



# Health Monitoring System Using Wireless Sensor Network

## Bakalářská práce

*Studijní program:*

B3944 Biomedicínská technika

*Studijní obor:*

Biomedicínská technika

*Autor práce:*

**Carlos Vladimír Díaz Shuňa, M.Sc.**

*Vedoucí práce:*

Ing. Jakub David

Fakulta zdravotnických studií





## Zadání bakalářské práce

# Health Monitoring System Using Wireless Sensor Network

*Jméno a příjmení:* **Carlos Vladimír Díaz Shuňa, M.Sc.**  
*Osobní číslo:* D18000105  
*Studijní program:* B3944 Biomedicínská technika  
*Studijní obor:* Biomedicínská technika  
*Zadávací katedra:* Fakulta zdravotnických studií  
*Akademický rok:* **2019/2020**

## **Zásady pro vypracování:**

### **Consultant:**

1. Ing. Stanislav Pecka, KNL.
2. Prof. Ing. Aleš Richter CSc.

### **Objectives:**

1. Design and develop a prototype ambulatory recording system and real-time ECG analysis.
2. Develop an ECG sensor that allows you to obtain a derivative of acceptable quality and transfer this signal over Bluetooth to an application on the patient's mobile phone.
3. Develop an application for the Android platform that receives the ECG signal transmitted by the sensor.

### **Theoretical background (including the output of the qualification work):**

A wireless sensor network could be defined as a network of devices that can communicate the information gathered from a monitored field through wireless links. The data is forwarded through multiple nodes, and with gateway, the data is connected to other networks. These networks are used to monitor physical or environmental conditions like sound, pressure, temperature, vital body functions, speed and co-operatively pass data through the network to a main location.

There are currently many researches in the field of data acquisition through wireless sensors. In this proposal, the device I will use an ECG (AD8232) sensor that collects physiological data wirelessly from medical staff and I will also use a receiver that receives the sensor data. As a result, a combination of software development and hardware programming on a wireless device, will provide an efficient network of wireless devices that can help in such situations.

The work is primarily aimed at students of biomedical technician, since they are the first audience, and finally the publication and expanded dissemination of it.

### **Research Prerequisites / Research Questions:**

1. We assume that the sensor catches ecg signals with a 10% error.
2. We assume that the acquisition software displays the ecg signals with a 10% error.

### **Method:**

Quantitative method.

### **Work technique, data evaluation:**

Experimental.

### **Location and time of research implementation:**

Faculty of Health Studies, Technical University of Liberec.

### **Sample:**

Students of 2nd and 3rd year of study Biomedical Technician (full-time form). Number of students: 25.

### **Scope of work:**

The scope of the bachelor thesis is 50-70 pages (i.e. 1/3 theoretical part, 2/3 research part).

Rozsah grafických prací:  
Rozsah pracovní zprávy:  
Forma zpracování práce:  
Jazyk práce:

tištěná/elektronická  
Angličtina



### Seznam odborné literatury:

1. MONK, Simon. *Hacking Electronics: An Illustrated DIY Guide for Makers and Hobbyists*. USA: McGraw-Hill Education, 2017. ISBN 978-1-26-001221-7.
2. BRONZINO, Joseph D. a Donald R., PETERSON. *Biomedical Signals, Imaging, and Informatics*. USA: CRC Press, 2017. ISBN 978-1-13-874811-8.
3. ZAPLATÍLEK, Karel. *MATLAB ? Začínáme se signály*. Praha: Tribun EU, 2015. EAN 9788026308980.
4. BULAVA, Alan. *Kardiologie pro nelékařské zdravotnické obory*. Praha: Grada, 2017. ISBN 978-80-271-0468-0.
5. STANĚK, Vladimír. *Kardiologie v praxi*. Praha: Axonite CZ, 2014. ISBN 978-80-904899-7.
6. LACKO, Ľuboslav. *Mistrovství – Android*. Brno: Computer Press, 2017. ISBN 978-80-251-4875-4.
7. KUBĚNOVÁ, Hana a VESELÁ, Ivana. *Jak funguje orgán*. Brno: Tribun EU, 2015. ISBN 978-80-263-0949-9.
8. HOUGHTON, Andrew R. a David GRAY. *Making Sense of the ECG: A Hands-On Guide*. Boca raton: CRC Press, 2014. ISBN 978-14-441-8182-1.
9. VEDRAL, Josef a Jakub, SVATOŠ. *Zpracování a digitalizace analogových signálů v měřicí technice*. Praha: ČVUT, 2018. ISBN 978-80-01-06424-5.
10. ROKYTA, Richard et al. *Fyziologie a patologická fyziologie: pro klinickou praxi*. Praha: Grada, 2015. ISBN 978-80-247-4867-2.
11. VODA, Zbyšek. *Průvodce světem Arduina*. Bučovice: Martin Stříž, 2017. ISBN 978-80-87106-93-8.
12. BULÍKOVÁ, Táňa. *EKG pre záchranárov nekaridiológov*. Praha: Grada, 2014. ISBN 978-80-247-5308-9.
13. MADEIRO, Joao P. et al. *Developments and Applications for ECG Signal Processing*. Fortaleza: Elsevier, 2018. ISBN978-01-281-4035-2

Vedoucí práce:

Ing. Jakub David  
Fakulta zdravotnických studií

Datum zadání práce:

2. září 2019

Předpokládaný termín odevzdání:

30. června 2020

L.S.

prof. MUDr. Karel Cvachovec, CSc., MBA  
děkan

## Prohlášení

Prohlašuji, že svou bakalářskou práci jsem vypracoval samostatně jako původní dílo s použitím uvedené literatury a na základě konzultací s vedoucím mé bakalářské práce a konzultantem.

Jsem si vědom toho, že na mou bakalářskou práci se plně vztahuje zákon č. 121/2000 Sb., o právu autorském, zejména § 60 – školní dílo.

Beru na vědomí, že Technická univerzita v Liberci nezasahuje do mých autorských práv užitím mé bakalářské práce pro vnitřní potřebu Technické univerzity v Liberci.

Užiji-li bakalářskou práci nebo poskytnu-li licenci k jejímu využití, jsem si vědom povinnosti informovat o této skutečnosti Technickou univerzitu v Liberci; v tomto případě má Technická univerzita v Liberci právo ode mne požadovat úhradu nákladů, které vynaložila na vytvoření díla, až do jejich skutečné výše.

Současně čestně prohlašuji, že text elektronické podoby práce vložený do IS/STAG se shoduje s textem tištěné podoby práce.

Beru na vědomí, že má bakalářská práce bude zveřejněna Technickou univerzitou v Liberci v souladu s § 47b zákona č. 111/1998 Sb., o vysokých školách a o změně a doplnění dalších zákonů (zákon o vysokých školách), ve znění pozdějších předpisů.

Jsem si vědom následků, které podle zákona o vysokých školách mohou vyplývat z porušení tohoto prohlášení.

9. května 2022

Carlos Vladimír Díaz Shuňa, M.Sc.

## Declaration

I declare that the presented work was developed independently and that I have listed all sources of information used within it in accordance with the methodical instructions for observing the ethical principles in the preparation of university thesis.

I hereby certify that I have written this bachelor thesis as an original and primary work using the literature listed below and consulting it with my thesis supervisor.

I acknowledge that my bachelor thesis is fully governed by Act No. 121/2000 Coll., the Copyright Act article 60 – School Work.

I acknowledge that the Technical University of Liberec does not infringe on my copyrights by using my bachelor thesis for the internal purpose of the Technical University of Liberec. I am aware of my obligation to inform the Technical University of Liberec on having used or granted a license to use the results of my bachelor thesis; in such a case the Technical University of Liberec may require reimbursement of the costs incurred for creating the results up to their actual amount.

At the same time, I honestly declare that the text of the printed version of my bachelor thesis is identical with the text of the electronic version up-loaded into the IS/STAG.

I acknowledge that the Technical University of Liberec will make my bachelor thesis public by following paragraph 47b of Act No. 111/1998 Coll., on Higher Education Institutions and Amendment to Other Acts (the Higher Education Act), as amended.

I am aware of the consequences which may under the Higher Education Act result from a breach of this declaration.

## Acknowledgement

My appreciation goes to my supervisor Ing. Jakub David for all his valuable advice, support, guidance, and time he dedicated during the work on my thesis.

## Anotace

**Autor** : Carlos Vladimír Díaz Shuňa, M.Sc.  
**Instituce** : Technická univerzita v Liberci  
Fakulta zdravotnických studií  
**Název práce** : Systém sledování srdce prostřednictvím sítě bezdrátových senzorů.

**Vedoucí práce:** Ing. Jakub David

**Počet stran** : 73

**Počet příloh** : 6

**Rok obhajoby:** 2022

**Anotace** : Cílem této práce je návrh a vývoj přenosného prototypu elektrokardiografu (EKG), který umožňuje zachytit biologický signál a bezdrátově jej přenést do chytrého zařízení – přes Bluetooth, pro následnou analýzu a vizualizaci v mobilní aplikaci. Tento prototyp pracuje se senzorem AD620AN, což je přístrojový zesilovač, který se používá k zesílení velmi slabých signálů, jako jsou biologické signály. Kromě toho byla prostřednictvím Android Studio vyvinuta mobilní aplikace, která přijímá EKG signál přenášený prototypem. Měření byla provedena u 25 účastníků, následně byla získaná data vyhodnocena a analyzována a vrcholy R byly detekovány pomocí programovacího prostředí MATLAB verze R2021b. Rozsah experimentální části byl však omezen z důvodu hygienických opatření uložených šířením viru SARS-CoV-2 (COVID-19).

**Klíčová slova** : EKG, AD620AN, Bluetooth, bezdrátový.



## Annotation

**Author** : Carlos Vladimir Díaz Shuňa, M.Sc.

**Institution** : Technical university of Liberec  
Faculty of Health Studies

**Title** : Health Monitoring System Using Wireless Sensor Network

**Supervisor** : Ing. Jakub David

**Pages** : 73

**Appendix** : 6

**Year** : 2022

**Annotation** : The aim of this work is focused on the design and development of a portable prototype of electrocardiograph (ECG) that allows capturing the biological signal and transferring it to a smart device wirelessly – via Bluetooth, for subsequent analysis and visualization from a mobile application. This prototype works with an AD620AN sensor, which is an instrumentation amplifier which is used for the treatment of very weak signals, such as biological signals. In addition, a mobile application was developed through Android Studio, which receives the ECG signal transmitted by the prototype. Measurements were made to 25 participants, subsequently the acquired data were evaluated and analysed, and the R waves were detected using the MATLAB programming environment of R2021b version. However, the scope of the experimental part was limited due to the sanitary measures imposed by the spread of the SARS-CoV-2 virus (COVID-19).

**Keywords** : ECG, AD620AN, Bluetooth, wireless.

# Content

List of Used Abbreviations .....	10
1 Introduction .....	12
1.1 Purpose of the study and Goals .....	14
1.2 Overview (structure) of the thesis .....	14
2 Theoretical Background .....	15
2.1 The Heart.....	15
2.1.1 Layers of the Heart Wall.....	16
2.1.2 The heart chambers .....	17
2.1.2.1 The right atrium.....	17
2.1.2.2 The right ventricle .....	17
2.1.2.3 The left atrium .....	18
2.1.2.4 The left ventricle .....	18
2.2 Principles of Electrocardiogram.....	18
2.2.1 Cardiac Conduction System.....	18
2.2.2 Detection of the Cardiac Conduction System.....	21
2.2.2.1 ECG Signal: Waves, segments, and intervals .....	21
2.2.2.2 ECG Leads .....	23
3 Monitoring System: Microcontrollers and Architecture .....	26
3.1 Microcontrollers .....	26
3.1.1 Arduino .....	26
3.1.1.1 Analog-Digital Converter (ADC) .....	27
3.2 Architecture.....	28
3.2.1 Design .....	30
4 Practical Part.....	31
4.1 Prototype: Electronic and modeling.....	31
4.1.1 Signal Acquisition: Instrumentation Amplifier .....	31
4.1.1.1 Gain selection.....	33
4.1.1.2 Common-Mode Rejection (CMR) .....	34
4.1.2 Signal Filtering .....	35
4.1.2.1 Low-Pass Filter .....	35
4.1.2.2 High-Pass Filter.....	36
4.1.2.3 Notch or Band-Stop Filter.....	37
4.1.3 Signal Digitization .....	38

4.1.4	Signal Processing .....	40
4.2	Prototype of the mobile application .....	47
4.2.1	Bluetooth Data Acquisition .....	47
4.2.2	Application Structure and User Interface .....	51
4.2.2.1	Fragment .....	51
4.2.2.2	Main Activity .....	52
4.2.2.3	Instructions Fragment.....	55
4.2.2.4	Bluetooth Manager.....	56
4.2.2.5	ECG Signal Fragment .....	58
4.2.2.6	About Fragment .....	61
4.3	Measurement and data analysis.....	63
4.3.1	Limitations .....	67
5	Discussion.....	68
6	Conclusion.....	71
7	Proposal of Recommendations for Further Work .....	73
	References.....	74
	List of tables.....	77
	List of figures.....	78
	List of graphs .....	80
	Appendix.....	81

## List of Used Abbreviations

<b>ECG</b>	Electrocardiograph
<b>EMG</b>	Electromyography
<b>SpO<sub>2</sub></b>	Oxygen saturation
<b>PCB</b>	Print circuit board
<b>mV</b>	millivolts
<b>μV</b>	microvolts
<b>SA</b>	Sinoatrial
<b>approx.</b>	Approximately
<b>ICs.</b>	Integrated circuits
<b>CPU</b>	Central Processing Unit
<b>ADC</b>	Analog-Digital Converter
<b>CMR</b>	Common-Mode Rejection
<b>CMV</b>	Common-Mode Voltage
<b>dB</b>	Decibels
<b>IDE</b>	Integrated development environment
<b>GUI</b>	Graphical user interface
<b>iOS</b>	iPhone Operating System
<b>KB</b>	Kilobyte
<b>SDK</b>	Software Development Kit
<b>TX</b>	Transmit
<b>RX</b>	Receive
<b>GHz</b>	Giga Hertz
<b>PIN</b>	Personal Identification Number

<b>F<sub>s</sub></b>	Sampling Rate
<b>T<sub>s</sub></b>	Sampling Period
<b>G</b>	Gain
<b>Std</b>	Standard Deviation
<b>FFT</b>	Fast Fourier Transform
<b>F<sub>max</sub></b>	Maximum Frequency
<b>FIR</b>	Finite Impulse Response
<b>HRV</b>	Heart Rate Variability

# 1 Introduction

Technological advances have helped treat various diseases, especially heart disease and neurodegenerative diseases, which in recent decades are no longer limited to elderly people but are affecting middle-aged people and young people due to the prevailing stress in daily life (Gupta and Biswas, 2020).

Currently, there are several healthcare providers that have developed mobile applications designed to promote and maintain health through the telecommunications infrastructure, also known as telemedicine. These applications run on mobile devices such as smartphones, tablets, and smartwatches.

In telemedicine, a wireless sensor network is defined as a network of devices that allow the information collected from a monitored area to be transferred through wireless ports. This data is sent through various links or nodes, connecting to other networks through data transfer links. These networks are used to monitor climatic, physical, or bodily functions and transmit these data through the network to a server.

From a clinical aspect, a personalized, wireless medical care model is required for 24-hour monitoring within the patient's home environment. This would reduce unnecessary visits to the clinic or rehabilitation centres. These medical care models feature a system of microprocessors and miniaturized wireless sensors capable of recording physiological parameters and differences over long periods of time (Gupta and Biswas, 2020).

An overview of a typical wireless system for remote healthcare monitoring is shown in Figure 1.1. Sensors include electrocardiogram (ECG), electromyography (EMG), and oxygen saturation (SpO<sub>2</sub>), among other sensors.

ECG is a diagnostic method for detecting the heart's electrical signal and its rhythm abnormalities. These heart conduction system disorders are usually sporadic in appearance and of limited duration. Personal ECG devices are typically divided into Holter devices and event monitoring devices. Holter devices record the ECG over a period of 1 to 7 days, storing the recorded data on a mobile device for further analysis. In the case of event monitoring, devices are divided into loop recording, where signal transmission is wireless via electrodes connected to the patient's surface, and post-event

recording, where the signal is transmitted directly to a data centre and then processed and analysed by an algorithm and a specialist.

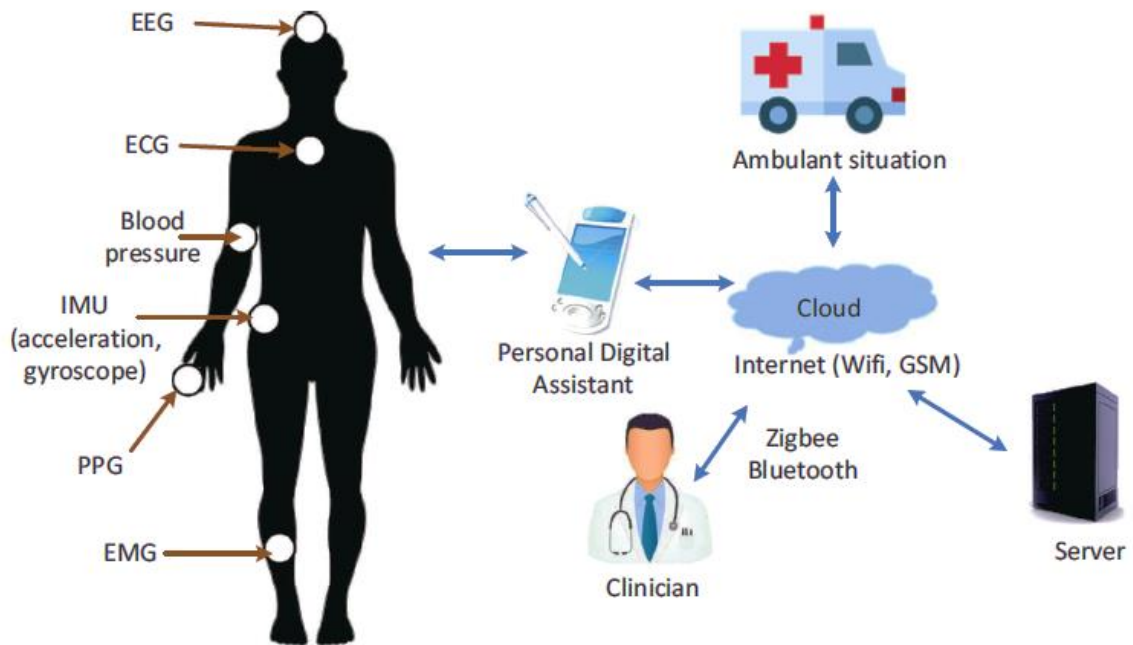


Figure 1.1: Typical remote monitoring system (Gupta and Biswas, 2020, fig. 1.1, p. 3)

As an alternative to ECG, the device in this proposal will use a post-event recording monitoring system with an AD620AN sensor from the company Analog Devices, which sends the physiological signal obtained via Bluetooth to an application on the patient's mobile phone, where it will be displayed and analysed in real-time.

As a result, a combination of software development and hardware programming in a wireless device will provide an efficient network of wireless devices that can help in such situations. To acquire the ECG signal, disposable electrodes and an analogy fronted circuit were used. As the signal captured by the electrodes is in the order of millivolts (mV), it must be amplified in the order of volts and then filtered to eliminate noise.

Once the signal is amplified and filtered, it is necessary to take samples at a certain frequency to obtain a digital signal that can be transmitted wirelessly to the mobile phone. The application was developed on Android Studio, and it can be downloaded on the Android platform. This application receives the signal wirelessly and allows it to be viewed in real-time.

## **1.1 Purpose of the study and Goals**

The main goal of this thesis consists of the design and development of an ECG sensor prototype which provides us with information and analysis in real-time through the implementation of a mobile application on the Android platform and the use of an Arduino microcontroller for the transmission of the ECG signal.

Besides, developing an ECG sensor that allows obtaining a signal of acceptable quality and transferable by Bluetooth to an application on the patient's mobile phone and the development of an application that allows us to visualize these signals.

## **1.2 Overview (structure) of the thesis**

This thesis is divided into seven chapters. Chapter 1 provides a general introduction to the problem and its objectives. Chapter 2 illustrates the theoretical basics which are relevant in the context of this thesis. The anatomy and electrophysiology of the heart and the functioning of the ECG are described. In Chapter 3, the operation of microcontrollers and their architecture are explained and described. The prototype of the ECG, the processing of the ECG signal, and the visualization of the application in Android Studio make up the practical part of this thesis, which is explained in Chapter 4. Chapter 5 consists of the discussion of the results. Finally, the proposals for the future work and recommendations and conclusions are presented in Chapters 6 and 7, respectively.



## 2 Theoretical Background

This part briefly discusses the main theoretical basics relevant to the research. The anatomy and physiology of the heart, as well as its electrical activity, are described. The functioning of ECG is also outlined.

### 2.1 The Heart

The heart is the pump for the circulatory system. It is located in the thoracic cavity in the mediastinum between the lungs and below the sternum. From its superior to inferior midpoints, it is tilted toward the left, so about two-thirds of the heart lies to the left of the median plane. The broad superior portion of the heart, called the base, is the point of attachment for the great vessels. The inferior end tapers to a blunt point, the apex of the heart immediately above the diaphragm (see figure 2.1 and figure 2.2). The adult heart weighs from 270 to 300g approximately and measures about 9cm wide at the base, 13cm from base to apex, and 6 cm from anterior to posterior at its thickest point (Saladin, Sullivan, and Gan, 2017). The heart is a muscular organ whose rhythmic contractions force blood to circulate within both circulation loops, systemic and pulmonary loops (Kaniusas, 2019).

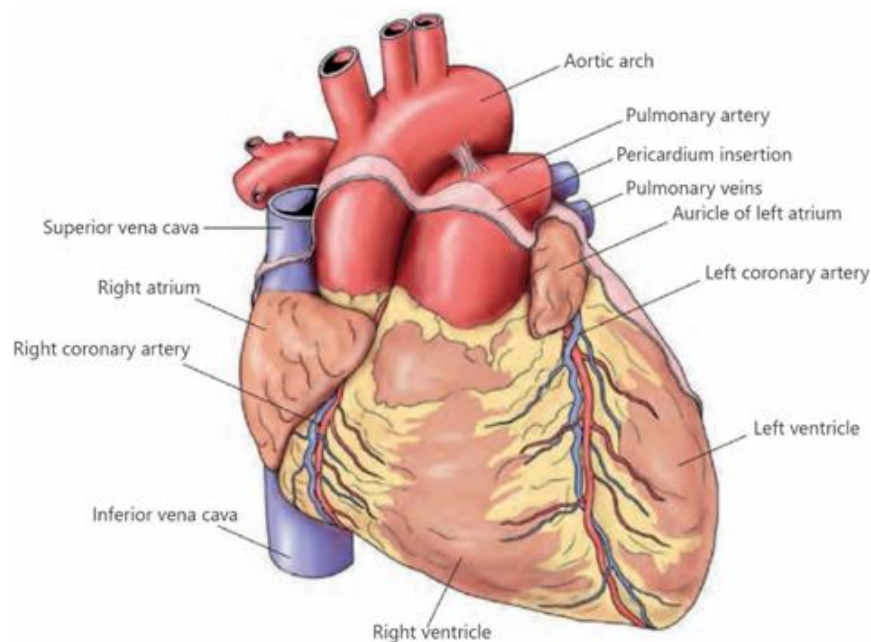


Figure 2.1: Front view of the heart (Staněk, 2014, p. 15)

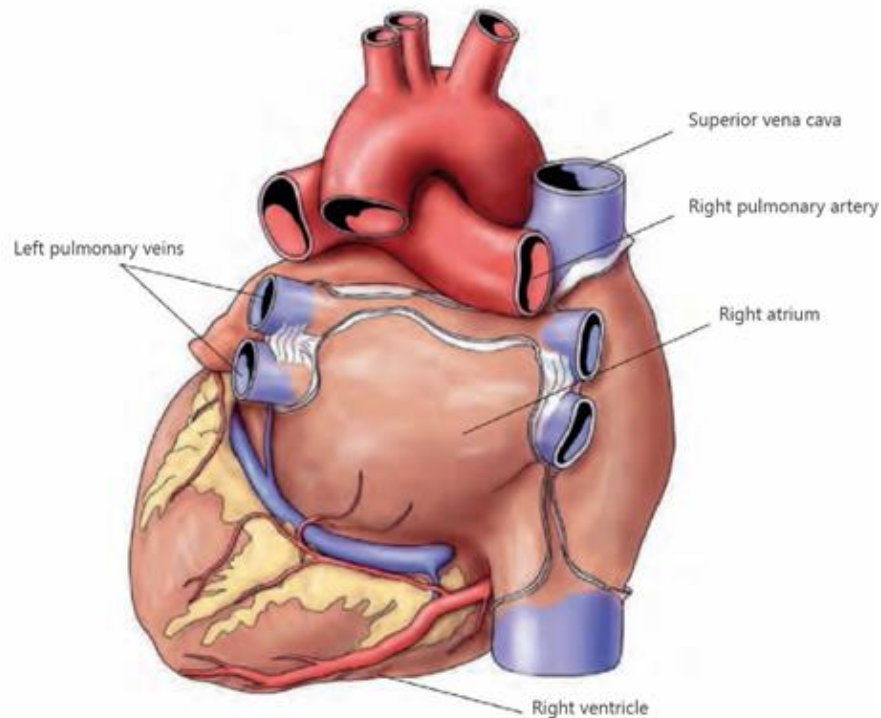


Figure 2.2: Back view of the heart (Staněk, 2014, p. 16)

### 2.1.1 Layers of the Heart Wall

The wall of the heart has three layers: a superficial epicardium, a middle myocardium, and a deep endocardium. All three layers are richly supplied with blood vessels. The epicardium is the visceral layer of the serous pericardium. This serous membrane is often infiltrated with fat, especially in older individuals (Saladin, Sullivan, and Gan, 2017).

According to Marieb (2017), the myocardium forms the bulk of the heart. It consists of cardiac muscle tissue and is the layer that actually contracts. Surrounding the cardiac muscle cells in the myocardium are connective tissues that bind these cells together into elongated, circularly, and spirally arranged networks called bundles. These bundles function to squeeze blood through the heart in the proper directions: inferiorly through the atria and superiorly through the ventricles. The connective tissues of the myocardium internally anchor the cardiac muscle fibers.

The endocardium, located beneath the myocardium, is a sheet of simple squamous epithelium resting on a thin layer of connective tissues. The endocardium lines the heart chambers and covers the heart valves (Marieb, Wilhelm, and Mallatt, 2017).

## **2.1.2 The heart chambers**

### **2.1.2.1 The right atrium**

The right atrium constitutes the entire right border of the human heart, where deoxygenated blood returns from the systemic loop. The right atrium receives blood through three veins: the superior and inferior vena cava and the coronary sinus. Externally, the right atrium has a small flap which projects anteriorly from the upper corner of the atrium. Internally, it is divided into two parts: the pectinate muscles (*musclea musculi pectinati*) and the crista terminalis (derived from the sinus venosus) (Marieb, Wilhelm, and Mallatt, 2017). The crista is important in locating the sites where the veins enter the right atrium. In addition, behind this end of the crista is the oval fossa (also called the limbus), a depression in the interatrial septum that marks the place where the foramen ovale existed. Inferiorly and anteriorly, the right atrium opens into the right ventricle through the tricuspid valve (McKinley et al., 2016).

### **2.1.2.2 The right ventricle**

The right ventricle forms most of the anterior surface of the heart. It receives blood from the right atrium and pumps it to the pulmonary circulation through the pulmonary trunk. Internally, the walls of the right ventricle are thicker than the walls of the atria and are also marked by irregular ridges of muscles called trabeculae carneae. In addition, the papillary muscles project from the walls into the ventricular cavity. The chordae tendineae are strong, thin bands that project upward from the papillary muscles to the flaps of the tricuspid valve. Superiorly, the opening between the right ventricle and the pulmonary trunk contains three semilunar cusps (semilunar pulmonary valves) (Marieb, Wilhelm, and Mallatt, 2017).

### **2.1.2.3 The left atrium**

The left atrium makes up most of the posterior surface or base of the heart. It receives oxygenated blood that returns from the lungs through the right and left pulmonary veins. Internally, the atrial wall is smooth, with pectinate muscles covering the entire atrium. The left atrium opens into the left ventricle through the mitral valve (McKinley et al., 2016).

### **2.1.2.4 The left ventricle**

The left ventricle forms the apex of the heart and dominates its inferior surface. The wall is considerably thicker than that of the right ventricle but with a similar structure containing trabeculae carneae, papillary muscles, chordae tendineae, and the cusps of an atrioventricular valve. The left ventricle wall is thick as it is necessary to pump high-pressure oxygenated blood through the systemic circulation, passing through the stem artery of the aorta through the aortic semilunar valve (McKinley et al., 2016).

## **2.2 Principles of Electrocardiogram**

The mechanical action of the heart is due to the generation of small electrical impulses and their propagation within the heart. The electrocardiograph (ECG) is the method that records the electrical activity of the heart, normally measured between two points on the surface of the body. As the activity of the cardiac chambers is rhythmic and totally ordered, the shape of the wave obtained is regular. In it, various waves whose amplitudes, durations, and morphologies are well defined and easily recognized.

### **2.2.1 Cardiac Conduction System**

The cells of the cardiac muscles have an intrinsic ability to generate and conduct electrical impulses to the contractile cells of the myocardium, where depolarization activates cardiac contraction. These properties are intrinsic to the muscles of the heart and

do not depend on extrinsic nerve impulses. Even if all nerve connections to the heart are severed, the heart continues to beat rhythmically. This is a property of these cells, known as "pacemaker cells" (Rokyta, 2015).

According to Morega (2020), the heart's conduction system is made up of specialized cardiac muscle cells that carry impulses throughout the heart muscles, which signal the chambers of the heart to contract in the corresponding sequence. It also begins each contraction sequence. Each muscle contraction is associated with a change in electrical potential. During depolarization, there is a change in resting potential from -80 mV to -90 mV by opening sodium ( $\text{Na}^+$ ) channels. As the potential between the external and internal environment of the cardiac cells decreases to a threshold value,  $\text{Na}^+$  channels close and potassium ( $\text{K}^+$ ) channels open until the balance of  $\text{Na}^+$  and  $\text{K}^+$  ions is restored between the external, and internal environment of the cardiac cells, this process is known as repolarization (see figure 2.3). The total time of both processes (repolarization and depolarization) is approx. 300ms.

The impulse that starts each beat begins in the sinoatrial (SA) node, which is made up of a crescent-shaped mass of muscle cells found in the wall of the right atrium, just below the superior vena cava's entrance point. The SA node also sets the basic heart rate by generating between 70 and 80 electrical pulses per minute. This signal, initiated by the SA node, propagates through the entire myocardium through the gap junctions in the intercalated discs, producing a high spontaneous depolarization and acting as a primary pacemaker.

From the SA node, the impulses travel in a wave along the muscle fibers of the atrium, initiating atrial contraction. Some of these impulses travel along the internodal pathway to the atrioventricular (AV) node at the bottom of the interatrial septum, where they are delayed before continuing through the AV bundle (previously called the bundle of His), dividing into two branches, right and left of the AV bundle. Approximately midway through the septum, the AV bundle branches propagate the action potential to the subendocardial conducting network (Purkinje fibers), which approaches the vertex of the heart to finally rotate up the ventricular walls (Subasi, 2021).

This arrangement ensures ventricular contraction, pushing the blood towards the semilunar valves so that it is expelled towards the great arteries.

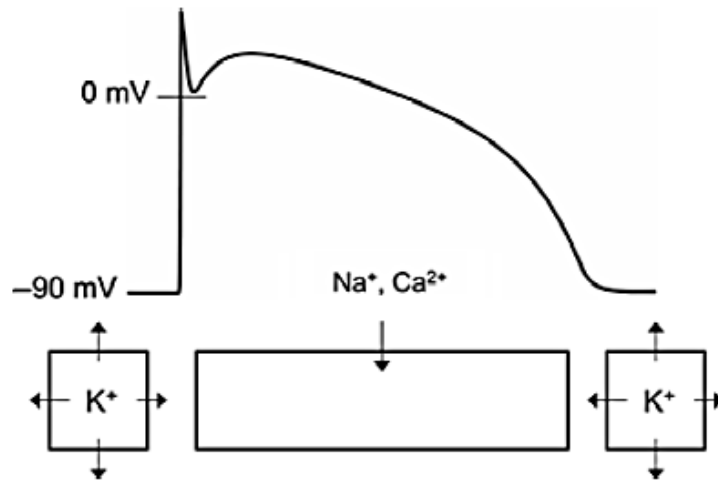


Figure 2.3: Cardiac action potential. (Goldberger & Ng, 2010, Fig. 10.1, p. 114)

The brief delay of the contraction signaling pulses at the AV node allows the ventricles to completely fill before they begin to contract. The membrane potential starts at approximately -60mV and then spontaneously depolarizes to the -40mV threshold, at which point an action potential is generated. After repolarization, the membrane potential begins to depolarize again and the cycle repeats (see figure 2.4).

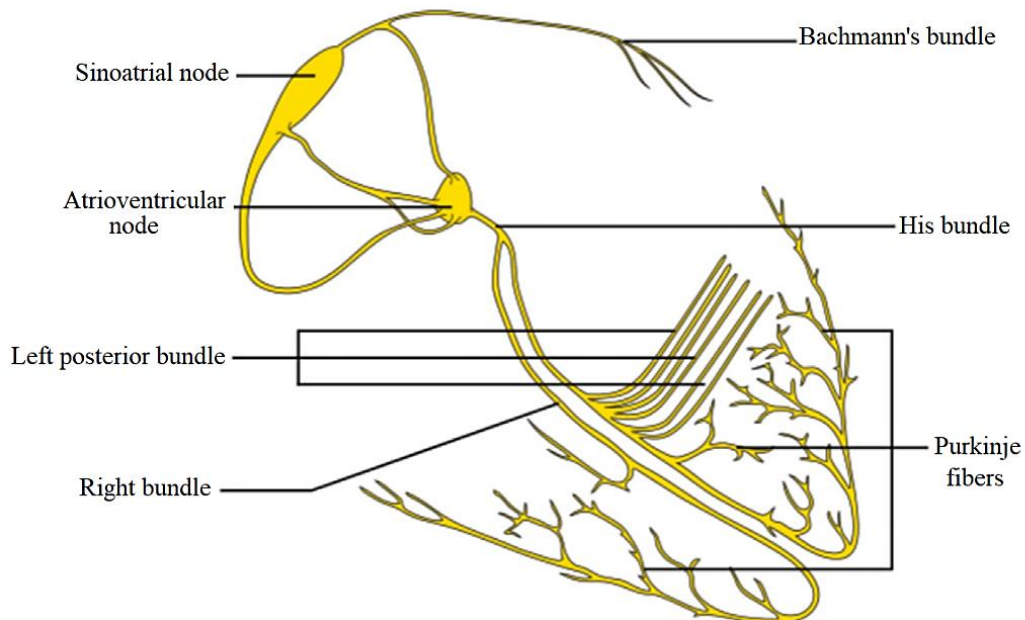


Figure 2.4: Conduction system of the heart (Morega et al., 2020, Fig. 4.1, p. 95)

## 2.2.2 Detection of the Cardiac Conduction System

ECG is a recording that reflects the electrical activity of the heart normally measured between two points on the surface of the body. As the activity of the rhythmic heart chambers is totally ordered, the waveform obtained is regular. It easily recognises various waves whose amplitudes, durations, and morphologies are well defined. ECG is used to investigate some types of abnormal cardiac function, including arrhythmias and conduction disturbances, as well as heart morphology (for example, heart orientation in the chest cavity, hypertrophy, and course of ischemia or myocardial infarction). It is also useful for evaluating pacemaker performance (Petty, 2016).

According to Golemati and Nikita (2019), ECG is a method that records electrical activity versus time. Changes in electrical potential difference (measured in mV) during depolarization and repolarization of myocardial fibres are recorded by electrodes normally placed between two points on the body surface. The sources of the electrical potentials are cells of the contractile heart muscle called cardiomyocytes. The generally accepted frequency range for a diagnostic ECG is 0.05 to 150 Hz.

### 2.2.2.1 ECG Signal: Waves, segments, and intervals

The QRS complex is the basis for automatic heart rate recognition and a fundamental part of ECG data compression schemes. According to Subasi (2021), the QRS complex describes the mechanical action of the heart. When the heart depolarizes, these waves spread through the cardiac cycle producing electrical impulses, which will be detected on the body's surface through the electrodes. For these signals to form the ECG wave, certain elements must be considered: the isoelectric line, which is a horizontal line when there is no electrical activity, the segments, which is the duration of the isoelectric line between the waves and the intervals, which are the time between the same adjacent wave segments.

The main features of ECG are as follows (see figures 2.5 and 2.6):

**P wave:** it is due to the electrical action that comes from the atrial contraction (systole), which is usually positive in most of the leads. It lasts no more than 0.12s, and the voltage in the limb leads should not exceed 0.25mV and 0.15mV in the precordial leads (Madeiro et al, 2019).

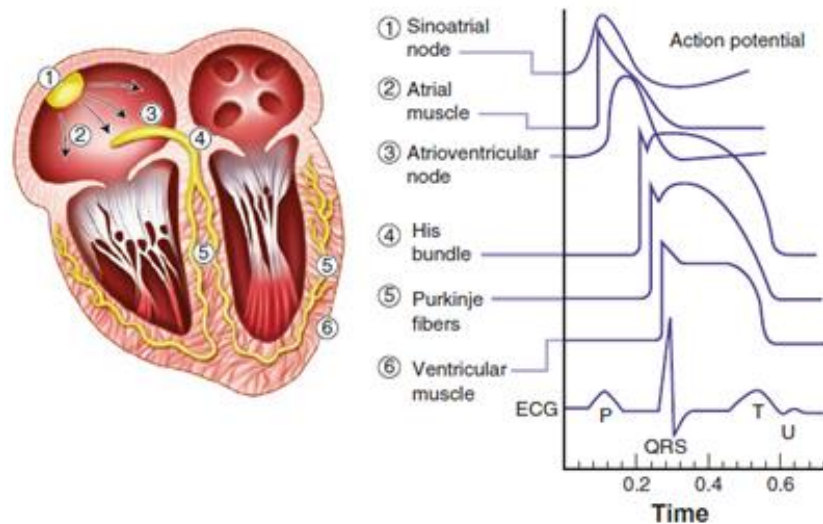


Figure 2.5: Normal activation of the heart (Kusumoto, 2020, fig. 1.5, p. 9)

**PR segment:** this corresponds to electrical impulses transmitted through the SA node, His bundle, and its branches, and the Purkinje fibers and is usually isoelectric (Zgallai, 2020).

**PR interval:** This extends from the beginning of the P wave to the beginning of the QRS complex. This should not exceed 0.2s, which expresses the time elapsed from the atrial depolarization to the onset of the ventricular depolarization (Zgallai, 2020) (Madeiro et al., 2019).

**QRS complex:** This is the largest group of waves in the ECG and represents ventricular depolarization. The first negative deviation (downward) is given by the Q wave representing the ventricular contraction (systole), followed by the R wave with a positive deviation (upward). Any negative deflection that follows the R wave is called the S wave. The normal duration of the QRS complex is not greater than 0.12s. The voltage usually varies between 1.5 to 2 mV (Madeiro et al, 2019).

**ST segment:** This is part from the QRS complex to the beginning of the T wave. Normally, it is isoelectric. It coincides with the slow and rapid repolarization of the ventricular muscle (Zgallai, 2020).

**T wave:** According to Madeiro (2019), when the ventricles relax (diastole), they produce a repolarization wave called the T wave, which lasts from 0.25 to 0.35s after the



ventricular depolarization. In this phase, the ventricles electrically relax and prepare for their subsequent muscle contraction. Atrial repolarization is also present.

**QT interval:** This is measured from the beginning of the QRS complex to the end of the T wave. It lasts approximately 0.35s and provides data on the status of the ventricular contractions. Its duration decreases as the heart rate increases, and this interval does not last more than half the time between the previous RR interval for rates between 60 to 90 beats per minute (Madeiro et al., 2019).

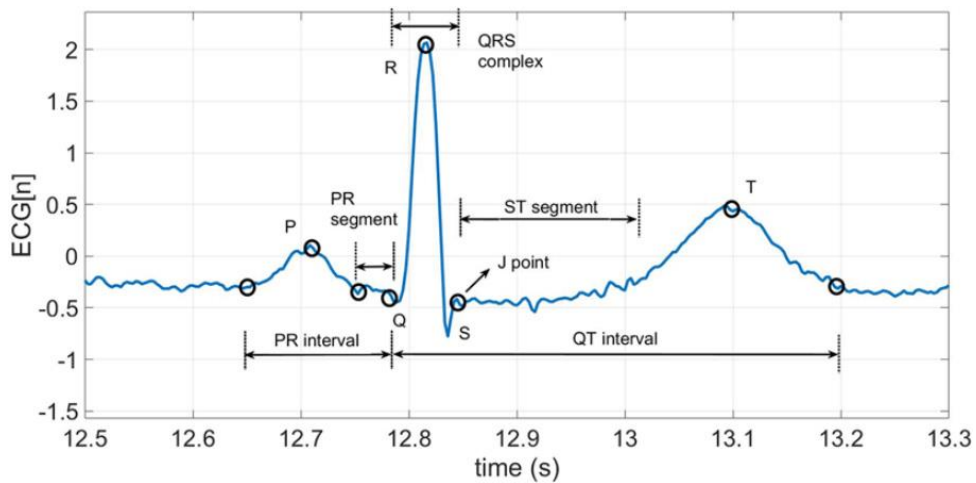


Figure 2.6: EKG signal (Madeiro et al., 2019, fig. 1.6, p. 10)

### 2.2.2.2 ECG Leads

ECG signals are representations of cardiac electrical activity, captured by two or more electrodes. The result will be the potential difference between the electrodes (one positive electrode and one negative electrode), which will comprise a single ECG lead. The most common electrodes are non-invasive surface electrodes, which have a conductive gel between the metal part of the electrode and the patient's skin, reducing the skin-electrode impedance (Madeiro et al., 2019).

Einthoven, in 1924, considered three leads which were placed on the right arm, left arm, and left leg of a person with hands stretched laterally, which formed an equilateral triangle with vertices in a circle.

Lead I:  $V_{LA} - V_{RA}$ , Lead II:  $V_{LL} - V_{RA}$ , and Lead III:  $V_{LL} - V_{LA}$ , where  $V_{LA}$  is a potential of the left arm,  $V_{RA}$  is a potential of the right arm, and  $V_{LL}$  is a potential of the left leg (see figure 2.7) (Bulíková, 2014).

Since the three branches lead to the construction of a closed circuit, Kirchhoff's voltage law can show the relationship between them as:  $I + III = II$ . Wilson defined and standardized unipolar leads with three unipolar limb leads ( $V_L$ ,  $V_R$ , and  $V_F$ ) and six precordial chest leads. Because the unipolar leads had a small amplitude, Goldberger modified these precordial leads to develop the increased limb leads,  $aVR$ ,  $aVL$ , and  $aVF$ , which increased the amplitude by 50% (see figure 2.8) (Kusumoto, 2020).

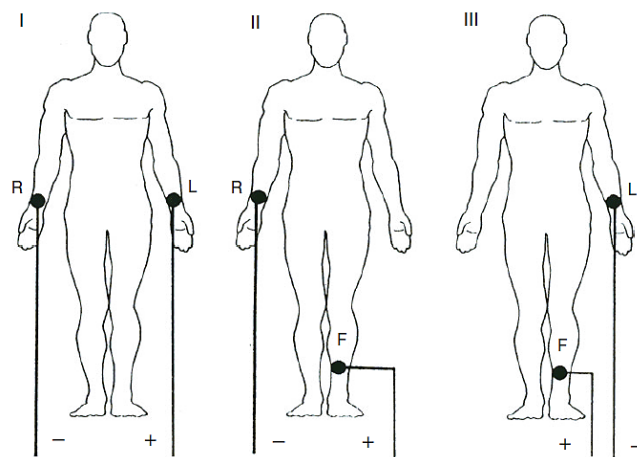


Figure 2.7: Leads location according to Einthoven (Kramme, 2017, Fig. 6, p.138)

Currently working with the 12-lead ECG system, which is accepted in the mapping of a patient's ECG signals. In this system, the leads  $V_1$ ,  $V_2$ ,  $V_3$ ,  $V_4$ ,  $V_5$ , and  $V_6$  measure cardiac potentials in the peripheral intercostal spaces of the chest from a horizontal plane, and leads I, II, III (6- in total) measure the potential from a frontal plane (see figure 2.9) (Gupta, Mitra and Bera, 2014).

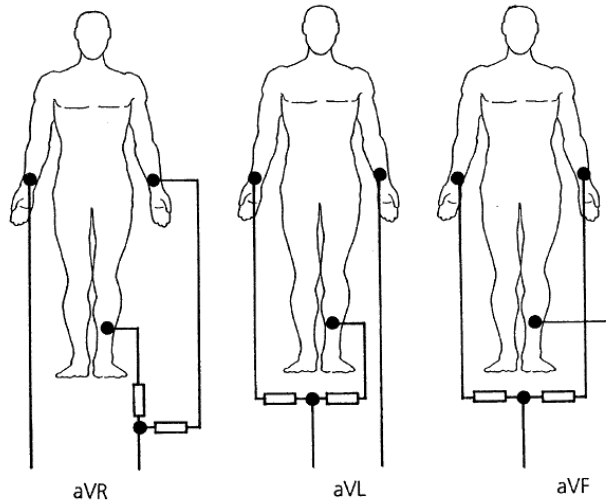


Figure 2.8: Lead circuit diagram according to Goldberger (Kramme, 2017, Fig. 8, p.139)

According to Lyon (2020), ten electrodes currently are used to produce electrical voltages ranging from 5 microvolts ( $\mu\text{V}$ ) to 5 mV. The bandwidth used by the ECG varies from 0.5Hz to 1MHz. AC noise (ranging from 50 to 60Hz), skin-electrode interface resistance, movement, muscle contractions, respiration, and other electromagnetic sources are often present in the sensors during the exam.

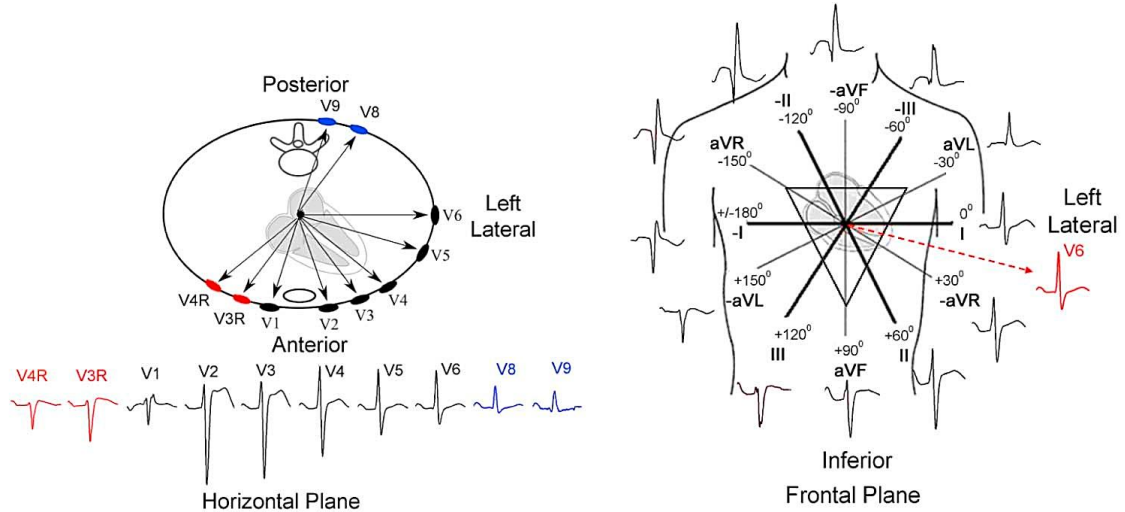


Figure 2.9: 12-lead ECG system (Jekova et al. 2016, Fig. 1, p. 32)

## 3 Monitoring System: Microcontrollers and Architecture

This chapter includes the development of the hardware, which will allow us to communicate with an external device with a microcontroller system such as Arduino. Such a device must be portable and have a low-power consumption. The Arduino system has the ability of physiological signal operation and signal processing. In addition, we will explain the architecture of the ECG device.

### 3.1 Microcontrollers

Microcontrollers are programmable integrated circuits (ICs) or small integrated circuit computers that contain a complex microprocessor system or central processing unit (CPU), memory, timers, and input/output peripherals.

The simplest microcontroller works with 8-bit words and is suitable for applications that require small amounts of memory and simple logical functions. They consume extremely small amounts of energy and include a sleep mode that reduces power consumption. 16-bit and 32-bit microcontrollers are much more powerful and expensive (Lee and Seshia, 2017).

Microcontrollers can become quite elaborate. In addition, they include an internal clock and a RAM and/or read-only memory (ROM or EFROM), and a flash memory to store data programs. Some typically include digital-analog converters and analog-digital converters (Dogan, 2014).

#### 3.1.1 Arduino

Arduino is a microcontroller development platform combined with an intuitive programming language that is developed using the integrated development environment. By equipping the Arduino with sensors, actuators, lights, speakers, add-on modules, and other ICs, they can turn the Arduino into a programmable "brain" for almost any control system (Perea, 2015).

Arduino boards are based on the Atmel Corporation's ATmega family of chips. The Arduino board model used in this project has been the Arduino UNO, which is based on the 8-bit ATmega328p chip (see figure 3.1).

Arduino is an open-source hardware company and technology community which designs and manufactures hardware and software development boards composed respectively of printed circuits that integrate a microcontroller and a development environment (Blum, 2020). The technical characteristics of the Arduino board are in table 3.1.

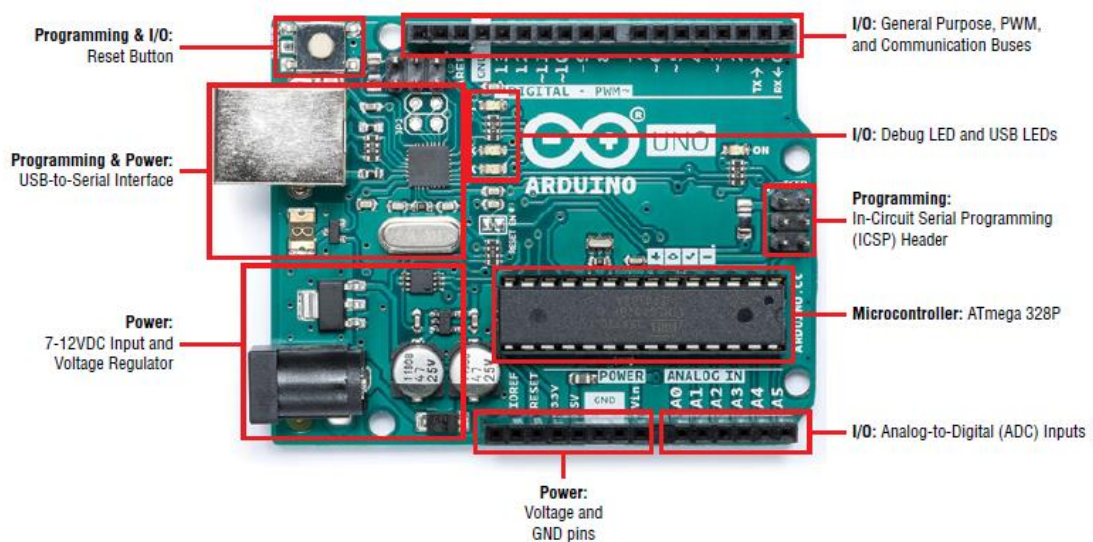


Figure 3.1:Arduino UNO components (Blum, 2020, fig. 1.1, p. 6)

### 3.1.1.1 Analog-Digital Converter (ADC)

ADC is an electronic system that converts analog voltage signal to digital values, allowing data to be sent and processed using Arduino software. This converter is limited to several physical parameters, including resolution and frequency.

**Resolution:** It is defined as the smallest difference between two successive values that the ADC can detect. The Arduino converter has a resolution of 10 bits, which limits the output range to 1024 values ( $2^{10}=1024$ , where 10 is the number of bits) (Perea, 2015).

**Frequency:** The frequency indicates the number of conversions that ADC can perform per unit of time. The ATmega328 chip converter requires 13 cycles to perform

a normal conversion and uses the oscillating crystal frequency of the Arduino board reduced through a pre-multiplier.

The oscillating glass frequency value is 16MHz, and the pre-multiplier value is a division of 128 ( $16\ 000\text{KHz}/128 = 125\text{KHz}$ ). Every 13 cycles per conversion, the converter can convert 9600 values per second ( $125\text{KHz}/13 = 9.6\text{KHz}$ ). To establish the sample rate for obtaining an ECG, must calculate the maximum and minimum values. The maximum value is given by the limitations of ADC, while the minimum values are given by the intervals or segments of the ECG. QRS complexes have a length of 100 to 200 milliseconds (Perea, 2015).

Table 3.1: Technical characteristics of Arduino board (Arduino, 2016)

Detail	Characteristics
Microcontroller	ATMega 328p
Operating Voltage	5V
Input Voltage (recommended)	7 – 12V
Input Voltage (limit)	6 – 20V
Digital I/O Pins	14 (of which 6 provide PWM output)
PWM Digital I/O Pins	6
Analog Input Pins	6
DC Current per I/O Pin	20mA
DC Current for 3.3V Pin	50mA
Flash Memory	32 KB (ATmega328P) of which 0.5 KB used by bootloader
SRAM	2 KB (ATmega328P)
EEPROM	1 KB (ATmega328P)
Clock Speed	16 MHz
Led_Builtin	13
Size	68.6 x 53.4 mm
Weight	25 g

## 3.2 Architecture

The complex telemedicine surveillance system in which the ECG device operates is shown in Figure 3.2. This system consists of 4 levels. The first level of the system is a portable patient device that provides recording, pre-processing, and storage of

physiological signals. At this level, ECG signals are sent and recorded to the algorithm and/or storage centre.

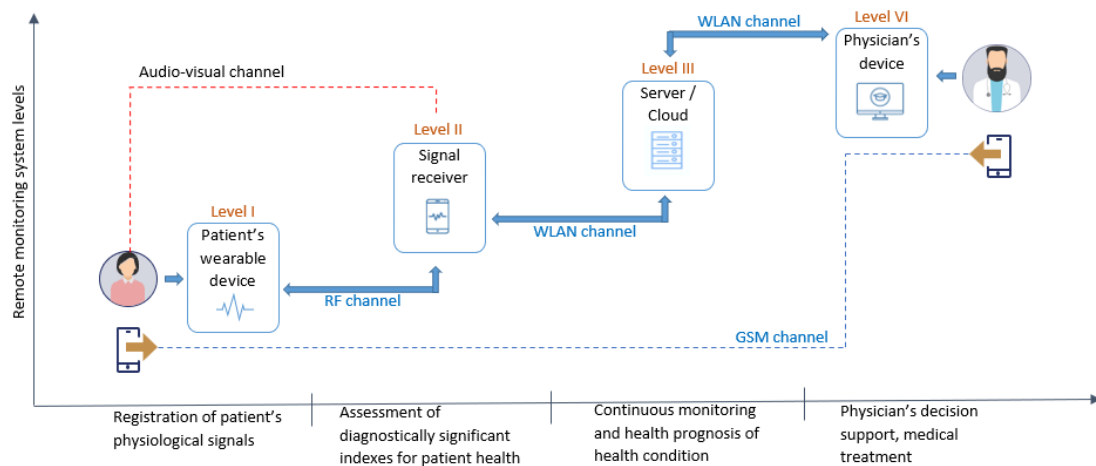


Figure 3.2: Basic diagram of the presented platform and its principal components (Courtesy of prof. Evgenii Pustozarov, PhD.)

At the next level of the system, signals are received from the patient's portable devices for detailed data analysis in order to track the patient's status. This is a level of mobile and web applications where we can see all the signals sent and proposed by the algorithms.

The third level of the system is the medical institution's server which collects data from different sources, including data related to the health of the patient's device. At this level, the recorded signal is sent from the ECG device to the storage algorithms via Bluetooth to the phone application, which will send it to the target web storage servers.

Signals received at the server will be processed according to algorithms and classified into critical (or urgent) and non-critical signals.

The fourth level is a physician's device with appropriate software that will help to support data analysis decisions. This portable device records complex biomedical signals and indicators of the activities of the body's systems. Monitoring systems may be suitable for monitoring daily life with a minimal level of a negative effect of the recording devices on the patient's life activities.

### 3.2.1 Design

The sensor should have a minimum size and weight, providing a non-invasive evaluation without disturbing the user during use. To ensure reliable and continuous recording, the device must have long battery life. That is why portable devices are not capable of complicated signal pre-processing, which requires a high-performance multiprocessor and a large power supply. A Bluetooth signal, having low interface energy, is recommended for data transmission.

Highly integrated analogue front-end modules are recommended for medical purposes for recording biopotentials such as ECG, SO<sub>2</sub>, pulse wave, respiratory rate, temperature, and others. The structure of a portable device contains a set of electrodes and sensors for signal acquisition and several channels and front-end modules, and a microcontroller (Gupta and Biswas, 2020).

While the radio channel transmits the signals, the power supply must provide continuous power. The selection of specific system modules may vary depending on the purpose of the device.

At the second level of the telemedicine system, it is common to use a smartphone or tablet, which provides preliminary processing of physiological signals. The transmission of biomedical information over a wireless channel to the server must also be included in the device. The server must be updated and configured for full operation (Gupta and Biswas, 2020).

Among the most common difficulties, we can mention organizational and technological barriers, threats to the confidentiality and privacy of the patient's personal information, legal, ethical, and administrative barriers, and high cost of implementation and maintenance.

There are also factors related to telecommunications and hardware, including reliability issues, sudden interruption of telecommunications networks, scalability in terms of data rate and power consumption, difficulty in processing some data due to the devices used in patient monitoring, and user training required to use the portable system.



## 4 Practical Part

This chapter analyzes and explains the experimental and practical configuration of this thesis, which focuses on the development of a portable ECG prototype and a mobile application where the ECG signal can be stored.

### 4.1 Prototype: Electronic and modeling

The design and creation of an ECG began by reading small electrical signals on a subject. These signals must be amplified and filtered in order to be acquired (see figure 4.1). These signals are then converted to digital format so they can be processed and finally sent wirelessly to an Android application.

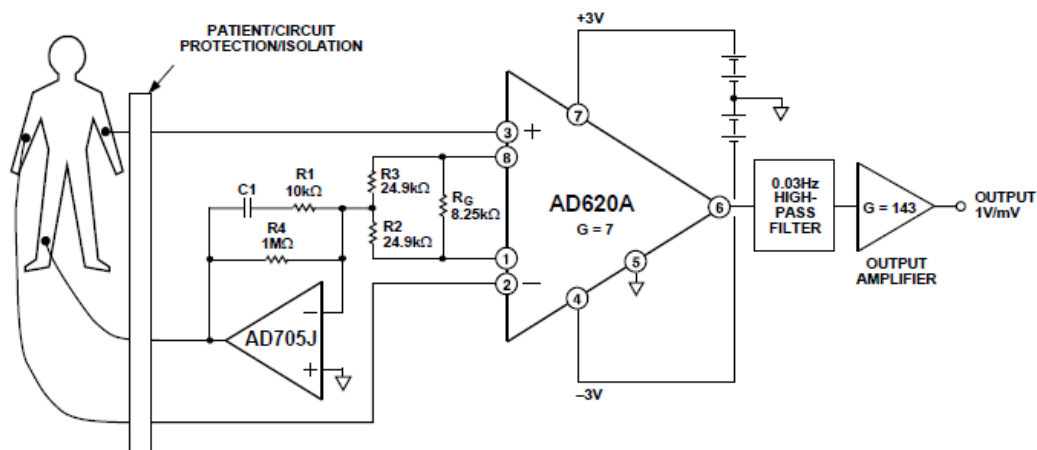


Figure 4.1: Medical ECG monitor circuit. (Analog-Devices, 2011)

#### 4.1.1 Signal Acquisition: Instrumentation Amplifier

The signals that are taken by the electrodes are too small (in the order of mVs) for the sensitivity of the Arduino board's ADC module, so amplification circuits are used to increase the voltage of the biosignals. The amplification circuits have an amplifier and other electronic components to make up an amplification stage. There are different types of amplification stages, among which are: adding, differentials, inverters, instrumentals, and others. The differential amplification stage allows us to amplify the difference

between two input signals, helping to eliminate noise. In the case of the signal obtained by the electrodes, the input impedance is too low; in this case, it is necessary to increase the input impedance while maintaining the same amplification behaviour of the difference between two waves to exclude noise. A combination of operational amplifiers that form a stage called an instrumentation amplifier is used. In this amplifier, the input impedance is infinite, which will avoid the appearance of noise in the signal (Hambley, 2019).

This project used the AD620, a high-precision, low-cost instrumentation amplifier which is based on a modification of the classic approach of three operational amplifiers. With only one resistance, the gain can be programmed (at 0.15% in  $G = 100$ ). The low noise and low power of the AD620 make it the best choice for medical applications such as EEG, ECG, and non-invasive blood pressure monitors. Low current noise allows its use in ECG monitors where high source resistances of  $1\text{ M}\Omega$  or higher are not uncommon. Due to its low power consumption and low supply voltage, the AD620 is recommended for battery-powered data recorders.

The AD620 has a monolithic construction and laser wafer trimming allows the combination and tracking of circuit components, ensuring a high level of inherent performance. The input transistors Q1 and Q2 provide a high precision bipolar input, as shown in figure 4.2. The main limitation of this circuit is that it is more exposed to external noises that interfere with the capture of biological signals (Analog-Devices, 2011).

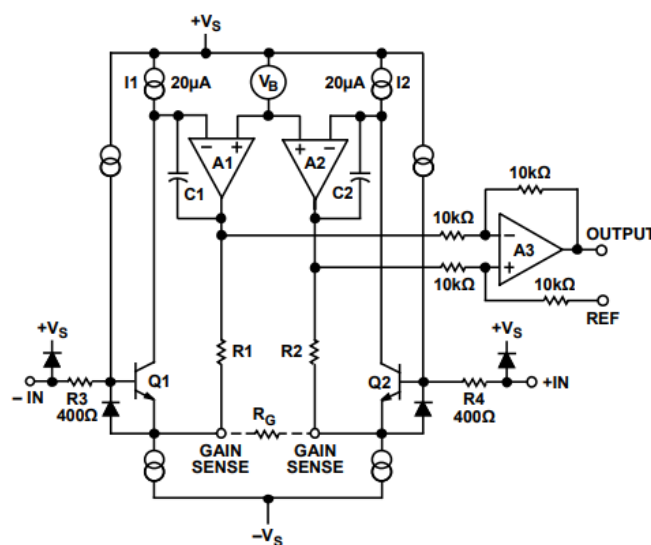


Figure 4.2: Simplified Schematic of AD620 (Analog-Devices, 2011)

#### 4.1.1.1 Gain selection

The AD620 gain is programmed by the gain resistance  $R_G$ , which gives us precise gains using resistances from 0.1% to 1%. The  $R_G$  value also determines the transconductance of the preamp stage. As  $R_G$  is reduced for higher gains, the transconductance increases up to the values of the input transistors. The internal gain resistances  $R_1$  and  $R_2$  are trimmed to an absolute value of  $24.7\text{k}\Omega$ , allowing to precisely program the gain with a single external resistance (Analog-Devices, 2011). To find the external resistance, it must calculate the  $R_G$  according to the equation number 1 and 2:

$$G = \frac{49.4\text{k}\Omega}{R_G} + 1 \quad (1)$$

$$R_G = \frac{49.4\text{k}\Omega}{G - 1} \quad (2)$$

The amplification instrument used has a gain of 1000 ( $G = 1000$ ). The gain equation was used to find the  $R_G$  according to the equation number 2.

$$R_G = \frac{49.4\text{k}\Omega}{1000 - 1} \rightarrow R_G = 49,4\Omega \quad (3)$$

Table 4.1 can visualize the calculation of the gain with respect to equation number 1, it depends on the value of  $R_G$ .

Table 4.1: Values of Gain Resistors (Analog-Devices, 2011)

<b>1% Std Table Value of <math>R_G(\Omega)</math></b>	<b>Calculated Gain</b>	<b>0.1% Std Table Value of <math>R_G(\Omega)</math></b>	<b>Calculated Gain</b>
49.9 K	1.990	49.3 K	2.002
12.4 K	4.984	12.4 K	4.984
5.49 K	9.998	5.49 K	9.998
2.61 K	19.93	5.61 K	19.93
1.00 K	50.40	1.01 K	49.91
499	100.0	499	100.0
249	199.4	249	199.4
100	495.0	98.8	501.0
49.9	991.0	49.3	1003.0

#### 4.1.1.2 Common-Mode Rejection (CMR)

The CMR is given when the same voltage with respect to the ground is applied to both inputs of an amplifier, where the output is not affected in an ideal system. Common mode voltage or CMV is commonly defined as a voltage difference between a neutral point of the DC load and a neutral point of the system load with DC-AC conversion; this results in decreased parasitic impedance that might exist at both points (Analog-Devices, 2011).

In other words, CMR is the relationship between the common-mode input voltage (also called CMV) and the input differential voltage that produces the same change in the output or error voltage. CMR is measured in decibels (dB), where 1dB will be equal to  $20\log(\text{CMV}/\text{Error Voltage})$ . When the CMR is equal to 80dB, it means that a CMV of 1V produces an error of 100mV referred as the input, which is in the range of 110 to 130dB. In the case of the AD620, the CMR has a wide frequency range, as shown in figure 4.3 (Analog-Devices, 2011).

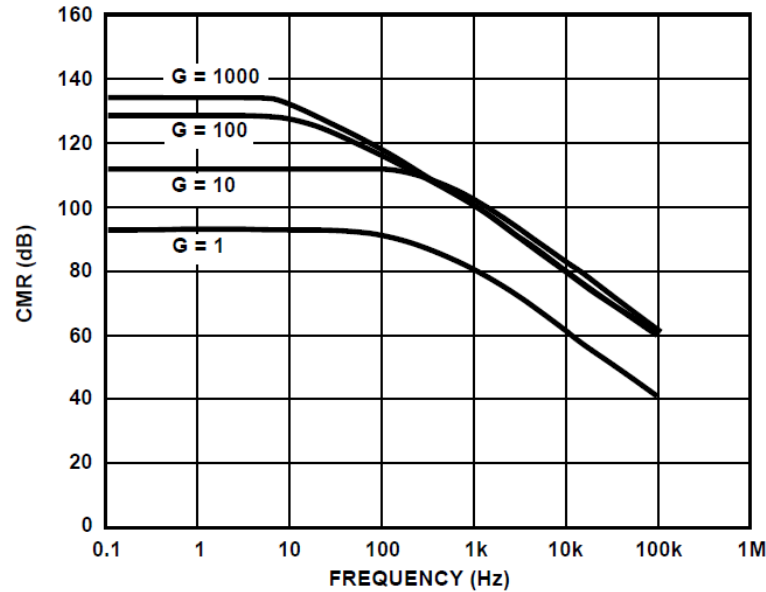


Figure 4.3: Typical CMR vs. Frequency (Analog-Devices, 2011)

## 4.1.2 Signal Filtering

A filter is a system that passes signals within a specific frequency band while attenuating those signals that are outside the band. They can be passive filters, which use passive components such as resistors, capacitors, and inductors, or active filters, containing passive and active components such as transistors and operational amplifiers. Passive filters generally have the advantage of not requiring an external power supply but use inductors that tend to be bulky and expensive. In the case of active filters, they use resistors and capacitors; also, they can produce signal gain and have high input and low output impedances, which allows a simple cascade connection with little or no interaction between them (Gift and Maundy, 2021). The project used three types of filters, low-pass filter, high-pass filter, and a notch or band-stop filter.

### 4.1.2.1 Low-Pass Filter

The basic function of a low-pass filter is to pass frequencies below a specified cut-off frequency. There are two well-differentiated areas in the filter response, the passband and the suppressed band (Gift and Maundy, 2021).

The passband defines the frequency content to be selected. In the ideal case, it is the area in which the signals will not be attenuated by the filter. This area is delimited by the cut-off frequency, which will hold a value of one in the case of being normalized. The frequency range contained in the passband is called filter bandwidth, which in the case of a low-pass filter matches the cut-off frequency. The suppressed band is ideally the area in which the filter no longer allows any frequency components through. The attenuation it offers is extremely high but does not become infinite (Gift and Maundy, 2021).

At this stage, the prototype uses an active first-order low-pass filter consisting of an operational amplifier with a cut-off frequency of 125Hz.

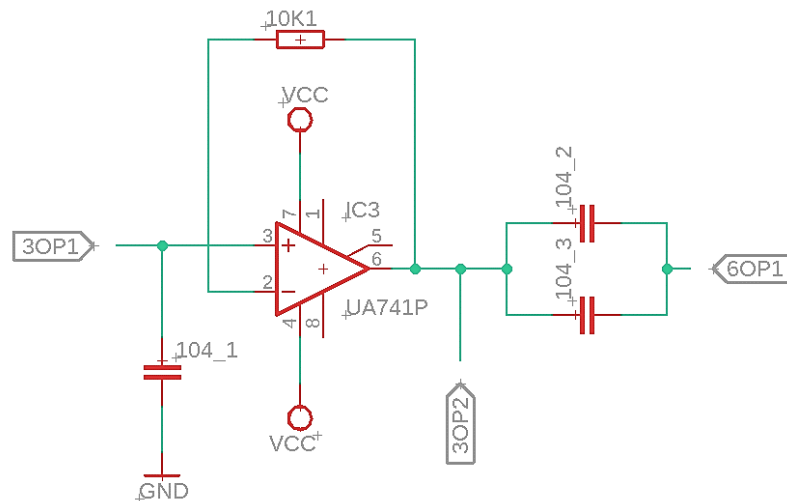


Figure 4.4: Low-pass filter (Source prepared by the author)

#### 4.1.2.2 High-Pass Filter

The function of a high-pass filter is to allow the high-frequency signals to flow through it and reject the low-frequency signals. The circuit diagram is like the low pass filter (Gift and Maundy, 2021). The simplest high-pass filter is a series RC circuit in which the output is the voltage drop across the resistor. In the case of extremely low frequencies, the capacitor behaves like an open circuit, so it will not let the current pass to the resistance, and the voltage difference will be zero. For an extremely high frequency, ideally infinite, the capacitor will behave like a short circuit, so the voltage drop of the resistance will be the same input voltage, which means that it would let the entire signal pass. The frequency of this filter is 0.5 Hz.

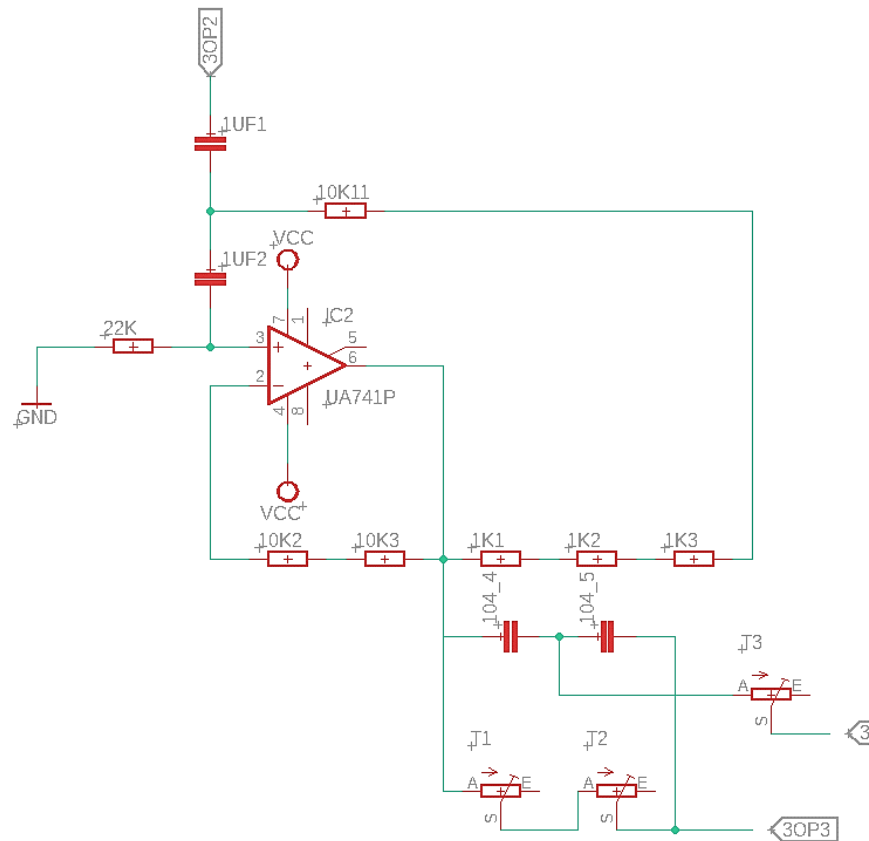


Figure 4.5: High-pass filter (Source prepared by the author)

### 4.1.2.3 Notch or Band-Stop Filter

A notch or band-stop filter is a special type of filter which combines low-pass and high-pass filters in parallel connection through an amplifier circuit. Unlike the filters mentioned above, these filters have two cut-off frequencies ((Gift and Maundy, 2021).

The notch filter that was used is a narrowband filter, which will attenuate a few hertz, i.e., attenuate single or exceedingly small frequencies instead of the entire bandwidth of different frequencies. This filter will have a value of 50 Hz.

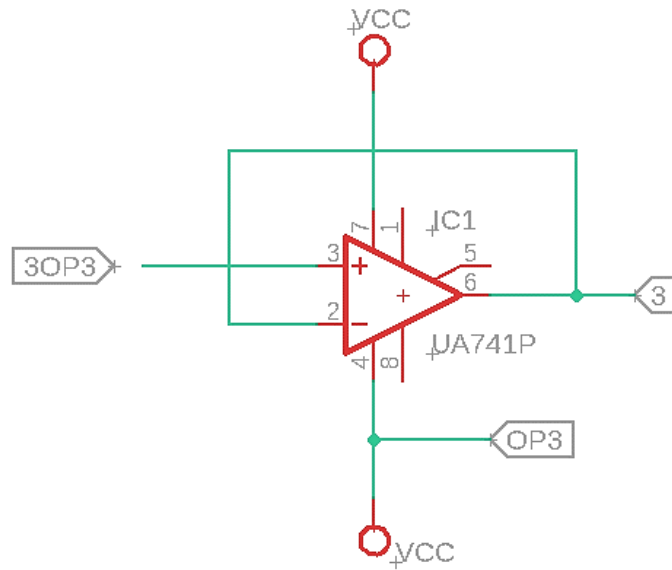


Figure 4.6: Notch or band-stop filter (Source prepared by the author)

### 4.1.3 Signal Digitization

Currently, there are several software that allow the development of the source code for the Arduino platform and, in this way, digitize the signal obtained by the AD620. This digitization will be done using the integrated development environment (IDE), which is a computer program composed of a set of programming tools that contains a code editor, a compiler, a debugger, and a graphical user interface builder or GUI (Voda, 2017).

The main advantages of this software are easy programming, free use, friendly compilation, and code-loading from any type of Arduino hardware, thus allowing real-time visualization of the executed code.

Before starting with the programming in Arduino, 3-lead electrodes will be used for data acquisition. These will be placed on the patient's chest where they will be responsible for taking the electrical information from the heart, and then it will be connected to the ECG module (AD620) in the RA, LA, and LL pins. Table 4.2 shows the PIN configuration of the AD620 module and Arduino UNO.



Table 4.2: PIN configuration of the AD620 and Arduino UNO module (source prepared by the author)

AD620 MODULE		ARDUINO UNO PIN
PIN	FUNCTION	
SDN	Shutdown control input	-
OUTPUT	Cardiac signal output (conditioned to connect to an ADC)	A0
3.3V	Supply voltage	3.3V
GND	Power supply to ground	GND

Figure 4.7 shows the setup () function; this function is executed at the start of each program only once and is used to configure the input pins (A0). The loop () function is also shown, which performs repetitive execution of the program all the time.

```

int ECG=A0;          //ECG Signal
int ECGsignal=0;    //Variable where the signal is saved

void setup() {
  Serial.begin(9600); //Serial communication
}

void loop() {
  ECGsignal=analogRead(ECG);
  Serial.print(ECGsignal);
  Serial.print(",");
  Serial.println(700);

  //If the signal peak exceeds 500 units
  if(ECGsignal>=500)
  {
    digitalWrite(12,HIGH);
    ECGsignal=analogRead(ECG);
    Serial.print(ECGsignal);
    Serial.println(900);
    delay(1000);
  }
  else
  {
    ECGsignal=analogRead(ECG);
    Serial.print(ECGsignal);
    Serial.print(",");
    Serial.print(700);
    digitalWrite(12,LOW);
  }
}

```

Figure 4.7:Startup the system in Arduino (Source prepared by the author)

After programming the microcontroller with the code shown in Figure 4.7, the raw ECG signal was obtained. Figures 4.8 and 4.9 show the ECG signals of two participants obtained from the ECG prototype.

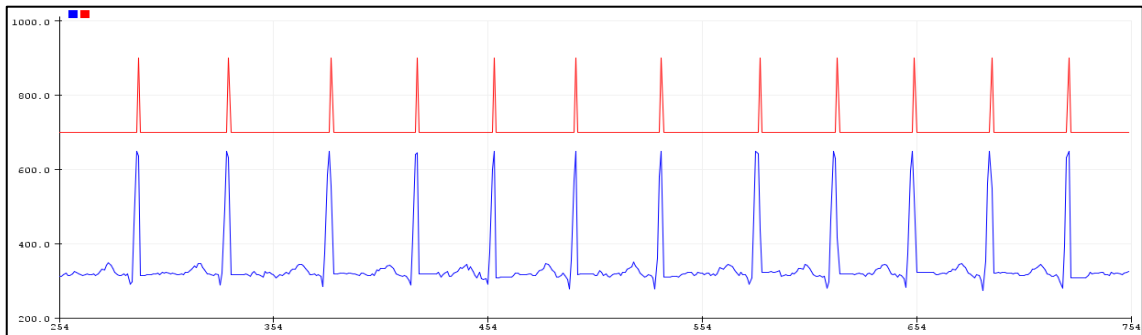


Figure 4.8: ECG signal. Sample subject ID 16 (Source prepared by the author)

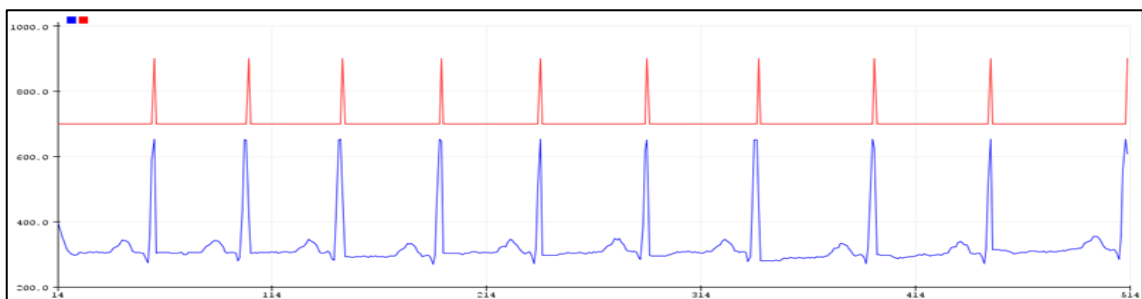


Figure 4.9: ECG signal. Sample subject ID 20 (Source prepared by the author)

#### 4.1.4 Signal Processing

ECG signals, after being acquired through the Arduino IDE, must be properly processed for analysis and interpretation. The ECG signals obtained are quasi-periodic waves that have a relatively low amplitude in the mV range. In some cases, additional processing had to be carried out for noise suppression.

Figure 4.10 shows the flowchart of the algorithm designed to open the acquisition data in .txt format. It will then be stored in a vector type variable to later be analysed and filtered, if necessary, to finally visualise the graph.

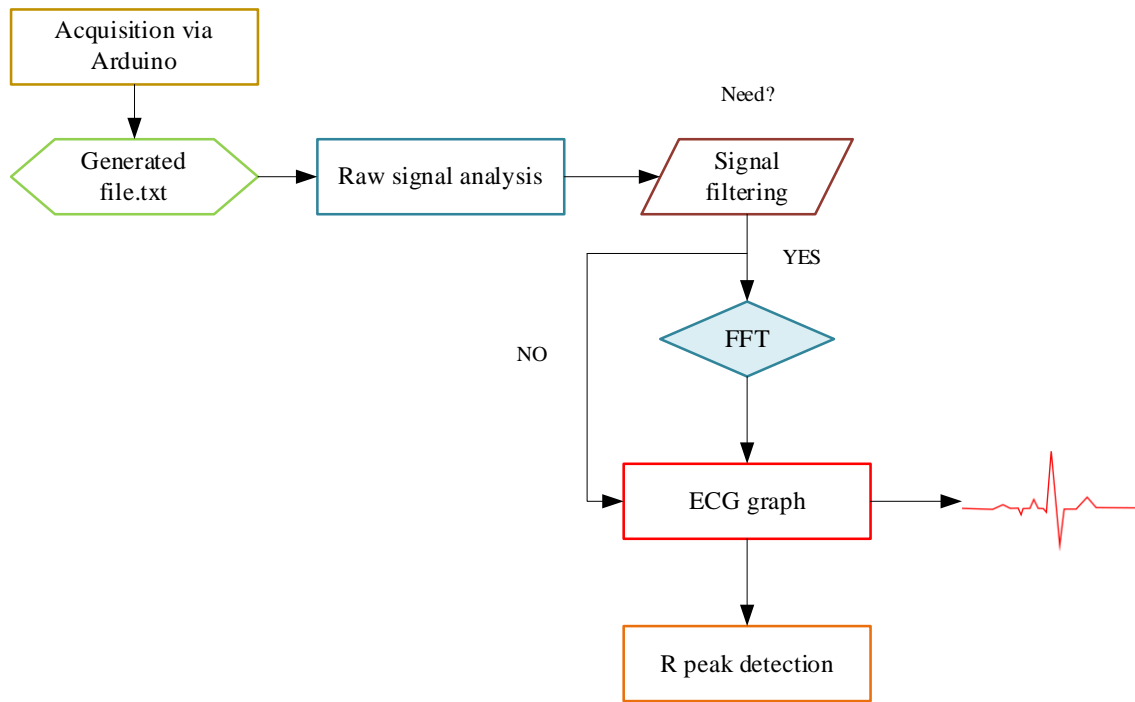


Figure 4.10: Flowchart for graphing the ECG signal (Source prepared by the author)

The signal analysis was performed with MATLAB, an IDE for numerical analysis programming and algorithm development used in engineering and science. According to the flowchart, the raw signal processing should be performed using the code shown in Figure 4.11. This code is divided into four phases: acquiring the signal, adjusting the amplitude, calculation of the sampling rate, and the calculation of the time vector.

The prototype of the ECG has a gain of 1000; in other words, for each integer value that the ECG vector has of 1000, it represents 1 mV at the physiological level. Also, to obtain the amplitude, the obtained signal is divided over the gain.

The sampling rate ( $F_s$ ) is 250 Hz, which means that for every second, 250 samples are taken on the signal; also, the sampling period ( $T_s$ ) is calculated as the inverse of the  $F_s$ . The  $T_s$  represents the distance between each sample, and it is represented in seconds.

To calculate the time vector, a vector like the raw ECG signal must be obtained, which will go from 1 to the length of the vector, then this vector will be multiplied by the  $T_s$  to obtain the X-axis in the variable of seconds. Likewise, these vectors are linear.

Finally, the signal will be centred at zero, this is calculated from the raw ECG signal to which the average of the entire signal is subtracted and then divided by the standard

deviation (Std) of the original signal to finally obtain the corrected signal. This corrected signal is shown in Figure 4.12.

```
%% ECG Signal Processing

clc;
close all;
clear;
ecg=load('id25.txt');
G=1000; %1mv
ecg_mv=ecg/G; %Amplitude

Fs=250; %(Hz)
Ts=1/Fs;
N=length(ecg);
vect=(1:1:N);
t=vect*Ts;

ecg_final = (ecg_mv - mean(ecg_mv))/std(ecg_mv);

figure;
plot(t,ecg_final);
ylabel('Amplitude [mV]');
xlabel('Time [s]');
xlim([0 4]);
title('ECG Signal without filter')
```

Figure 4.11: Code for raw signal analysis (Source prepared by the author)

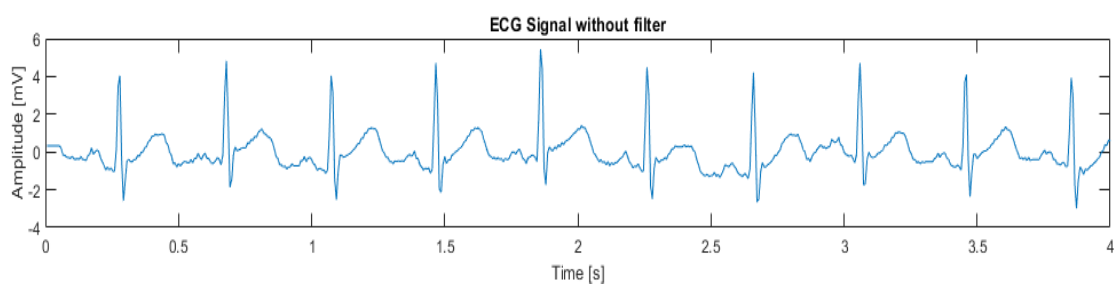


Figure 4.12: Corrected ECG signal without filter (Source prepared by the author)

Once the data has been previously processed, it must be analyzed according to the flowchart to determine whether the ECG signal should be filtered or not. This analysis relies heavily on quantifying the digitally recorded ECG waveform in the parameters of voltage, amplitude, and frequency.

In case the signal needs to be filtered, the Fourier transform was applied over that signal. The Fourier transform is a method that allows the transformation of the signal from the time domain to the frequency domain where we can see characteristics that are not appreciated in the time domain (Ulrich and Weber, 2017). Since the ECG signal is a discrete and physiological signal, Fast Fourier Transform (FFT) filtering was applied.

In the code shown in Figure 4.13, an arrangement of a mathematical expression with real and complex values is made through the abs function, where a real value is obtained, which is represented as the frequency domain of the signal. Then the vector of the signal must be cut halfway, for which the ceil function is needed, allowing for rounding up to the nearest integer.

Likewise, the frequency vector must have the same length as the Fourier transform, which is represented by the variable L. To create this frequency vector, which has a length of 1 to L, it was multiplied by the maximum frequency (Fmax), which is equal to the Fs divided by 2 (ELDAR, 2015).

```
%% Fourier Transform

F=fft(ecg_final);
F= abs(F);
F=F(1:ceil(end/2));
F= F/max(F);

L= length(F);
f=(1:1:L)*((Fs/2)/L);
figure;
plot(f,F)
xlabel ('Frequency [Hz]');
ylabel('Normalized Magnitude');
title('ECG in frequency');
```

Figure 4.13: Fourier Transform (Source prepared by the author)

After applying the Fourier transform, the upper and lower limit of the band-reject filter must be determined. Then the finite impulse response filter (FIR) was created, where the coefficient a is equal to 1, and the coefficient b is given by the variable fir1. Then the frequencies of the upper and lower limits are normalized by dividing them over the Fmax.

Those values are used in coefficient b. To filter the signal, the `filtfilt` function is used, which allows an adjustment in the phase. The code used is shown in figure 4.14.

```
%Frequency Normalization
limi_n=limi/(Fs/2);
lims_n=lims/(Fs/2);

%Create filter
a=1;
b=fir1(orden,[limi_n lims_n],'stop');

%Filtered signal
ecg_limpio = filtfilt(b,a,ecg_final);
figure;
plot(t,ecg_limpio);
xlim([0 4]);
```

Figure 4.14: FIR filter and Frequency Normalization (Source prepared by the author)

Figure 4.15 shows the pre-processed signal and the filtered signal as well as the ECG signal in frequency, before and after filtering. To carry out the verification of the generated filter, the function `freqz(b, a)` is used, where the attenuation of the filter and its phase are displayed, which is shown in figure 4.16.

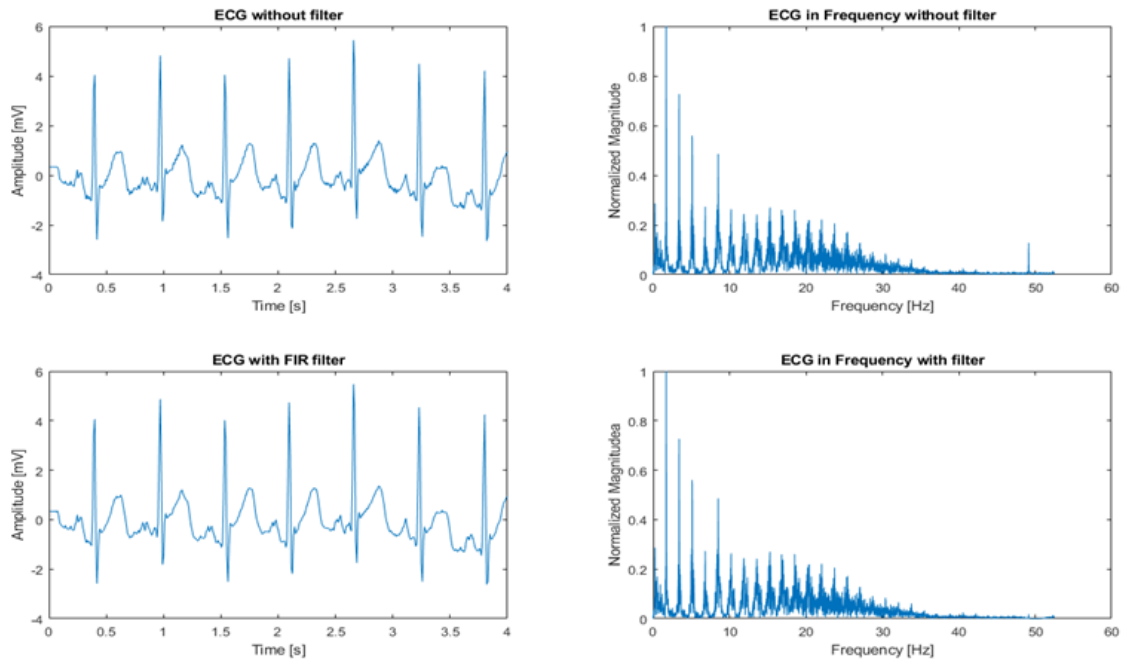


Figure 4.15: ECG Signal without and with filter (Source prepared by the author)

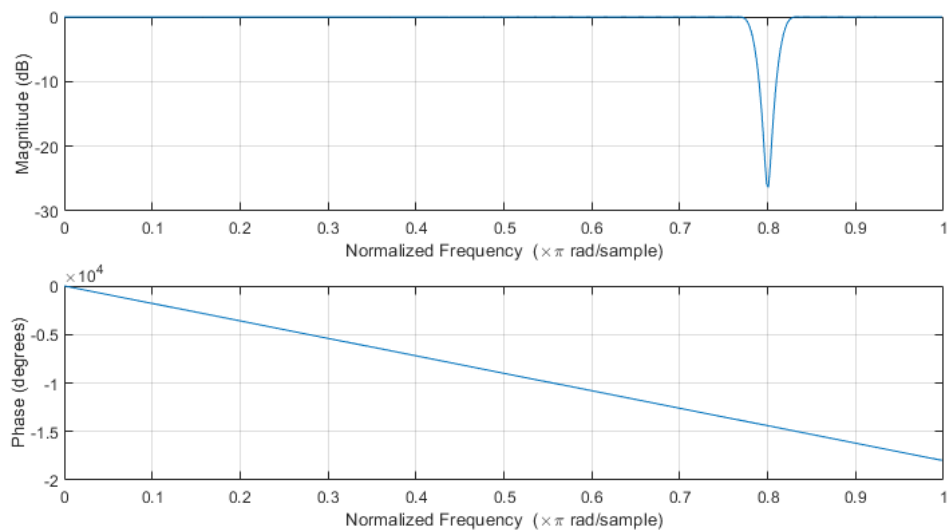


Figure 4.16: Verification of the generated filter (Source prepared by the author)

The locations of the R peaks can be obtained from the processed ECG signal. Due to its characteristic shape, the QRS complex is the prominent part of an ECG wave. For this reason, the detection of these peaks is taken as a starting point for different ECG analysis algorithms for subsequent clinical review. For the analysis of the R peaks, the code shown in figure 4.17 is used. The algorithm is going to look for the locations within the sample,

and then it is going to plot and locate the R peak according to time. To locate only the R peaks within the ECG wave, the threshold variables on the X- and Y-axes were used.

The threshold for the Y-axis is calculated as six times the average of the absolute value of the ECG signal. Then the threshold X is calculated as 60/300 beats per minute, which is equal to 0.2 seconds, then multiplied by the Fs. The threshold X allows to calculate the minimum distance between the peaks R, and the threshold Y shows the location of these peaks. Figure 4.18 shows the processed ECG signal and the R peak detection.

```

%% R Peak Detection
ecg1=ecg_limpio;
figure;
hold on;
plot(t, ecg1);
xlabel('Time [s]');
ylabel('Magnitude [mV]');
xlim([0 4]);
title('R peak detection');

%Threshold
umbral_y=6*mean(abs(ecg1));
umbral_x=0.2*Fs;

%findpeaks
[pks,locs]=findpeaks(ecg1,'MinPeakHeight',umbral_y, ...
    'MinPeakDistance',umbral_x);
scatter(t(locs),pks)

```

Figure 4.17: Algorithm to detect the R peak (Source prepared by the author)

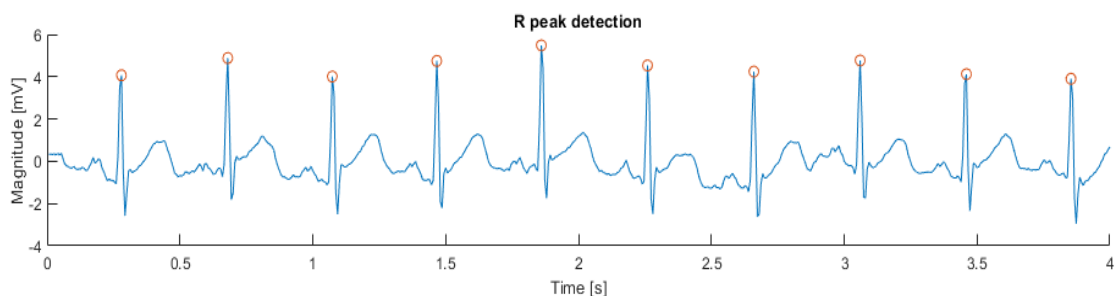


Figure 4.18: R peak detection signal (Source prepared by the author)



## 4.2 Prototype of the mobile application

Once the electronics of the ECG prototype had been defined, an application needed to be developed to be able to visualize the acquired data. Within the market, there are two systems, the iOS created by Apple and the Android system created by Google.

Within the iOS group, the offer of mobile phones and tablets is very limited; Furthermore, it is impossible to develop a high-quality application for these devices without making a considerable financial outlay, which is not feasible.

In contrast, there are multiple options from manufacturers that present devices with the Android system; it is also extremely simple and almost cost-free to develop an application on this system. All you need to do is download and install the Android Software Development Kit (Android SDK), which is public and accessible at no cost. Additionally, a version of the IDE prepared for Android devices is also available from the developer's website. It is also possible to debug the application on a real device through the IDE.

Building the application has been an extensive and tedious process. Even so, there are some aspects of the implementation that should receive attention due to the specificity of the result. Among these is the creation of a stable and strong Bluetooth system and a simple interface for the final user.

### 4.2.1 Bluetooth Data Acquisition

In Chapter 4.1, the conversion of the analog signal obtained by our ECG prototype is explained. Every time this signal is obtained, it is necessary to send it by Bluetooth to the mobile application, where it is graphed and analyzed. According to Usama bin Aftab (2017), Bluetooth communication is carried out through radiofrequency waves of 2.4 GHz. Advantages of Bluetooth connectivity over Wi-Fi include being universal to all smart devices, constant availability, and bearing no additional cost to users.

The module used is the HC-05 which is connected to the Arduino UNO, as shown in Figure 4.19. This module or "serial port" is responsible for sending and receiving data serially to a peripheral device. The data is received through the RX buffer, and the

information is transmitted through the TX buffer to the registration software that presents the module.

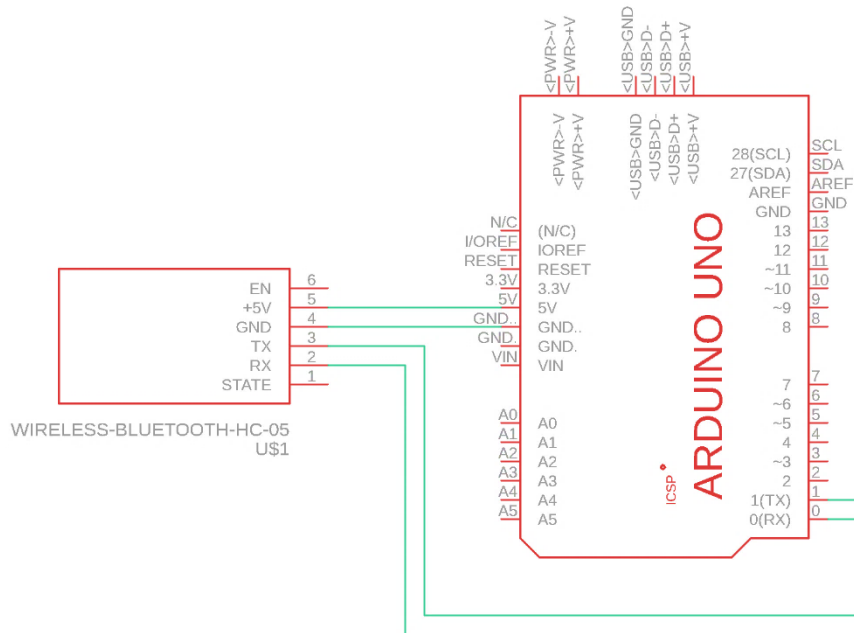


Figure 4.19: Module HC-05 and Arduino UNO schema (Source prepared by the author)

To acquire the data sent by the HC-05 Bluetooth module that contains the ECG prototype, the application must perform a scan of the available devices to link to them, starting the connection process. To link both devices (module - mobile), the password requested is "1234". Finally, both devices are paired.

The red LED on the HC-05 module flashes continuously when it is available to initiate a connection. When the devices are connected, the LED flashes/blinks and stays off for 3 seconds and then flashes/blinks again, repeating this action consecutively.

Once the connection is finished, the application begins to receive the signal sent by the Bluetooth module.

The most important aspect of serial port communication between the microcontroller and the HC-05 module is the baud rate. This refers to the rate of transmitting binary code symbols per second over a serial port. The reverse of this rate is the period for which a symbol remains available for transmission. The default baud rate is 9600 bits per second.

As mentioned by Usama bin Aftab (2017), when a byte of information is sent, 10 bits and not 8 bits are actually sent because 1 bit represents START, 1 bit represents STOP, and 8 bits correspond to information. This implies that the number of data transmitted per second according to the selected baud rate is calculated with equation 4 (Ward, 2022).

$$\text{Bytes per second} = \frac{\text{Bits per second}}{10} = \frac{9600}{10} = 960 \quad (4)$$

To calculate the transmission time of each byte is the reverse, which is expressed in equation number 5 (Ward, 2022):

$$\text{One - byte transmission time} = \frac{1}{\text{Bytes per second}} = \frac{1}{960} \approx 1.042 \text{ ms} \quad (5)$$

The time of 1,042ms represents the time needed to transmit the reading from the HC-05 module to the smart device. On the other hand, it is necessary that the baud rate of the HC-05 module and device are the same; for this, it is necessary to determine the real baud rate, which is calculated from equation 6 (Ward, 2022).

$$\text{Real Baud Rate} = \frac{F_{osc}}{16(n + 1)} = \frac{4\text{MHz}}{16(25 + 1)} \approx 9615.38 \text{ baud} \quad (6)$$

$F_{osc}$  represents the oscillation frequency; in other words, it is the clock that controls the execution of the instructions. This value is 4MHz.  $n$  represents the value of the transmission rate. For the baud rate of 9600 baud, the value of  $n$  is 25. With respect to equation 6, the real baud rate is 9615.38 baud. Also, the calculation of the absolute error is given with equation 7 (Ward, 2022).

$$\begin{aligned}
 \text{Error} &= \frac{\text{Real Baud Rate} - \text{Used Baud Rate}}{\text{Used Baud Rate}} \cdot 100\% \\
 &= \frac{9615.38 - 9600}{9600} \cdot 100\% = 0.16\%
 \end{aligned}
 \tag{7}$$

To configure the parameters of the HC-05 module with the Arduino UNO microcontroller, the code shown in Figure 4.20 was executed.

```

#include <SoftwareSerial.h>
#define rxPin2
#define txPin3
#define baudrate 9600
String msg;
SoftwareSerial hc05 (rxPin, txPin);

void setup() {
  pinMode (rxPin, INPUT);
  pinMode (txPin, OUTPUT);
  Serial.begin(9600);
  Serial.println("Enter at commands:");
  hc5.begin(baudrate);
}

void loop() {
  readSerialPort();
  if(msg!="")hc05.println(msg);
  if(hc5.available()>0){
    Serial.write(hc05.read());
  }
}

void readSerialPort(){
  msg="";
  while(Serial.available()){
    delay(10);
    if(Serial.available()>0){
      char c = Serial.read();
      msg +=c;
    }
  }
}

```

Figure 4.20: HC-05 connection algorithm (Source prepared by the author)

After correctly configuring the HC-05 module, the communication between the module and the smartphone was tested. To perform the pairing, the device must be

searched from the smartphone, then the system will ask for the password, which is "1234". After providing the password, the user must see that the LED of the HC-05 module flashes every 2 seconds.

## 4.2.2 Application Structure and User Interface

During the design and implementation of the application structure, the Android Studio design guides have been followed to create a modern and functional application. For the creation of modular interfaces, interactive menus called fragments were applied. The creation of these menus was done by using the `NavigationUI` class. To represent the ECG signal in real time, an implementation was created from the `View` class.

Graphical interfaces or layouts in Android Studio are defined in XML files and are displayed by the running application or created dynamically using code.

### 4.2.2.1 Fragment

Fragment is a specific class to Android development libraries. It represents a graphical interface section that can be reused throughout different application activities. Fragments are useful when the developer wants to create an app that addresses devices with panels of different sizes.

The main reason why fragment objects have been used in this application has been the integration of a `NavigationUI`, which are hidden menus that allow navigating between different functionalities of the application.

The application structure presents a simple hierarchy, which has `Main_Activity` as the main fragment where the following fragments will be stored. These stored fragments are `Instructions_Fragment`, `Bluetooth_Manager`, `ECG_Signal_Fragment`, and the `About_Fragment`. In figure 4.21, the application structure is graphically shown.

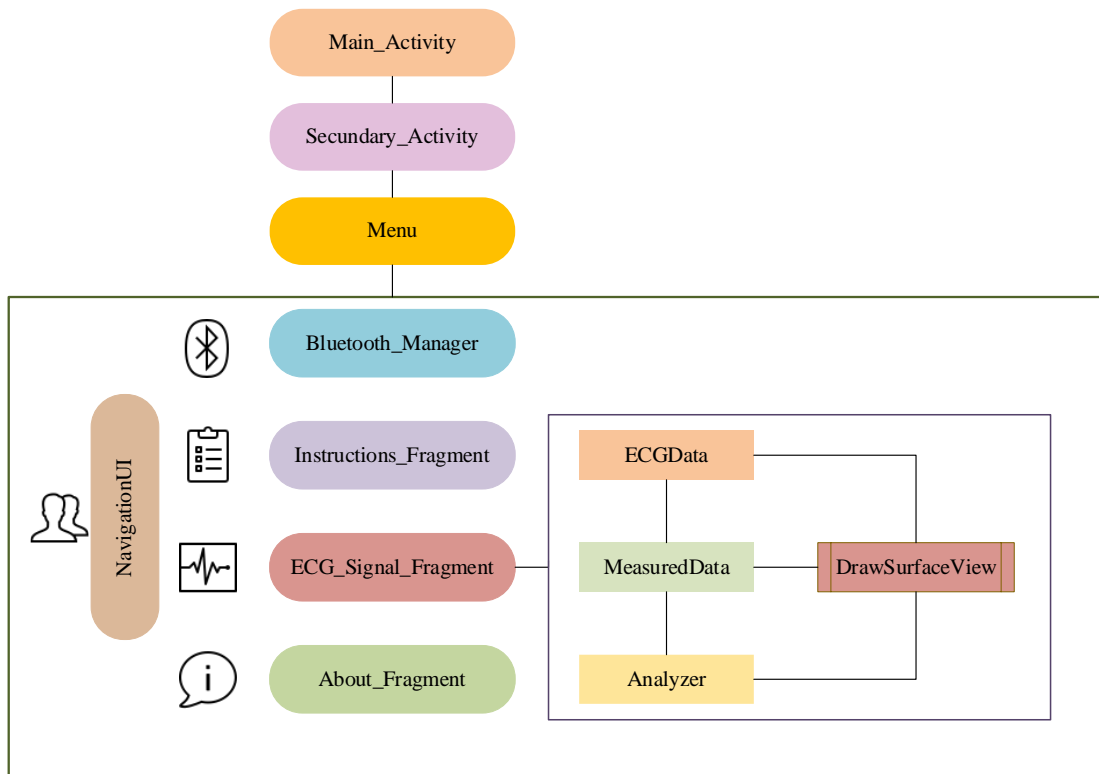


Figure 4.21: Application Structure (Source prepared by the author)

#### 4.2.2.2 Main Activity

In section 4.2.2.1 it is mentioned that the main activity is divided into four fragments. According to the menu settings, the `Instructions_Fragment` is presented as the main startup view. The main activity toolbar is configured through `activity_main.xml`, in which the design, size, color, and display of the options are configured.

To start the application, press the `START` button (as shown in fig. 4.22), which is programmed according to the following code:

```
@Override
protected void onCreate (Bundle savedInstanceState) {
    super.onCreate(savedInstanceState);
    setContentView(R.layout.activity_main);
    Button button = findViewById(R.id.btn);
    button.setOnClickListener(new View.OnClickListener() {
```

```

@Override
    public void onClick(View v) {
        Intent intent = new Intent(MainActivity.this,
MainActivity2.class);
        startActivity(intent);
    }
});
}
}
}

```

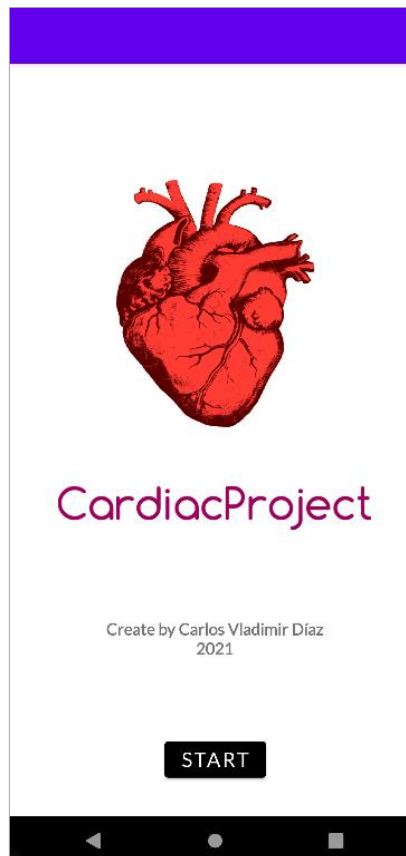


Figure 4.22: Main window layout (Source prepared by the author)

In the case of the implementation of the menu layout, the `NavigationView` option is used, which is designed in the `activity_main_drawer.xml` file. To create the design of the fragments, the following code is used:

```

DrawerLayout drawer = binding.drawerLayout;
NavigationView navigationView = binding.navView;
mAppBarConfiguration = new AppBarConfiguration.Builder(
    R.id.nav_instructions, R.id.nav_ecg, R.id.nav_about)
    .setOpenableLayout(drawer)

```

```

        .build();
        NavController navController =
Navigation.findNavController(this,
R.id.nav_host_fragment_content_main);
        NavigationUI.setupActionBarWithNavController(this,
navController, mAppBarConfiguration);
        NavigationUI.setupWithNavController(navigationView,
navController);
    }

```

The figure 4.23 shows the main activity layout, which shows the toolbar that the user will use to navigate over the application.

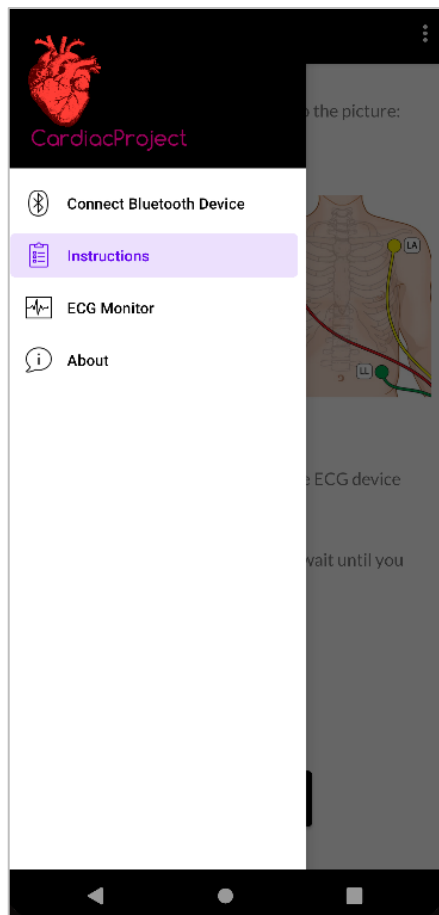


Figure 4.23: Main activity layout (Source prepared by the author)



### 4.2.2.3 Instructions Fragment

To start the study and use of the application, the user must enable the Bluetooth of the smartphone through the application to detect the signal of the ECG prototype. Once the pairing – or linking has been completed, the instructions in the `Instructions_Fragment` must be followed.

Depending on the version of Android that the smart device has, it is necessary for the user to provide the permissions previously. These permissions are declared in a file that contains the essential information of the application. In current versions of Android, the user can decline these permissions at any time. However, in versions prior to Android 6.0 (Marshmallow), this option is explicit.

This fragment shows, by default, the instructions on how to use the application. Contains a text box represented by a `TextView` class and a button, which pressed takes us directly to `ECG_Signal_Fragment`. Figure 4.24 shows the layout of this fragment.

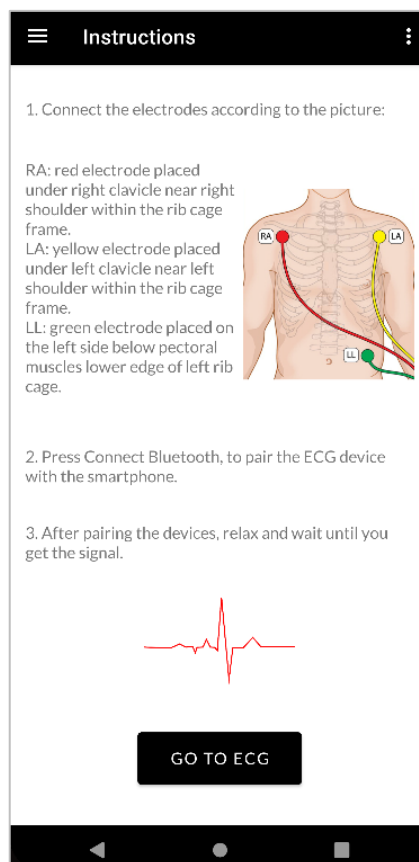


Figure 4.24: Instructions\_Fragment layout (Source prepared by the author)

#### 4.2.2.4 Bluetooth Manager

Bluetooth technology is considered one of the most secure and reliable wireless connections, so its configuration is tedious. The pairing between the ECG prototype and the mobile application is handled by the `bluetoothManager` class. First, the connection must be configured through the Bluetooth address. The code used is as follows:

```
public class bluetoothManager extends BroadcastReceiver {
    public final String btAdress = "00:21:13:01:28:FE";
    public bluetoothManager(android.os.Handler handler) {
        uiRefreshHandler = handler; }

    public void enableBluetooth(boolean startDiscovery) {
        if(!myBtAdapter.isEnabled()) {
            myBtAdapter.enable();
        }
        if(startDiscovery)
            myBtAdapter.startDiscovery();
    }

    public void disableBluetooth() {
        if (myBtAdapter.isEnabled()) {
            myBtAdapter.disable();
        }
    }
}
```

After configuring the Bluetooth address, the configuration of the reception of the information coming from the ECG prototype must be carried out. To do this, the `BroadcastReceiver` subclass is created, which controls each broadcast received. The code used is shown below:

```
public class bluetoothReceiver extends BroadcastReceiver {
    @Override
    public void onReceive(Context context, Intent intent) {
        String action = intent.getAction();
        String targetName = "HC-05";
```

```

        if (BluetoothDevice.ACTION_FOUND.equals(action)) {
            BluetoothDevice currentDevice =
intent.getParcelableExtra (BluetoothDevice.EXTRA_DEVICE);
            if
(currentDevice.getAddress().equalsIgnoreCase(btAddress)) {
                myBtDevice =
myBtAdapter.getRemoteDevice(btAddress);
                Toast.makeText(context, "DEVICE FOUND:" +
myBtDevice.getName(), Toast.LENGTH_LONG).show();
                CONNECT_STATE = true;
                myBtClientThread = new clientThread();
                myBtClientThread.start();
            }
        } else if
(BluetoothAdapter.ACTION_DISCOVERY_FINISHED.equals(action)) {
            if (!isConnected()) {
                Toast.makeText(context, "DEVICE NOT FOUND",
Toast.LENGTH_LONG).show();
            }
        } else if
(BluetoothAdapter.ACTION_DISCOVERY_STARTED.equals(action)) {
            Toast.makeText(context, "START
SEARCHING", Toast.LENGTH_LONG).show();
        } else if
(BluetoothDevice.ACTION_ACL_DISCONNECTED.equals(action)) {
            CONNECT_STATE = false;
            Toast.makeText(context, "DEVICE DISCONNECTED, TRY TO
RECONNECT", Toast.LENGTH_LONG).show();
            Message uiRefreshMessage = Message.obtain();
            uiRefreshMessage.what=1;
            uiRefreshHandler.sendMessage(uiRefreshMessage);
        }
    }
}

```

As shown in the code above, the `BluetoothDevice` class allows the HC-05 Bluetooth device presented by the ECG prototype to be created. This link is provided by the `onReceive` method, which finds the device remotely, and with the `Thread` subclass

several threads are executed within the Java virtual machine. All of this are used for signal processing.

#### 4.2.2.5 ECG Signal Fragment

This fragment covers the treatment of the ECG signal and its visualization through the `DrawSurfaceView`. Figure 4.25 shows the fragment's operating diagram, which is made up of 4 classes: `ECGData`, `MeasuredData`, `Analyzer`, and the `DrawSurfaceView`.

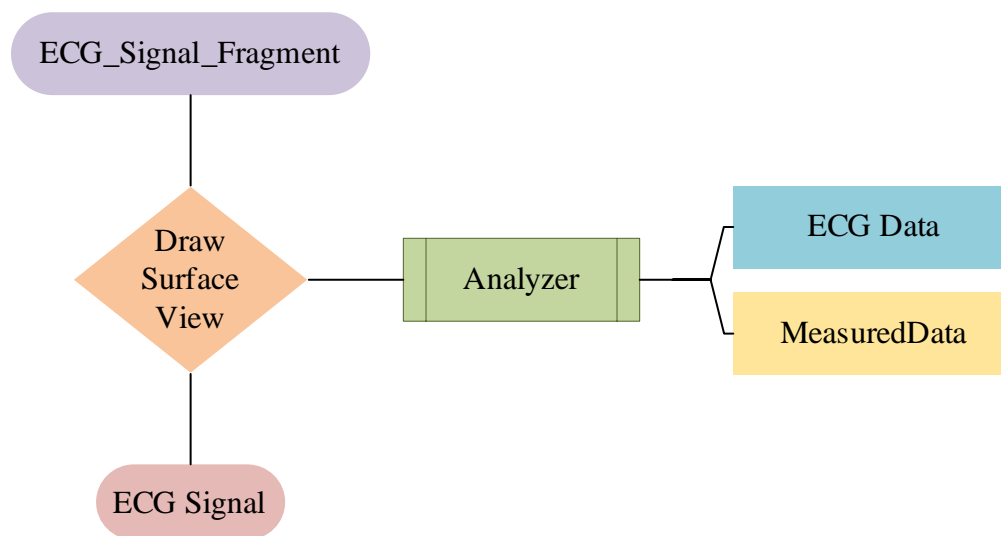


Figure 4.25: Diagram of ECG Signal Fragment (Source prepared by the author)

The `ECGData` class records the signal measurement time through the `recordTime` subclass. Through the `RECORDRATE` subclass, the frequency is recorded. To better understand this action, the code used is as follows:

```
public class ECGData extends MeasuredData{
    private double recordTime = 0.000;
    private int dataId;
    private static double RECORDRATE = 1.0/500.0;

    public ECGData (int data, int dataId) {
        super("ECG", data);
    }
}
```

```

        this.dataId = dataId;
        recordTime = (double) dataId * RECORDRATE;
    }
    public double getRecordTime() {
        return recordTime;
    }
    public int getDataId() {
        return dataId;
    }
    public static void setRecordRate (double hertz) {
        RECORDRATE = 1.0/hertz;
    }
}

```

The **MeasuredData** class measures the signal values stored in the **ECGData** class and return that value to be analysed in the next following class. The code used is the following:

```

public class MeasuredData {
    private String typeName;
    private int value;

    public MeasuredData(String typeName, int value) {
        super();
        this.typeName = typeName;
        this.value = value;
    }
    public String getTypeName() {
        return typeName;
    }
    public String getValueInString() {
        return String.valueOf(value);
    }
    public int getValueInInt() {
        return value;
    }
}

```

To perform the signal analysis, the code made by Ji (2018) was used, which is stored in the **Analyzer** class. The code performs automatic detections of the R peaks, heart rate, and the duration of the ECG signal. The algorithm features a cyclic control structure,

which captures the maximum R peak through each cardiac cycle. It also has a conditional control structure according to the amplitude of the waves. For a better understanding of the process, part of the code used is shown:

```

for (cnt = 0; cnt < 80; cnt++) {
    dataAvgValue += dataTemp[cnt].getData();
    if (rpeakLocalMax.getData() < dataTemp[cnt].getData()) {
        rpeakLocalMax = dataTemp[cnt];
    }
}
dataAvgValue = dataAvgValue / 80;

if (ifFirstRpeakDetected) {
    if ((Math.abs((rpeakMaxTemp.getData() - lastAvgValue) /
        (rpeakLocalMax.getData() - dataAvgValue) - 1) < 0.5)
        &&
        ((rpeakLocalMax.getDataId() - rpeakMaxTemp.getDataId()) >
60)) {
        rpeakMaxTemp = rpeakLocalMax;
        lastAvgValue = dataAvgValue;
        Log.v("hit", Double.toString(rpeakMaxTemp.getData()));
        rpeaksHandling(rpeakMaxTemp);
    }
} else {
    if (rpeakMaxTemp.getData() < rpeakLocalMax.getData()) {
        rpeakMaxTemp = rpeakLocalMax;
        lastAvgValue = dataAvgValue;
    }
    if ((dataTemp[0].getDataId() > 200) && ((rpeakMaxTemp.getData() /
Math.abs(dataAvgValue)) > 1.1)) {
        Log.v("get first", Double.toString(rpeakMaxTemp.getData()));
        ifFirstRpeakDetected = true;
        lastRpeak = rpeakMaxTemp;
    }
}
}

```

Finally, with the use of the `DrawSurfaceView` class, the signal is displayed and shows the value of the heart rate. Figure 4.26 shows the layout of the

`ECG_Signal_fragment`, which is made up of a display window, a box of buttons with options, and the main button.



Figure 4.26: ECG\_Signal\_fragment layout (Source prepared by the author)

#### 4.2.2.6 About Fragment

This fragment is the last element of the user interface, here the contact information and the purpose of the application are displayed. This fragment contains a text box represented by the `TextView` class.

For XML layout and text modification, the following code has been used:

```
<FrameLayout xmlns:android="http://schemas.android.com/apk/res/android"
    xmlns:tools="http://schemas.android.com/tools"
    android:layout_width="match_parent"
```

```

android:layout_height="match_parent"
tools:context=".About">
<TextView
    android:layout_width="match_parent"
    android:layout_height="match_parent"
    android:text="..."
    android:textDirection="firstStrongRtl"
    android:textSize="16sp"/>
</FrameLayout>

```

The layout of `About_Fragment` is shown in figure 4.27.

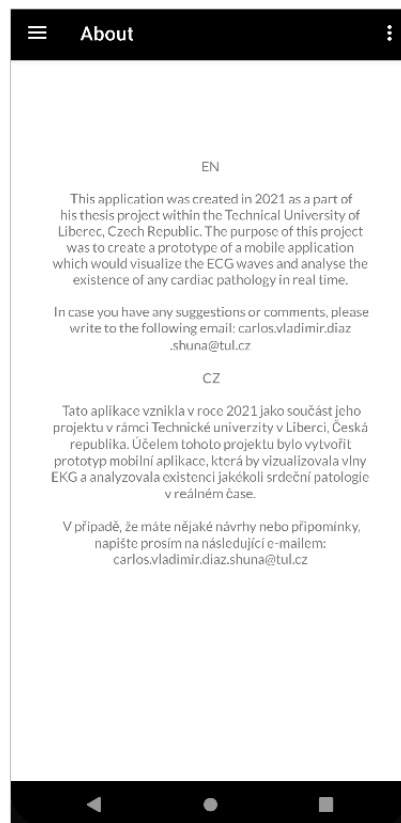


Figure 4.27: `About_Fragment` layout (Source prepared by the author)

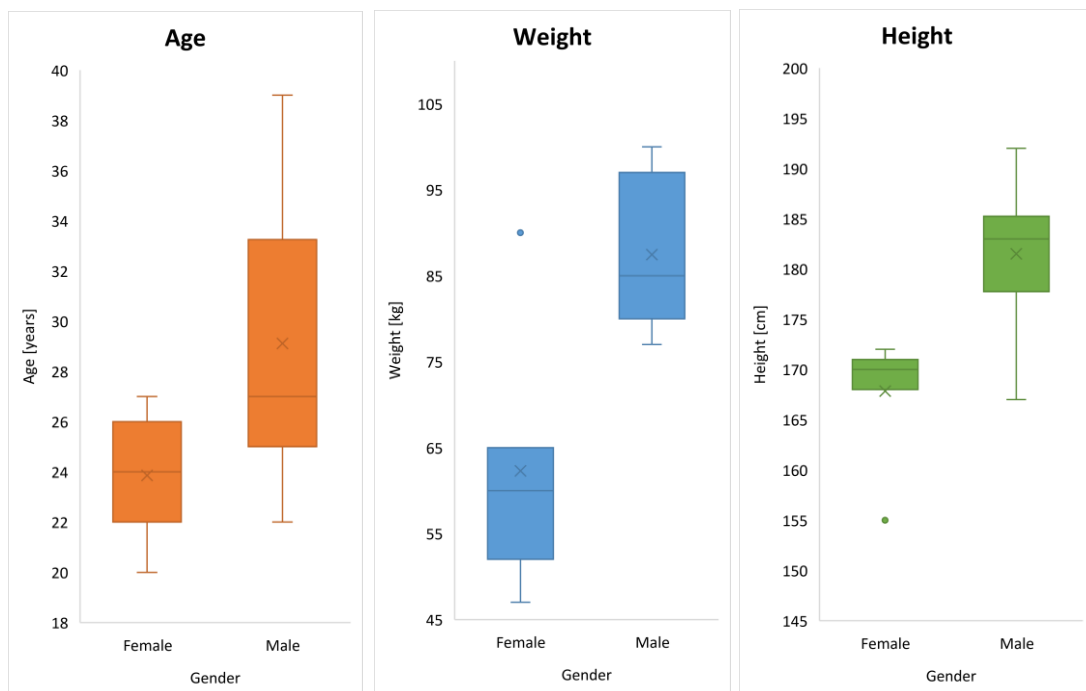


### 4.3 Measurement and data analysis

After explaining the implementation of the ECG prototype (see chapter 4.1), technical tests were carried out, and finally, ECG signal were measured in 25 participants who participated voluntarily.

The study consisted of two parts; in the first part, a questionnaire was carried out, in which personal data of the participant were asked, as well as a history of previous pathologies (see appendix B).

The selection criteria of the participants cover: age range, which is between 18 to 40 years, the weight, between 45 to 100 kg., and the height, between 145 to 210cm. Graph 4.1 shows the maximum, minimum, and mean values of the ranges of each selection criteria compared to the gender of the participant.



Graph 4.1: Ranges of each selection criteria vs gender. (Source prepared by the author)

The second part of the study was developed as follows; the participant was asked to remove any metallic objects (necklaces, chains) and electronic devices (mobiles, watches, and others) due to the appearance of artefacts in the signal. The participant was asked to

remove any clothing covering the chest. The electrode placement areas were cleaned to have an improvement in the adhesion of the electrodes and obtain a high-quality ECG signal. The electrodes were placed two centimetres below the right and left clavicles (clavicular fossa) and at the lower left costal edge, thus forming Einthoven's triangle (see chapter 2.2.2.2). Likewise, the 3 leads were determined as follow: lead I: RA – LA, lead II: RA – LL, and lead III: LA – LL. The ECG signal displayed is determined by the lead I (electrodes in position RA and LA), in the case of electrode LL was used to ground the terminal (see figure 4.28 and figure 4.29). The electrodes were then connected to the ECG prototype (see figure 4.30). The ECG signal was captured from each participant, and then the signal processing was performed (see chapter 4.1.4).

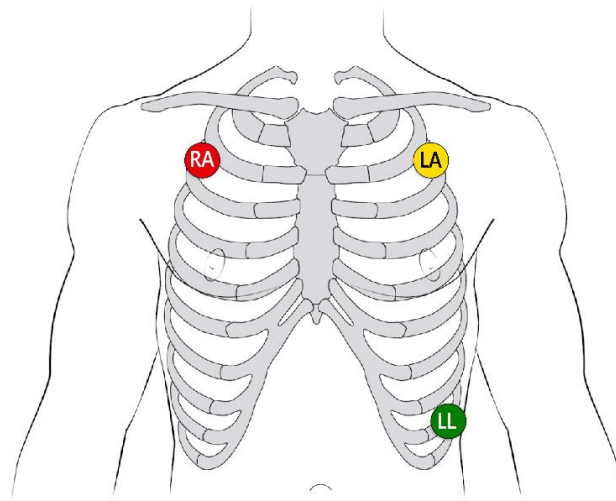


Figure 4.28: 3-lead electrode placement (Source taken from <https://litfl.com/ecg-lead-positioning/>)



Figure 4.29: 3-lead electrode placement in a participant. (Source prepared by the author)

The measurement data obtained were subsequently exported for processing to the MATLAB environment. The chosen  $F_s$  is 150Hz, in other words, for every second, 150 samples are taken from the signal. A lower frequency was not chosen, due to the phenomenon of aliasing, to wit, a possible distortion, and loss of information in the signal (see chapter 4.14).

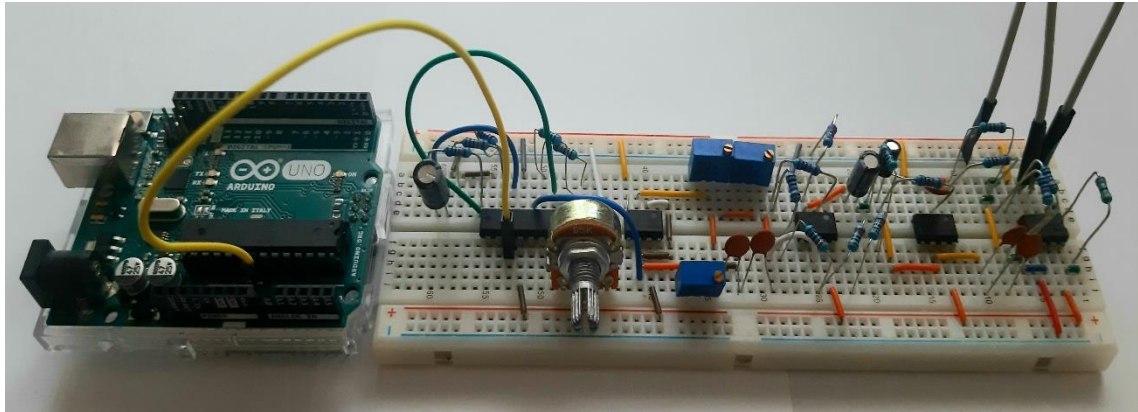


Figure 4.30: ECG prototype (Source prepared by the author)

Figure 4.31 shows the ECG signal, where the approximate amplitude of  $\pm 5\text{mV}$  peak to peak is displayed on the horizontal axis, and the cardiac period is displayed on the vertical axis, which is  $\pm 0.8$  seconds. Both magnitudes are physiologically acceptable (see chapter 2.2.2.1).

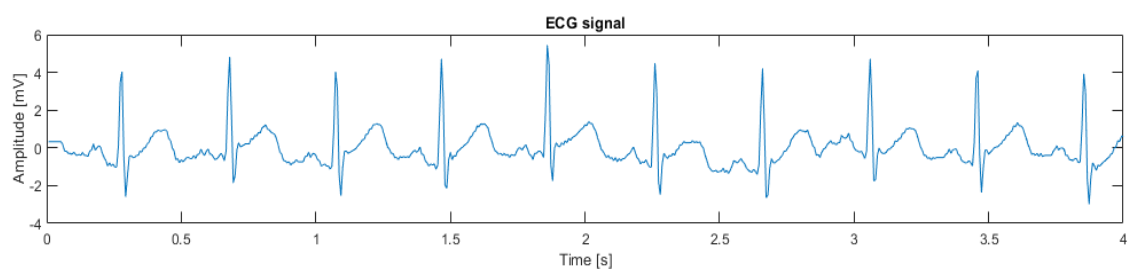


Figure 4.31: ECG signal (Source prepared by the author)

Figure 4.32 shows the spectral component of the signal, which must be in the range of 0.7 to 100 Hz. This spectral component is important for the analysis of the variance distribution of a signal as a function of frequency and thus being able to identify the most important frequency components (see Chapter 4.1.4).

The spectral component can also visualise possible interferences, which can corrupt the ECG signal and lead to misdiagnosis. There is a particular frequency component, which consists of environmental interference, which must be attenuated in the ECG signal; this frequency is 50 Hz and comes from the electromagnetic induction of the power line. For this reason, all acquired ECG signals were filtered (see Chapter 4.1.2.3). However, during the study, spectral components approximately in the range of 45 to 55Hz were captured.

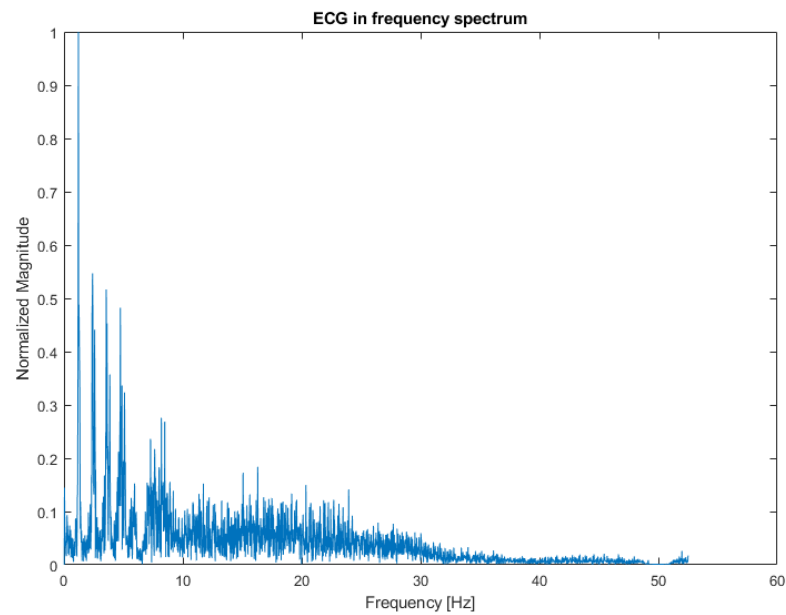


Figure 4.32: Spectral component of the ECG signal (Source prepared by the author)

Finally, figure 4.33 shows the detection of the R peaks, and the duration of the R-R interval is calculated. This detection is important for verifying the heart rate variability due to the predictive factor of cardiovascular diseases that the individual could present.

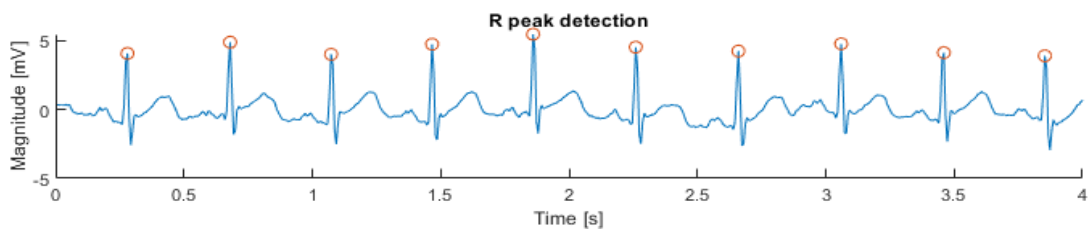


Figure 4.33: R peak detection (Source prepared by the author)

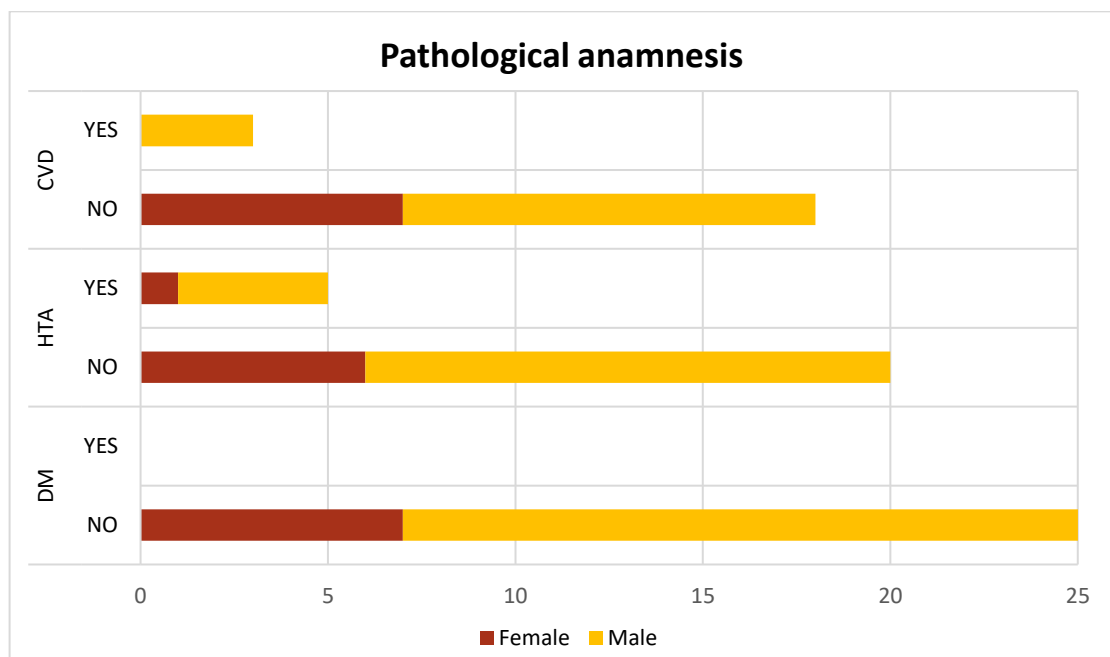
The duration time for the measurement of the ECG signal was 5 minutes, of which only the first 4 seconds are shown for educational and practical purposes. The processing of each participant's ECG signals can be visualized in Appendix C.

#### **4.3.1 Limitations**

There were several factors that limited the study, mainly due to the SARS-CoV-2 virus (COVID-19) pandemic. For this reason, the search for participants and the respective measurements were delayed since the country was in a state of a health emergency. In addition to this, it was necessary to preserve the health of both sides, the participants and the responsible of the study; for this reason, it was advisable to carry out rapid tests to avoid any mishap.

## 5 Discussion

For the elaboration of the tests of this project, 25 participants, of which 18 were men (72%) and 7 were women (28%), underwent an ECG measurement. Likewise, this data collection was carried out voluntarily, where 0% of the participants declared to have diabetes mellitus, 5 (20%) declared suffering from arterial hypertension, and 3 (12%) suffered from some heart disease, which can be seen in Graph 5.1.



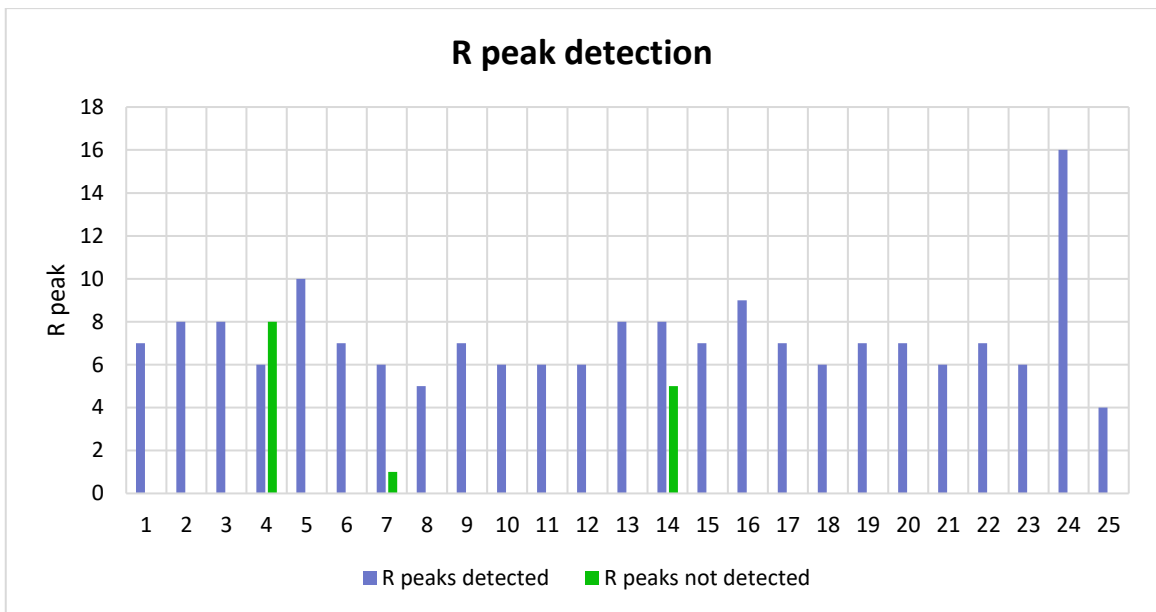
Graph 5.1: Pathological anamnesis vs. gender (Source prepared by the author)

In the tests that were carried out, certain very significant aspects can be observed. First, the production of the antenna effect is observed, which is produced on the electrodes and the connection cables. This effect could be reduced by placing the ECG prototype inside an insulating box. The amplitude and duration of the waves and segments of the ECG signal obtained were also measured to corroborate with the standard ECG signal.

The application of FFT, as a simple digital filter using digital processing in MATLAB, was also evaluated. This filter achieves the rejection of the 50 Hz frequency and its harmonic component. However, peaks at the 55 Hz frequency were observed at times during the test. By performing the filtering at this frequency, the noise was

eliminated from the entire signal, which makes us consider some interference during the measurement.

Likewise, an algorithm was used for the detection of QRS complexes or R peaks. It is observed that in almost all tests, the algorithm works with 100% efficiency. Only in two cases is the detection error greater than 30%. This is due to some cardiovascular pathology presented in sample 4 and, in the case of sample 14, a very variant potential is observed although the QRS complex is maintained. Graph 5.2 shows the difference between the detected and undetected R peaks of each participant.



Graph 5.2: R peak detection of each participant (Source prepared by the author)

The total detection efficiency of R peaks is 92.8%, and the detection error is 7.2%, resulting in less than 10%, which is mentioned in the project proposal. Formulas 8 and 9 respectively were used to calculate efficacy and error.

$$Efficacy = \frac{R_{detected}}{R_{total}} \cdot 100\% = \frac{180}{194} \cdot 100\% = 92.8\% \quad (8)$$

$$Error = \frac{|R_{detected} - R_{total}|}{R_{total}} \cdot 100\% = \frac{|180 - 194|}{194} \cdot 100\% = 7.2\% \quad (9)$$

Among the limitations of the prototype, a decrease in wireless transmission via Bluetooth from 960 to 910 bps is shown. This speed is ,nonetheless sufficient. Some defects were also found in the mobile application regarding the graph of the ECG signal.



## 6 Conclusion

During the development of the thesis, an ECG prototype, and an application where the obtained signal is displayed have been created. The experimental part of the thesis has been divided into three phases, which have been developed in parallel.

The first phase is composed of the electronics used for the elaboration of the ECG prototype. This phase involved basic knowledge and systems outside the scope of the study, thus requiring extensive external research and development. The points included in this phase are the analog electronics and the filtering of ECGs.

ECG signals are susceptible to noise and interference from sources both outside and inside the circuit. The fact that these signals are small motivated the creation of an amplifier, which allowed the ECG signal to be amplified in several stages.

The most relevant interference signals appear in the signal measurement, so the acquisition and amplification circuit have a high common mode rejection rate to eliminate these defects. Likewise, the common mode rejection rate has been a critical design parameter when designing the circuit.

Filters are another element designed to eliminate frequency components that do not provide information. The filters that were created for the attenuation of interference are the low-pass filter, which filters signals above 125 Hz; high-pass filter, which filters signals below 0.5 Hz; and the notch filter or band-stop filter, which attenuates the signal with a value of 50 Hz.

The second phase is composed of the processing of the ECG signal. This phase was carried out using an algorithm developed in the MATLAB tool, which did not require many mathematical parameters, allowing the elimination of the undesirable noise that was acquired during the sampling. Likewise, the detection of the R waves of each sample was performed. The algorithms implemented in this phase have been created based on already existing literature.

The final phase of the thesis is composed of the development of the mobile application through Android Studio. The previous knowledge and knowledge acquired during the development of the thesis in this environment have helped in the programming of the structure of the application and its basic aspects. However, complex components

have been developed to provide the application with other necessary functionalities such as Bluetooth communication and real-time ECG visualization. The algorithms implemented in this phase have been created based on existing literature, and another part has been implemented with the help of a professional in the creation of mobile applications.

Although the prototype presented offers functionality like that described in the original proposal, it is still a prototype, meaning that there is still a wide set of improvements and opportunities for expansion. The associated permissive license will allow future development of the project.

## **7 Proposal of Recommendations for Further Work**

There are several areas in which the present project could be followed up for future work. The first could be analysis of heart rate variability (HRV) through the Poincare diagram and comparative analysis of FFT and Wavelet filters. In addition, upon the verification of the sensor and the algorithms used, the monitoring of the respiratory rate and its analysis can be focused on.

## References

- GUPTA, Rajashi and Dwaipayan, BISWAS. *Health monitoring systems: an enabling technology for patient care*. New York: CRC press, 2020. ISBN 978-14-987-7582-3.
- SALADIN, K. S., SULLIVAN, S.J. and C. A. GAN. *Human Anatomy*. 5<sup>TH</sup>ed. New York: McGraw-Hill Education, 2016. ISBN 978-00-734-0370-0.
- KANIUSAS, Eugenijus. *Biomedical Signals and Sensors III*. Cham: Springer, 2019. ISBN 978-33-197-4916-7.
- STANĚK, Vladimír. *Kardiologie v praxi*. Praha: Axonite CZ, 2014. ISBN 978-80-904899-7.
- MARIEB, E., WILHELM, P. and J. MALLATT. *Human anatomy*. 7<sup>th</sup> ed. Sao Paulo: Pearson, 2014. ISBN 978-85-430-1496-8.
- MCKINLEY, Michael P. et al. *Human Anatomy*. 5<sup>th</sup> ed. La Vergne: McGraw Hill Education, 2016. ISBN 978-12-592-8527-1.
- ROKYTA, Richard et al. *Fyziologie a patologická fyziologie: pro klinickou praxi*. Praha: Grada, 2015. ISBN 978-80-247-4867-2.
- MOREGA, A., MOREGA, M. and A. DOBRE. *Computational Modelling in Biomedical Engineering and Medical Physics*. Cambridge: Academic Press, 2020. ISBN 978-01-281-7897-3.
- SUBASI, Abdulhamit. *Practical Guide for Biomedical Signals Analysis Using Machine Learning Techniques: A MATLAB Based Approach*. Cambridge: Academic Press, 2019. ISBN 978-01-281-7444-9.
- GOLDBERGER, Jeffrey J and Jason NG. *Practical Signal and Image Processing in Clinical Cardiology*. London: Springer, 2010. ISBN 978-18-488-2514-7.
- PETTY, Brent G. *Basic Electrocardiography*. New York: Springer New York, 2016. ISBN 978-14-939-2412-7.
- GOLEMATI, Spyretta and Konstantina S. NIKITA. *Cardiovascular Computing: methodologies and clinical applications*. Singapore: Springer Singapore, 2019. ISBN 978-98-110-5091-6.

ZGALLAI, Walid A. *Biomedical Signal Processing and Artificial Intelligence in Healthcare*. Cambridge: Academic Press, 2020. ISBN 978-01-281-8946-7.

BULÍKOVÁ, Táňa. *EKG pre záchranárov nekaridiológov*. Praha: Grada, 2014. ISBN 978-80-247-5308-9.

KUSUMOTO, Fred. *ECG Interpretation: from pathophysiology to clinical application*. Switzerland: Springer International Publishing, 2020. ISBN 978-30-304-0340-9.

LYON, Douglas. *Biomedical Signal Processing: Applications with Arduino and Java*. USA: Independently published, 2020. ISBN 979-86-077-9974-8.

GUPTA, Rajarshi, Madhuchhanda MITRA and Jitendranath BERA. *ECG Acquisition and Automated Remote Processing*. New Delhi: Springer India, 2014. ISBN 978-81-322-1556-1.

KRAMME, Rüdiger. *Medizintechnik: Verfahren, Systeme und Informationsverarbeitung*. 5. Auflage. Berlin: Springer Berlin Heidelberg, 2017. ISBN 978-36-624-8770-9.

JEKOVA, Irena et al. Inter-lead correlation analysis for automated detection of cable reversals in 12/16-lead ECG. *Computer Methods and Programs in Biomedicine*. 2016, **134**, 31-41. ISSN 0169-2607.

MADEIRO, Joao P. et al. *Developments and Applications for ECG Signal Processing*. Fortaleza: Elsevier, 2018. ISBN 978-01-281-4035-2.

DOGAN, Ibrahim. *PIC Microcontroller projects in C: basic to advanced*. USA: Elsevier, 2014. ISBN 978-00-809-9924-1.

LEE, Edward and Sanjit SESHIA. *Introduction to embedded systems: a cyber-physical systems approach*. 2<sup>nd</sup> ed. USA: MIT PRESS, 2017. ISBN 978-02-625-3381-2.

MONK, Simon. *Hacking Electronics: an Illustrated DIY Guide for Makers and Hobbyists*. USA: McGraw-Hill Education, 2017. ISBN 978-12-600-1221-7.

PEREA, Francis. *Arduino essentials: enter the world of Arduino and its peripherals and start creating interesting projects*. UK: Packt Publishing Ltd., 2015. ISBN 978-17-843-9856-9.

BLUM, Jeremy. *Exploring Arduino: tools and techniques for engineering wizardry*. 2<sup>nd</sup> ed. Indianapolis: Wiley, 2020. ISBN 978-11-194-0537-5.

ARDUINO. Arduino UNO technical specification. USA: Arduino, 2016. Retrieved from <https://www.arduino.cc/en/Main/arduinoBoardUno>&gt;.

ANALOG-DEVICES. *AD620 technical document*. USA: Analog-Devices, 2011. Retrieved from <https://www.analog.com/media/en/technical-documentation/data-sheets/AD620.pdf>.

HAMBLEY, Allan R. *Electrical Engineering: Principles and applications*. 7<sup>TH</sup> ed. UK: Pearson, 2019. ISBN 978-01-344-8414-5.

GIFT, Stephan J. G. and Brent MAUNDY. *Electronic Circuit Design and Application*. Cham: Springer International Publishing, 2021. ISBN 978-3-030-46988-7.

VODA, Zbyšek. *Průvodce světem Arduina*. Bučovice: Martin Stríž, 2017. ISBN 978-80-871-0693-8.

USAMA BIN AFTAB, Muhammad. *Building Bluetooth low energy systems*. UK: Packt Publishing Ltd., 2017. ISBN 978-17-864-6108-7.

WARD, Hubert Henry. *Programming Arduino Projects with the PIC Microcontroller*. Berkeley: Apress, 2022. ISBN 978-14-842-7232-9.

ULRICH, Helmut a Hubert WEBER. *Laplace, Fourier und z-Transformation*. Wiesbaden: Springer, 2017. ISBN 978-36-580-3449-8.

ELDAR, Yonina. *Sampling theory: beyond bandlimited systems*. Cambridge: Cambridge University Press, 2015. ISBN 978-11-070-0339-2.

JI, Tianchu. *ECG Monitor on Android [Source Code]*. USA: New York, 2018. Retrieved from [https://github.com/chickenjohn/ECG\\_Monitor\\_on\\_Android](https://github.com/chickenjohn/ECG_Monitor_on_Android) (2022).

## List of tables

Table 3.1: Technical characteristics of Arduino board.....	28
Table 4.1: Values of Gain Resistors (Analog-Devices, 2011).....	34
Table 4.2: PIN configuration of the AD620 and Arduino UNO module (source prepared by the author) .....	39

## List of figures

Figure 1.1: Typical remote monitoring system (Gupta & Biswas, 2020, fig. 1.1, p. 3).	13
Figure 2.1: Front view of the heart (Staněk, 2014, p. 15).....	15
Figure 2.2: Back view of the heart (Staněk, 2014, p. 16) .....	16
Figure 2.3: Cardiac action potential. (Goldberger & Ng, 2010, Fig. 10.1, p. 114) .....	20
Figure 2.4: Conduction system of the heart (Morega et al., 2020, Fig. 4.1, p. 95).....	20
Figure 2.5: Normal activation of the heart (Kusumoto, 2020, fig. 1.5, p. 9).....	22
Figure 2.6: EKG signal (Madeiro et al., 2019, fig. 1.6, p. 10).....	23
Figure 2.7: Leads location according to Einthoven (Kramme, 2017, Fig. 6, p.138) .....	24
Figure 2.8: Lead circuit diagram according to Goldberger (Kramme, 2017, Fig. 8, p.139) .....	25
Figure 2.9: 12-lead ECG system (Jekova et al. 2016, Fig. 1, p. 32).....	25
Figure 3.1:Arduino UNO components (Monk, 2017, fig. 6.1, p. 106).....	27
Figure 3.2: Basic diagram of the presented platform and its principal components (Courtesy by prof. Evgenii Pustozarov, PhD.) .....	29
Figure 4.1: Medical ECG monitor circuit. (Analog-Devices, 2011). .....	31
Figure 4.2: Simplified Schematic of AD620 (Analog-Devices, 2011).....	32
Figure 4.3: Typical CMR vs. Frequency (Analog-Devices, 2011).....	35
Figure 4.4: Low-pass filter (Source prepared by the author).....	36
Figure 4.5: High-pass filter (Source prepared by the author). .....	37
Figure 4.6: Notch or band-stop filter (Source prepared by the author). .....	38
Figure 4.7:Startup the system in Arduino (Source prepared by the author). .....	39
Figure 4.8: ECG signal. Sample subject ID 16 (Source prepared by the author). .....	40
Figure 4.9: ECG signal. Sample subject ID 20 (Source prepared by the author). .....	40
Figure 4.10: Flowchart for graphing the ECG signal (Source prepared by the author). .....	41
Figure 4.11: Code for raw signal analysis (Source prepared by the author). .....	42
Figure 4.12: Corrected ECG signal without filter (Source prepared by the author).....	42
Figure 4.13: Fourier Transform (Source prepared by the author) .....	43
Figure 4.14: FIR filter and Frequency Normalization (Source prepared by the author) .....	44
Figure 4.15: ECG Signal without and with filter (Source prepared by the author).....	45
Figure 4.16: Verification of the generated filter (Source prepared by the author) .....	45
Figure 4.17: Algorithm to detect the R peak (Source prepared by the author).....	46



Figure 4.18: R peak detection signal (Source prepared by the author).....	46
Figure 4.19: Module HC-05 and Arduino UNO schema (Source prepared by the author) .....	48
Figure 4.20: HC-05 connection algorithm (Source prepared by the author).....	50
Figure 4.21: Application Structure (Source prepared by the author) .....	52
Figure 4.22: Main window layout (Source prepared by the author).....	53
Figure 4.23: Main activity layout (Source prepared by the author).....	54
Figure 4.24: Instructions_Fragment layout (Source prepared by the author).....	55
Figure 4.25: Diagram of ECG Signal Fragment (Source prepared by the author). .....	58
Figure 4.26: ECG_Signal_fragment layout (Source prepared by the author) .....	61
Figure 4.27: About_Fragment layout (Source prepared by the author).....	62
Figure 4.28: 3-lead electrode placement (Source taken from <a href="https://litfl.com/ecg-lead-positioning/">https://litfl.com/ecg-lead-positioning/</a> ).....	64
Figure 4.29: 3-lead electrode placement in a participant. (Source prepared by the author) .....	64
Figure 4.30: ECG prototype (Source prepared by the author).....	65
Figure 4.31: ECG signal (Source prepared by the author) .....	65
Figure 4.32: Spectral component of the ECG signal (Source prepared by the author) ..	66
Figure 4.33: R peak detection (Source prepared by the author) .....	66

## List of graphs

Graph 4.1: Ranges of each selection criteria vs gender. (Source prepared by the author). .....	63
Graph 5.1: Pathological anamnesis vs. gender (Source prepared by the author). ....	68
Graph 5.2: R peak detection of each participant (Source prepared by the author).....	69

## Appendix

Appendix A: Informed consent.

Appendix B: Table with all participants' data.

Appendix C: ECG signal and R peak's detection obtained of the participants generated by the prototype.

Appendix D: ECG's electronic diagram.

Appendix E: Arduino UNO board.

Appendix F: Content of attached CD.

## Appendix A: Informed consent

### INFORMED CONSENT

Informovaný souhlas

CODE: ID\_

#### Health Monitoring System Using Wireless Sensor Network Systém sledování srdce prostřednictvím sítě bezdrátových senzorů

##### Responsible of the project Odpovědný za projekt

Name : Carlos Vladimír Díaz Shuňa  
Phone : +420602449969  
Email : carlos.vladimir.diaz.shuna@tul.cz

##### Dear participant, Vážený účastníku,

The purpose of this document is to let you know the details of the study and to request your informed consent to participate in it.

*Účelem tohoto dokumentu je informovat vás o podrobnostech studie a vyžádat si váš informovaný souhlas s účastí v ní.*

##### Introduction and Purpose of the study

###### Úvod a účel studie

You are being asked to take part in a research study. Before you decide to participate in this study, it is important that you understand why the project is being done and what it will involve. Please read the following information carefully. Please ask the responsible of the project if there is anything that is not clear or if you need more information.

*Jste požádáni, abyste se zúčastnili výzkumné studie. Než se rozhodnete zúčastnit se této studie, je důležité, abyste pochopili, proč se projekt provádí a co bude zahrnovat. Přečtěte si prosím pozorně následující informace. Pokud vám něco není jasné nebo potřebujete další informace, zeptejte se odpovědného za projekt.*

The purpose of this study is to design and development of an ECG sensor prototype which provides us with information and analysis in real-time.

*Účelem této studie je návrh a vývoj prototypu EKG senzoru, který nám poskytuje informace a analýzy v reálném čase.*

##### Description of the study

###### Popis studie

ECG is a diagnostic method for detecting the electrical signal of the heart and its rhythm abnormalities. These disorders of the conduction system of the heart are usually sporadic in onset and of limited duration. As an alternative, an ECG prototype has been made which uses a post-event recording monitoring system with an AD620AN sensor, which sends the physiological signal obtained via Bluetooth to an application on the patient's mobile phone, which supervises the real-time analysis of the obtained signal.

*EKG je diagnostická metoda pro detekci elektrického signálu srdce a jeho rytmických abnormalit. Tyto poruchy vodivého systému srdce jsou obvykle sporadické v nástupu a omezené trvání. Jako alternativa byl vyroben prototyp EKG, který používá monitorovací systém pro záznam po události se senzorem AD620AN, který odesílá fyziologický signál získaný přes Bluetooth do aplikace na mobilním telefonu pacienta, která dohlíží na analýzu získaného signálu v reálném čase.*

##### Methodology

###### Metodika

The present project consists of two stages, in the first a series of questions will be asked regarding pathological antecedents. During the second stage, the measurement of the ECG signal will be carried out, by means of our ECG prototype. These stages together will last 20 minutes.

*Tento projekt se skládá ze dvou fází, v první bude položena řada otázek týkajících se patologických předchůdců. Během druhé etapy bude provedeno měření EKG signálu pomocí našeho prototypu EKG. Tyto fáze dohromady budou trvat 20 minut.*

##### Participation in the study

###### Účast ve studii

Your participation in this study is free and voluntary, and you may request to be excluded from this research and that your interventions not be considered in this research without prior justification or prejudice to you. If you participate in this study, you do so with your express informed consent, which you sign and authorize.

*Vaše účast v této studii je bezplatná a dobrovolná a můžete požádat o vyloučení z tohoto výzkumu a o to, aby vaše intervence v tomto výzkumu nebyly brány v úvahu bez předchozího zdůvodnění nebo újmy vůči vám. Pokud se účastníte této studie, činíte tak se svým výslovným informovaným souhlasem, který podepisujete a autorizujete.*

## Appendix B: Table with all participants' data

<b>ID</b>	<b>GENDER</b>	<b>AGE</b>	<b>WEIGHT [Kg]</b>	<b>HEIGHT [cm]</b>	<b>DM</b>	<b>HTA</b>	<b>CVD</b>
1	Male	32	95	177	NO	NO	NO
2	Female	27	90	155	NO	YES	NO
3	Female	25	65	169	NO	NO	NO
4	Male	22	80	185	NO	YES	YES
5	Male	33	100	171	NO	YES	YES
6	Male	25	78	182	NO	NO	NO
7	Male	39	81	167	NO	NO	NO
8	Male	24	85	181	NO	NO	NO
9	Male	25	77	188	NO	NO	NO
10	Male	38	80	178	NO	NO	NO
11	Female	24	52	172	NO	NO	NO
12	Female	26	64	170	NO	NO	NO
13	Female	22	47	168	NO	NO	NO
14	Male	25	79	183	NO	NO	NO
15	Male	30	100	181	NO	NO	NO
16	Female	20	58	170	NO	NO	NO
17	Male	34	85	170	NO	NO	NO
18	Male	28	100	184	NO	YES	NO
19	Male	25	84	192	NO	NO	NO
20	Female	23	60	171	NO	NO	NO
21	Male	26	80	185	NO	NO	NO
22	Male	29	96	186	NO	YES	NO
23	Male	38	100	183	NO	NO	NO
24	Male	26	89	185	NO	NO	YES
25	Male	25	85	189	NO	NO	NO

## Appendix C: ECG signal and R peak's detection obtained of the participants generated by the prototype.

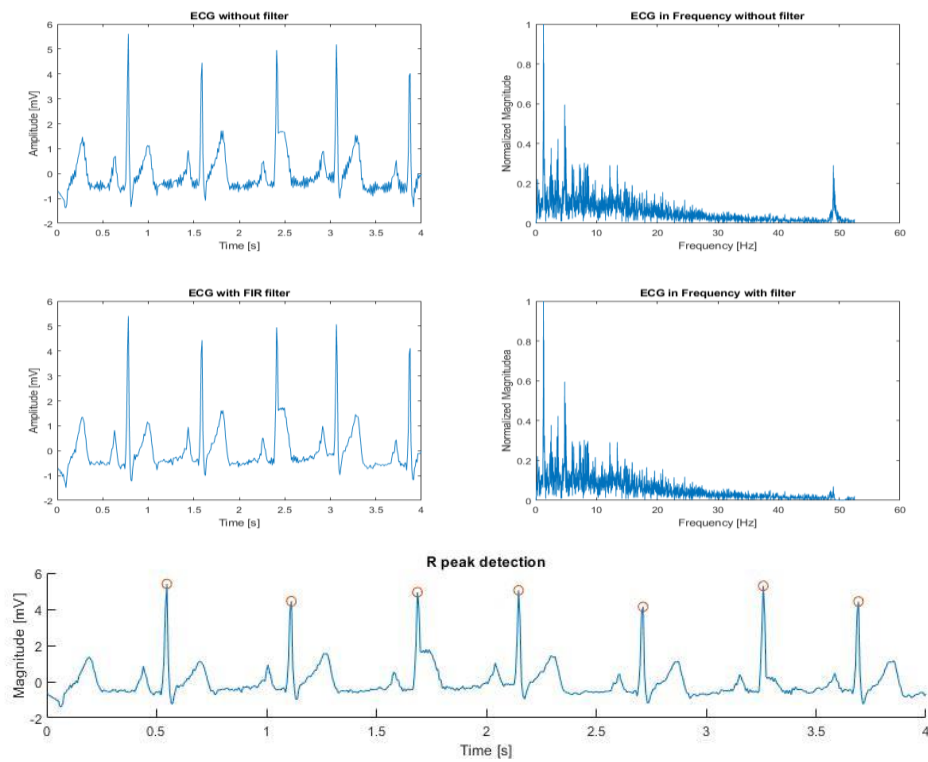


Figure C. 1: ECG and R peak analysis for subject 1.

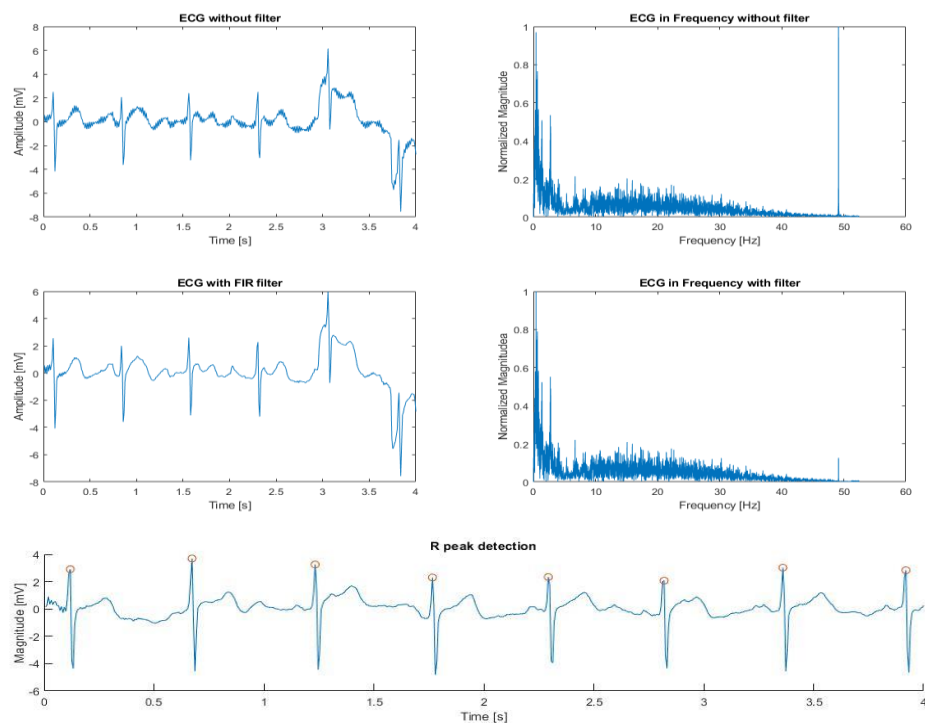


Figure C. 2: ECG and R peak analysis for subject 2.

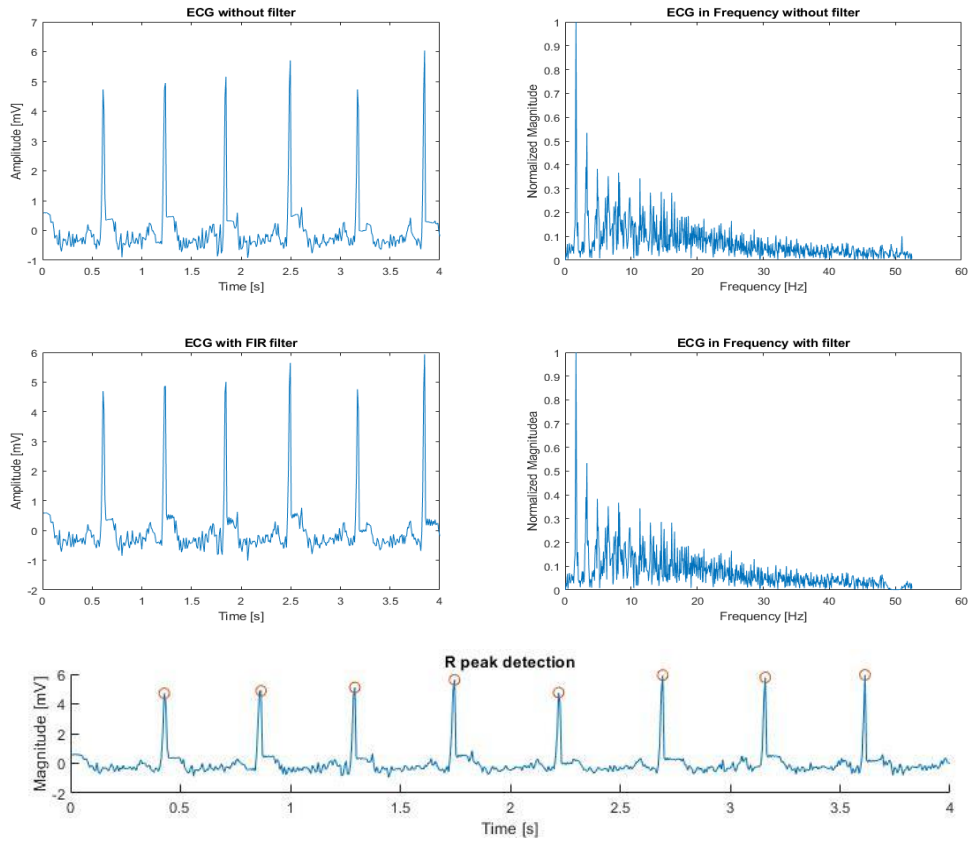


Figure C. 3: ECG and R peak analysis for subject 3.

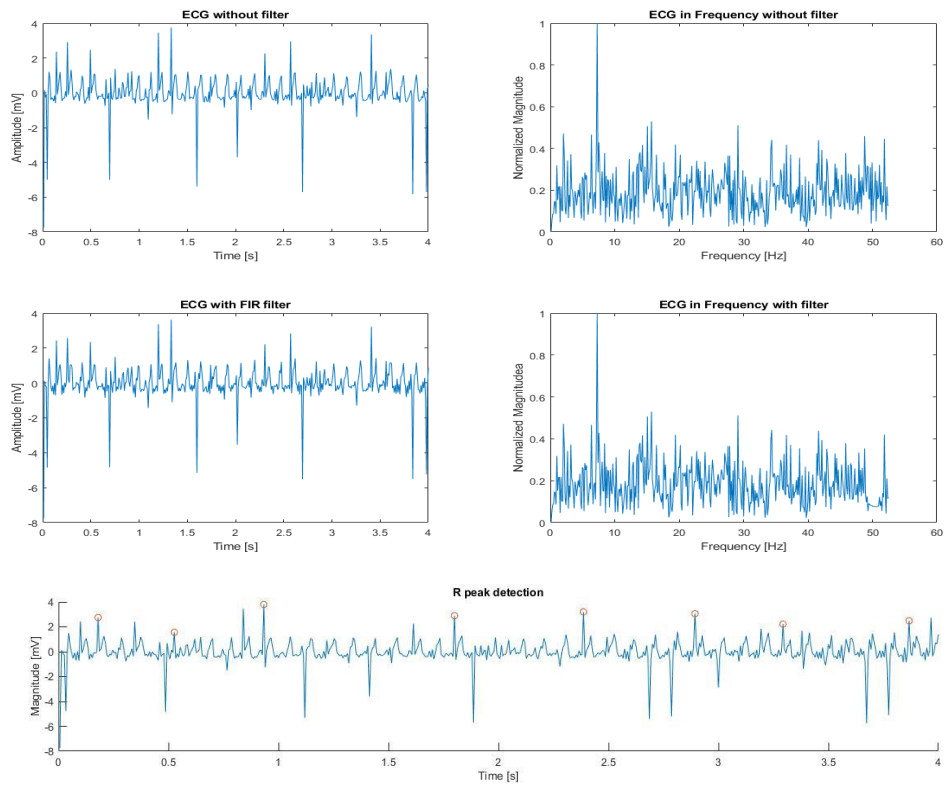


Figure C. 4: ECG and R peak analysis for subject 4.

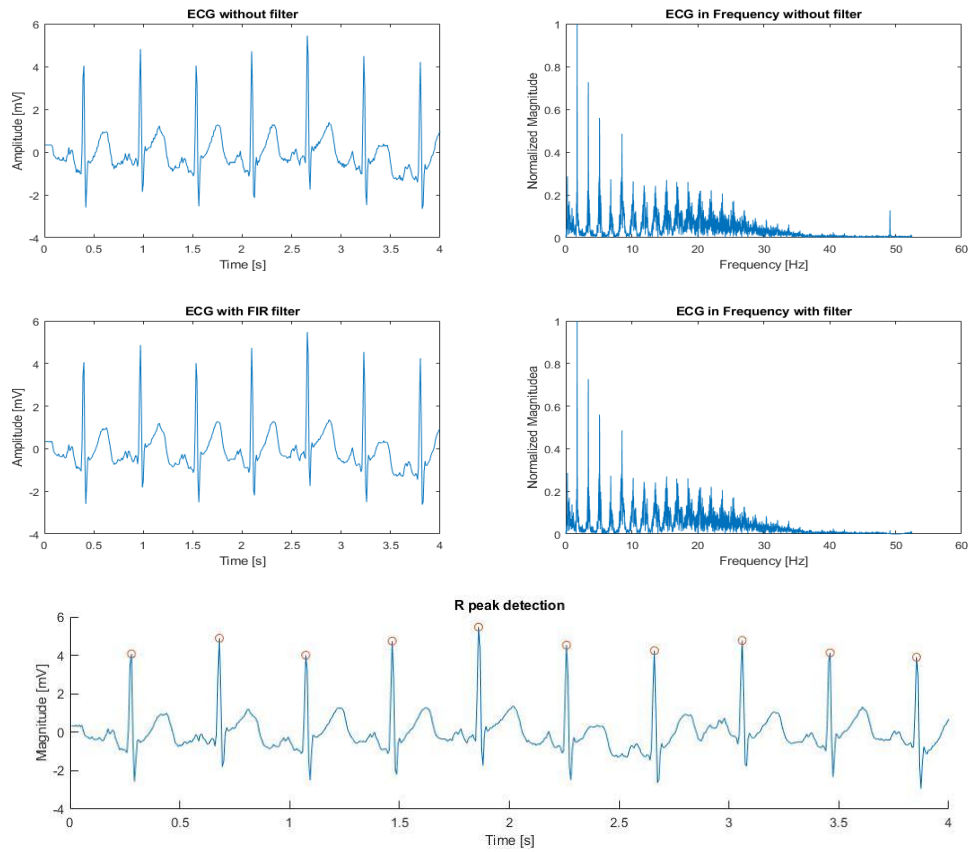


Figure C. 5: ECG and R peak analysis for subject 5.

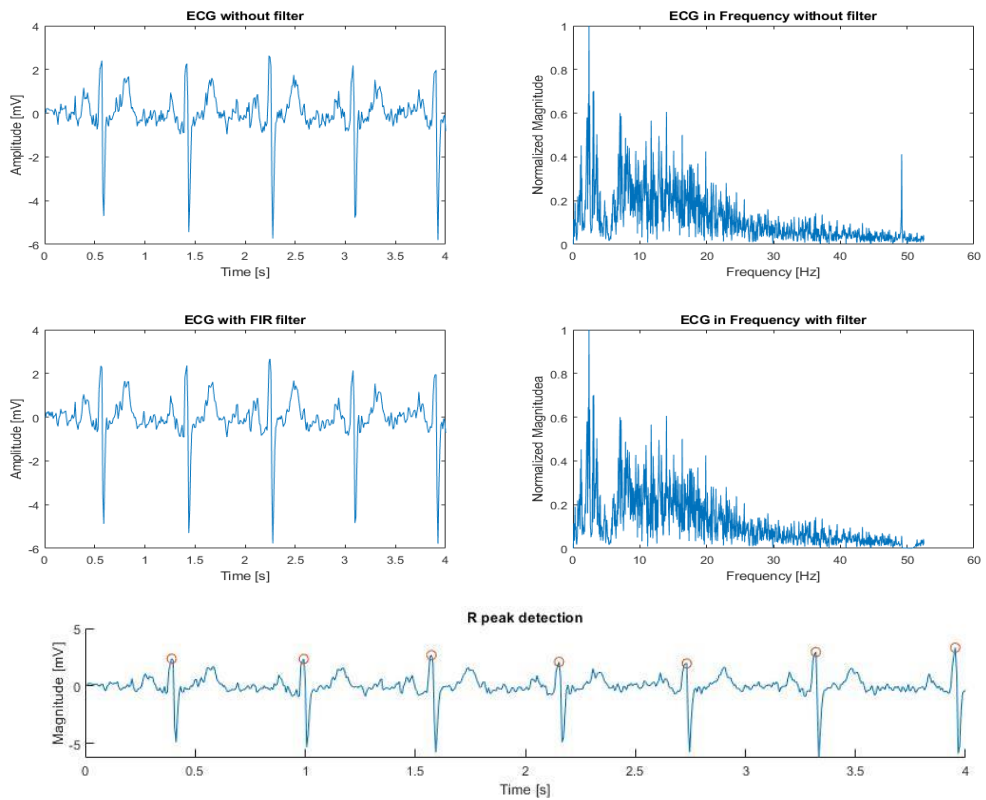


Figure C. 6: ECG and R peak analysis for subject 6.



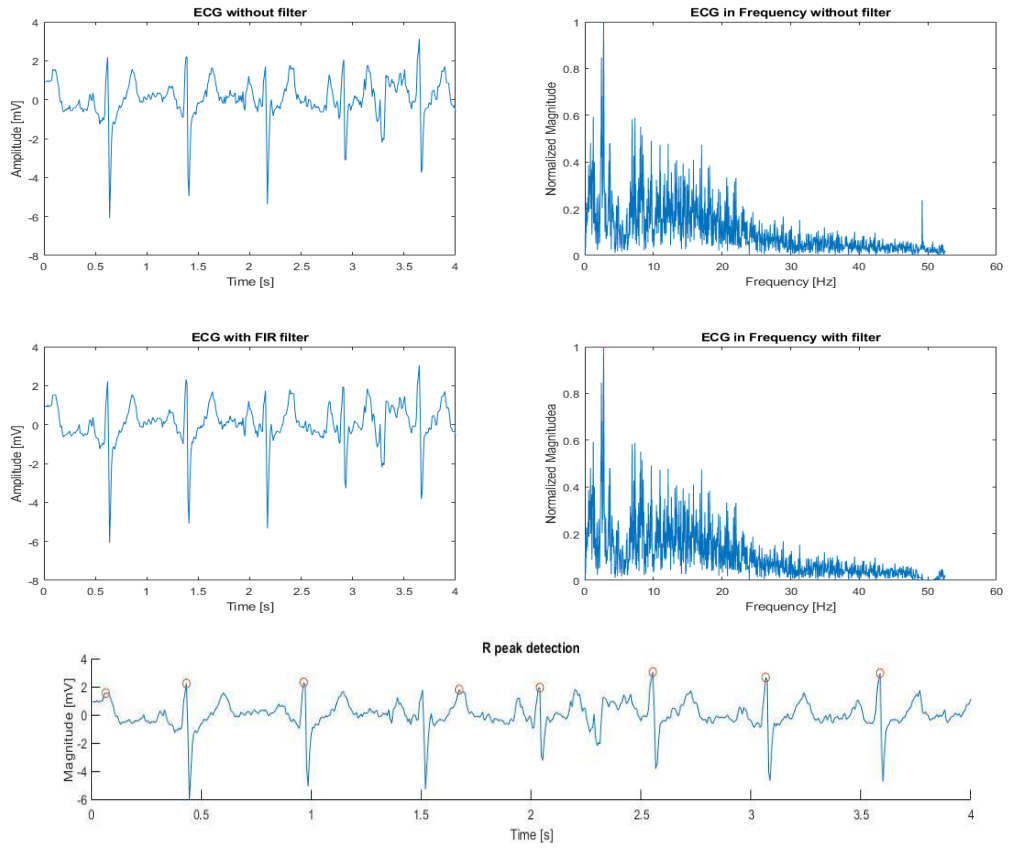


Figure C. 7: ECG and R peak analysis for subject 7.

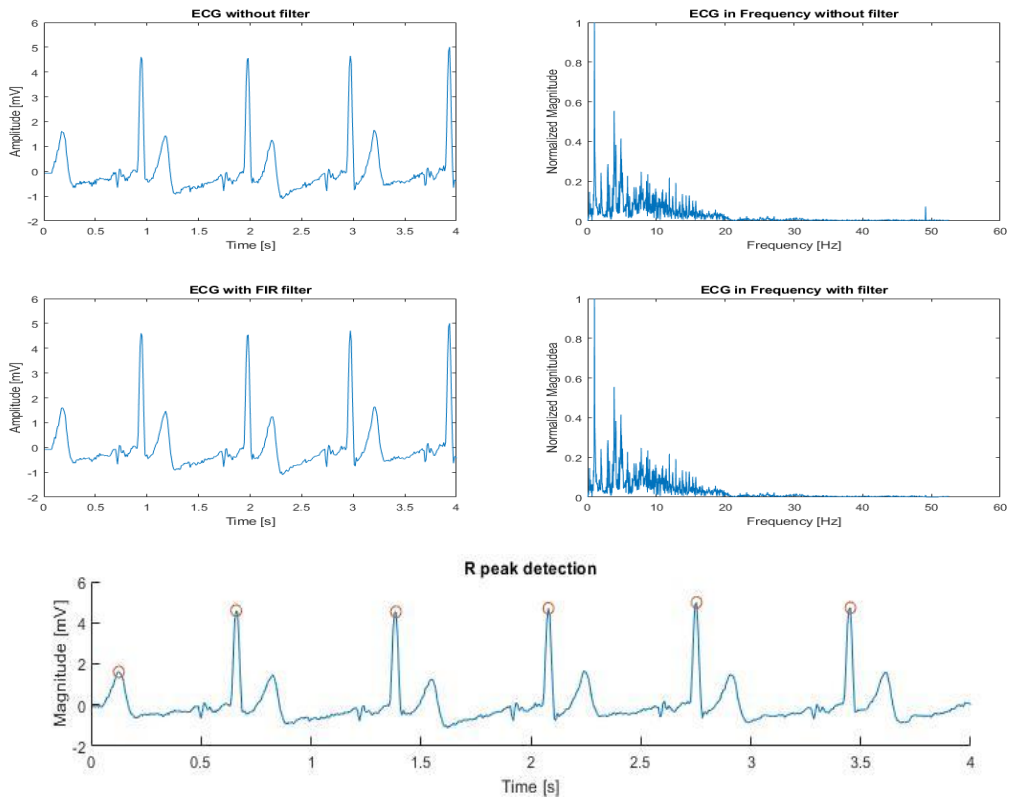


Figure C. 8: ECG and R peak analysis for subject 8.

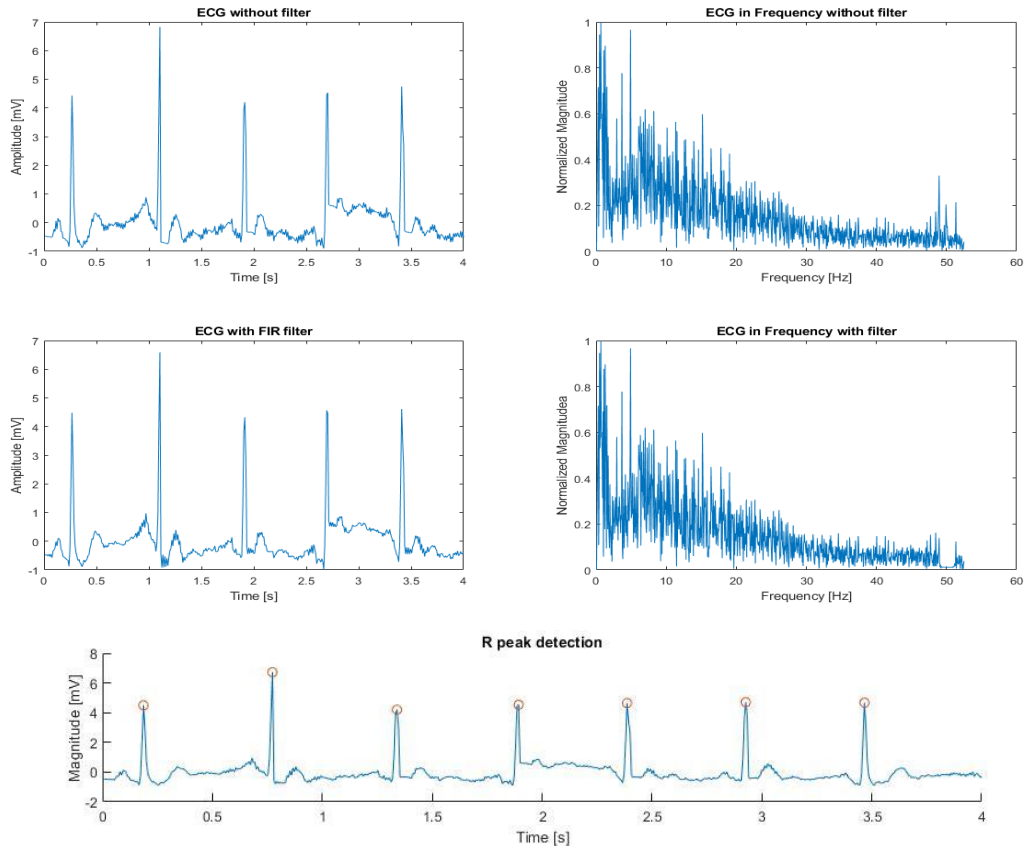


Figure C. 9: ECG and R peak analysis for subject 9.

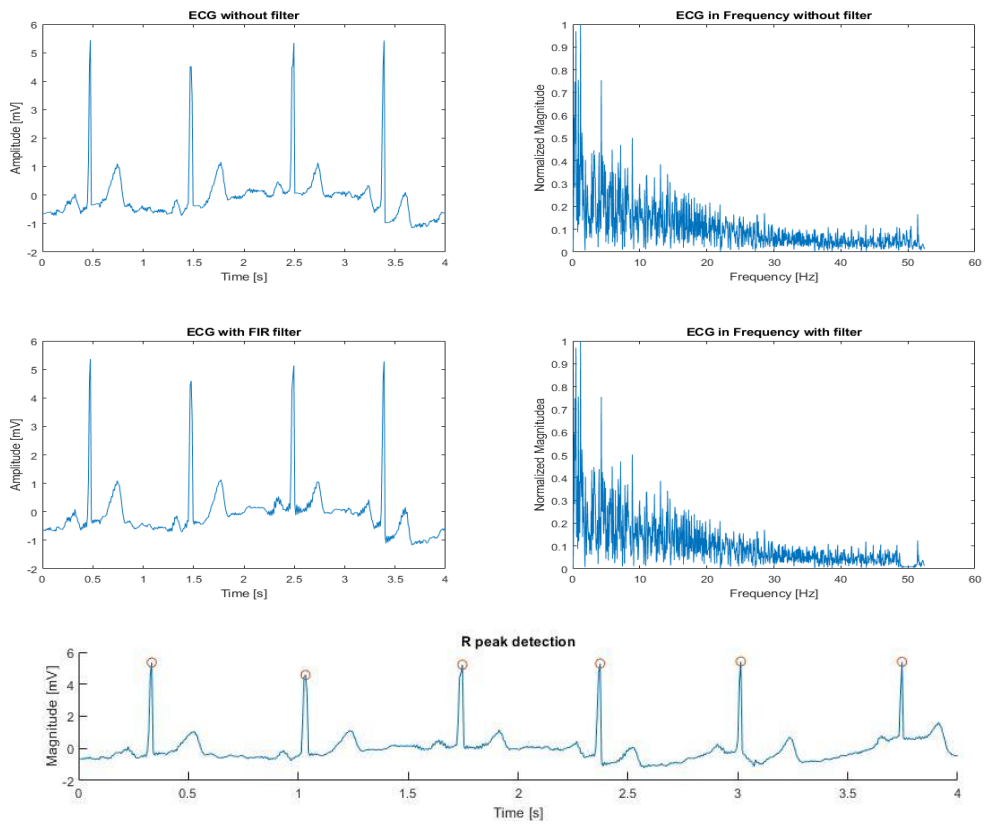


Figure C. 10: ECG and R peak analysis for subject 10.

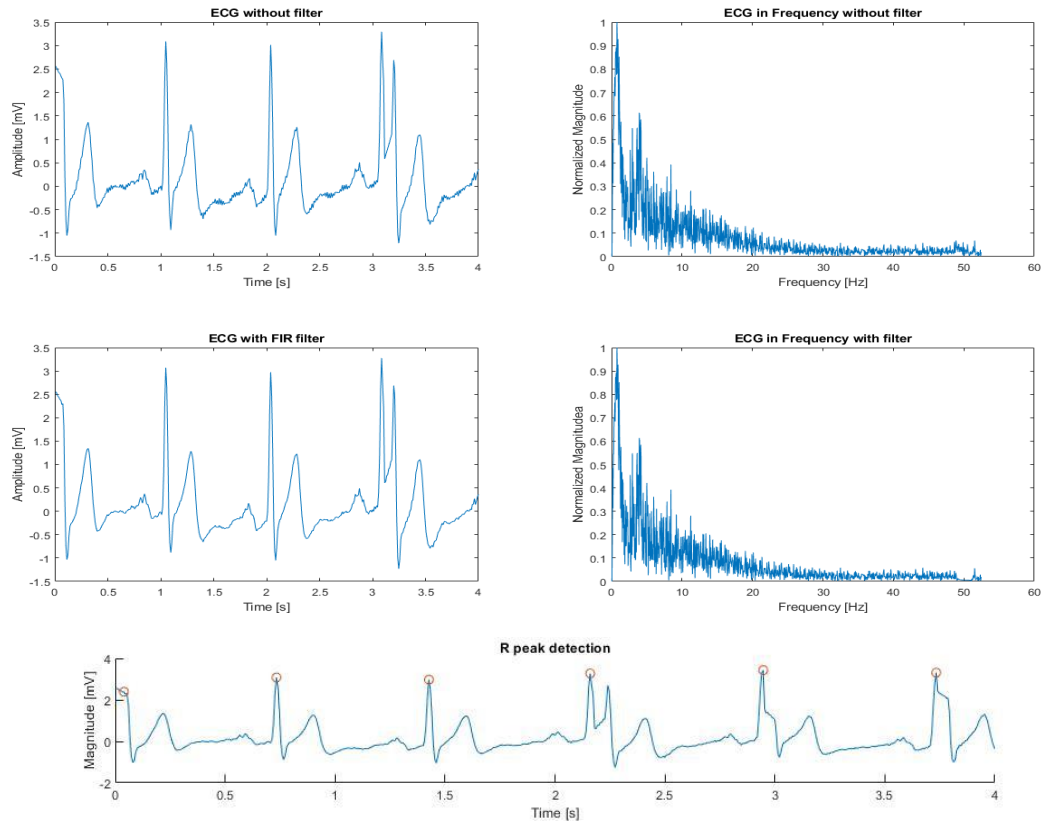


Figure C. 11: ECG and R peak analysis for subject 11.

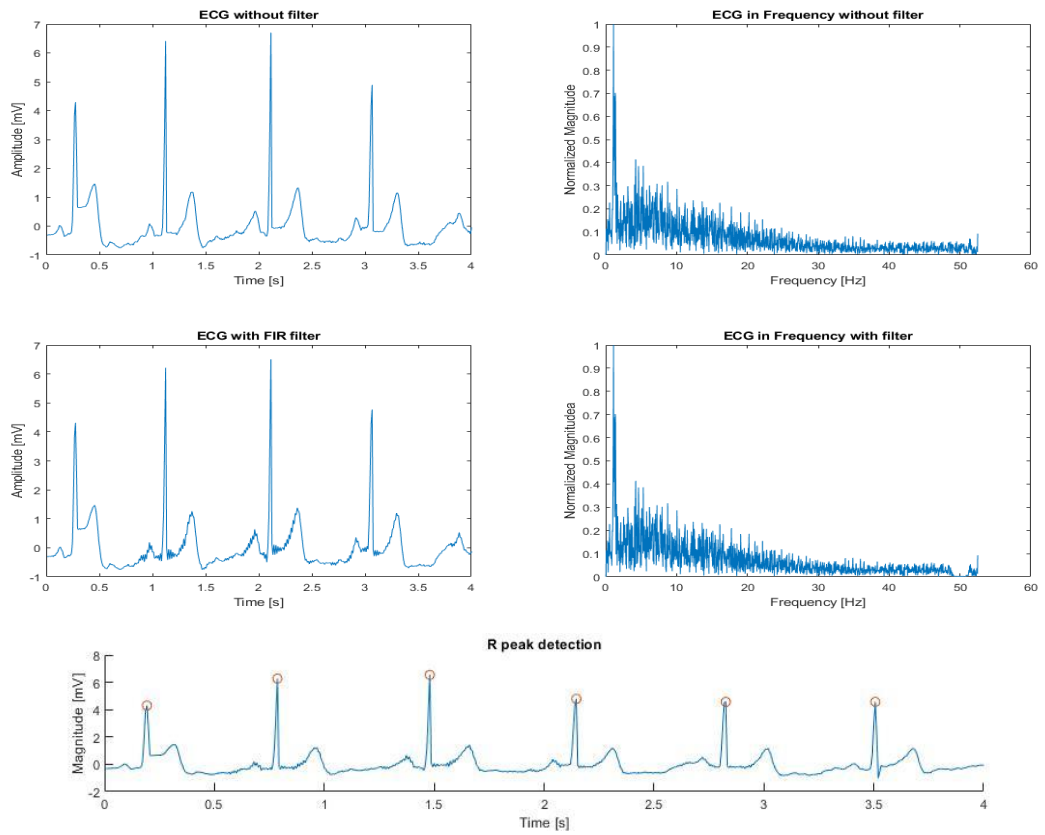


Figure C. 12: ECG and R peak analysis for subject 12.

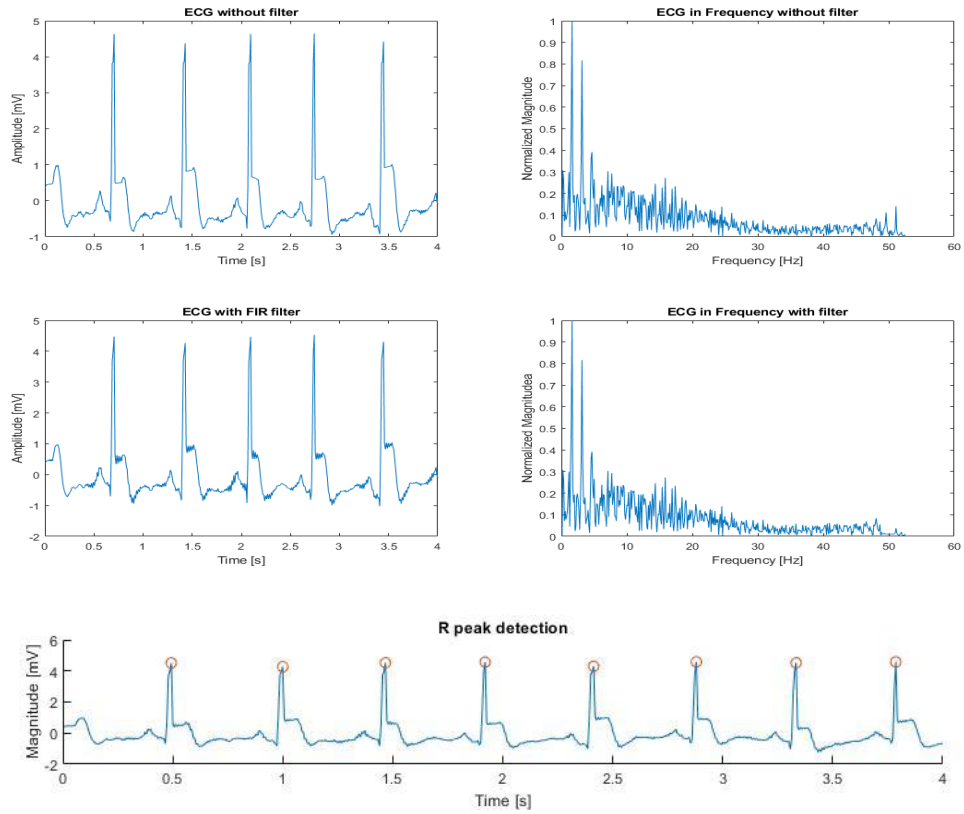


Figure C. 13: ECG and R peak analysis for subject 13.

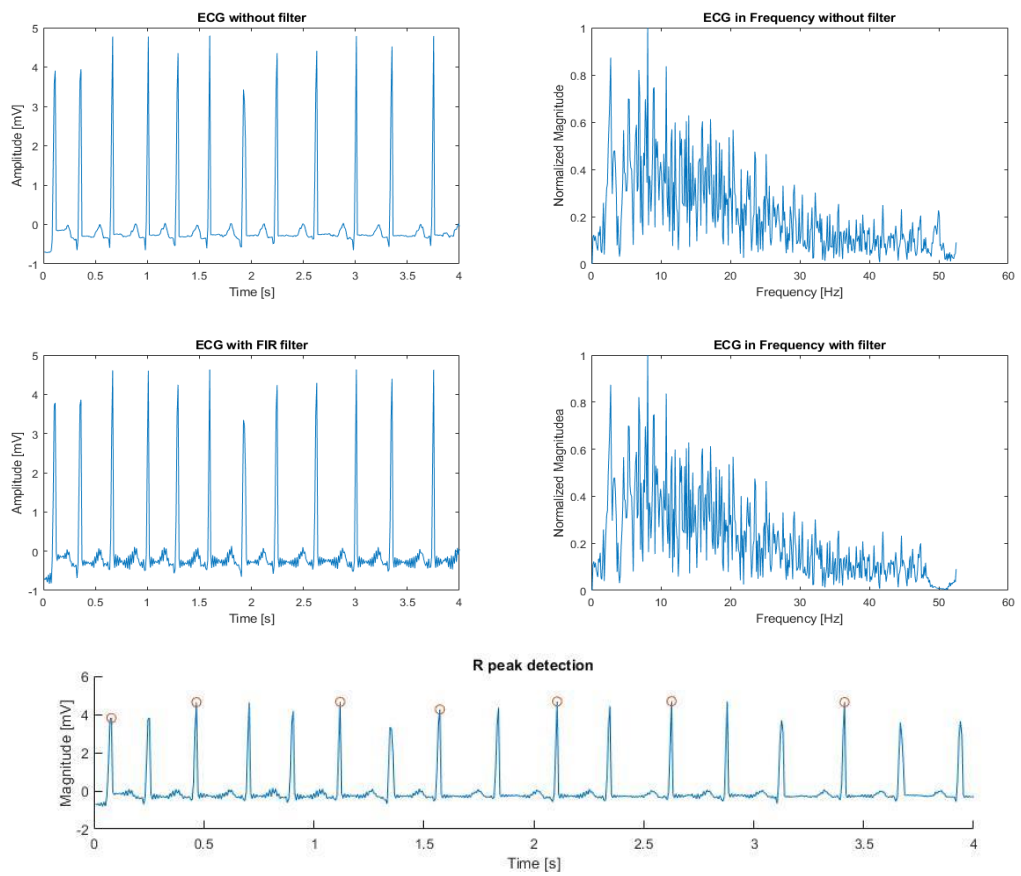


Figure C. 14: ECG and R peak analysis for subject 14.

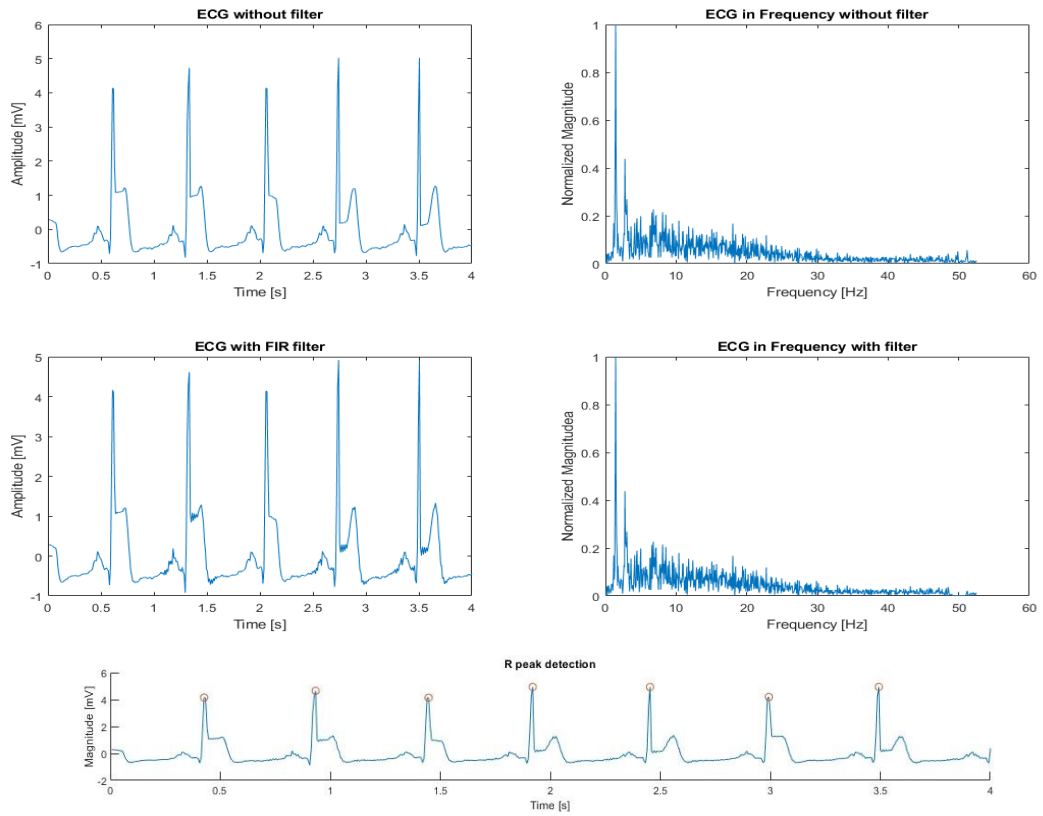


Figure C. 15: ECG and R analysis for subject 15.

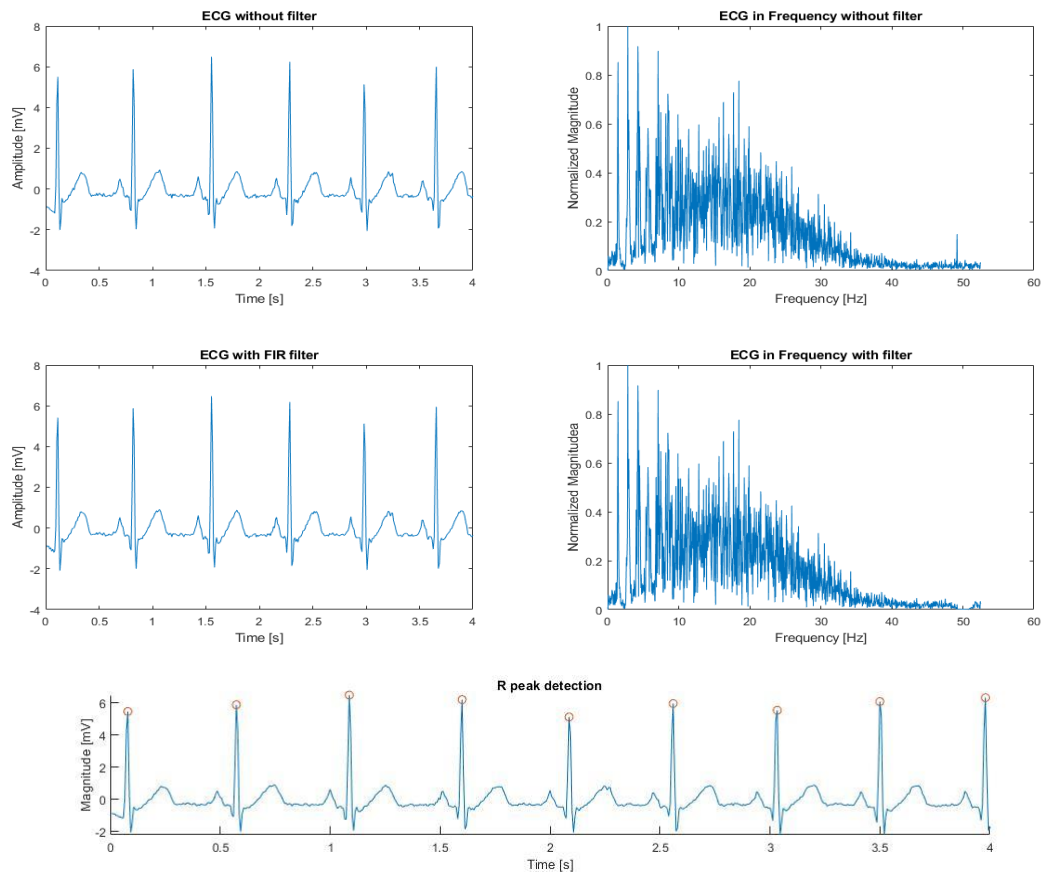


Figure C. 16: ECG and R peak analysis for subject 16.

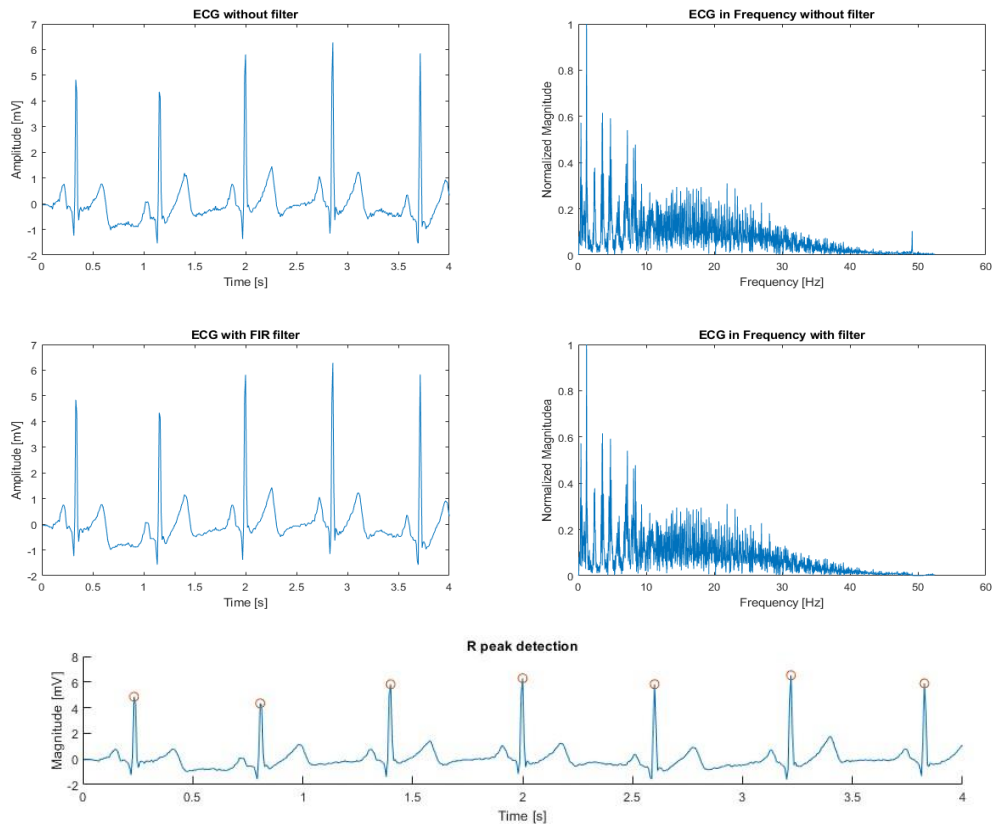


Figure C. 17: ECG and R peak analysis for subject 17.

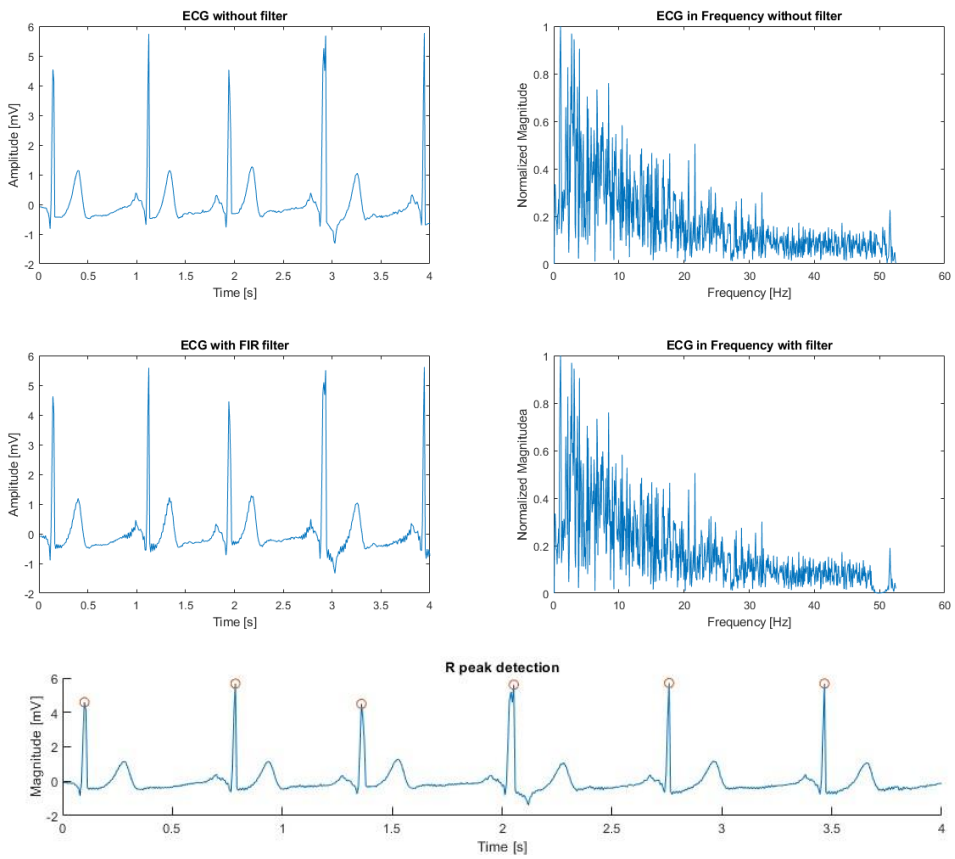


Figure C. 18: ECG and R peak analysis for subject 18.

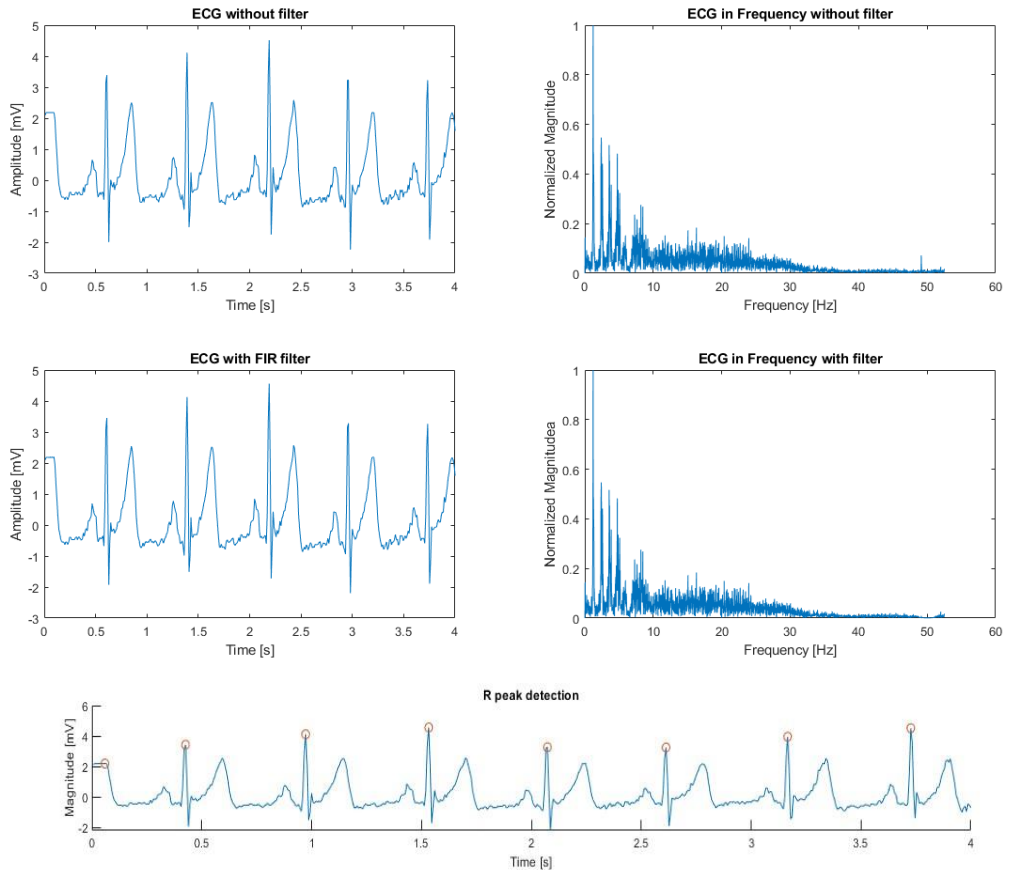


Figure C. 19: ECG and R peak analysis for subject 19.

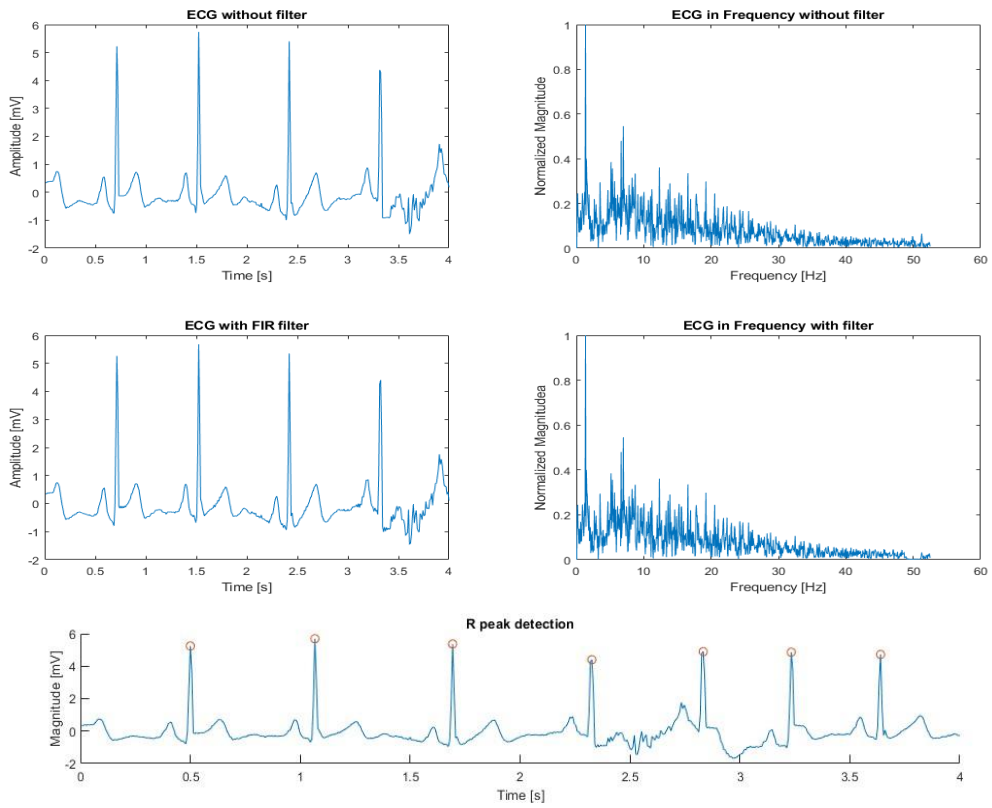


Figure C. 20: ECG and R peak analysis for subject 20.

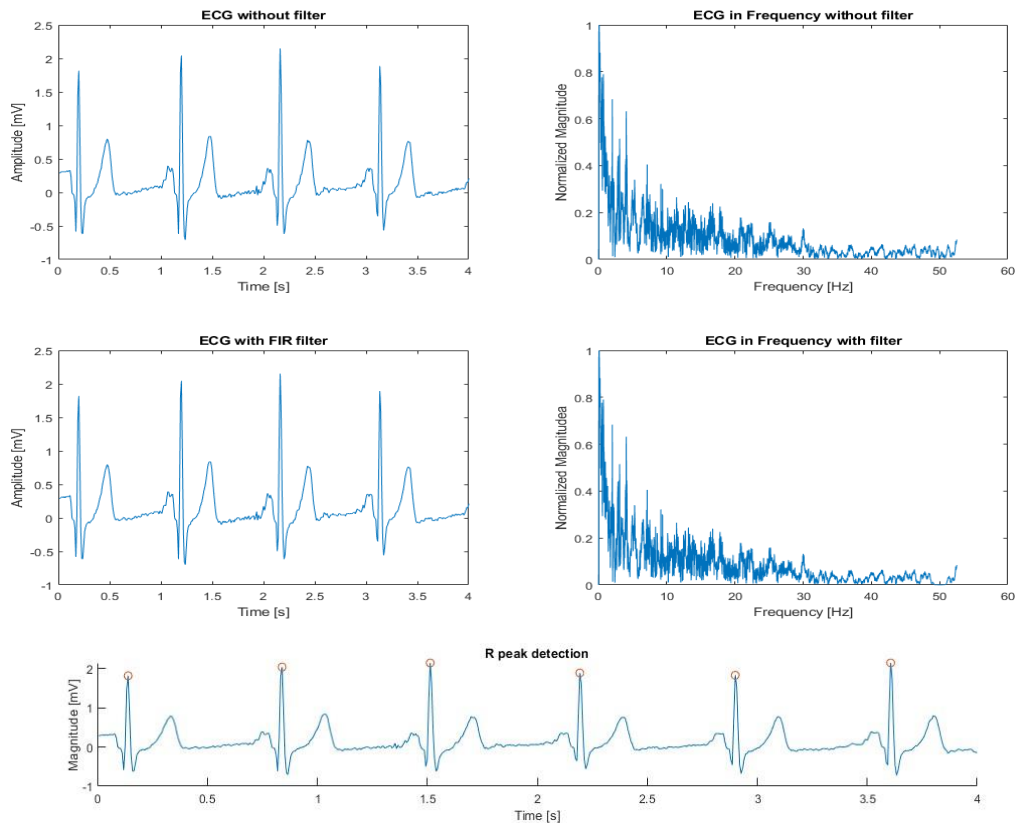


Figure C. 21: ECG and R peak analysis for subject 21.

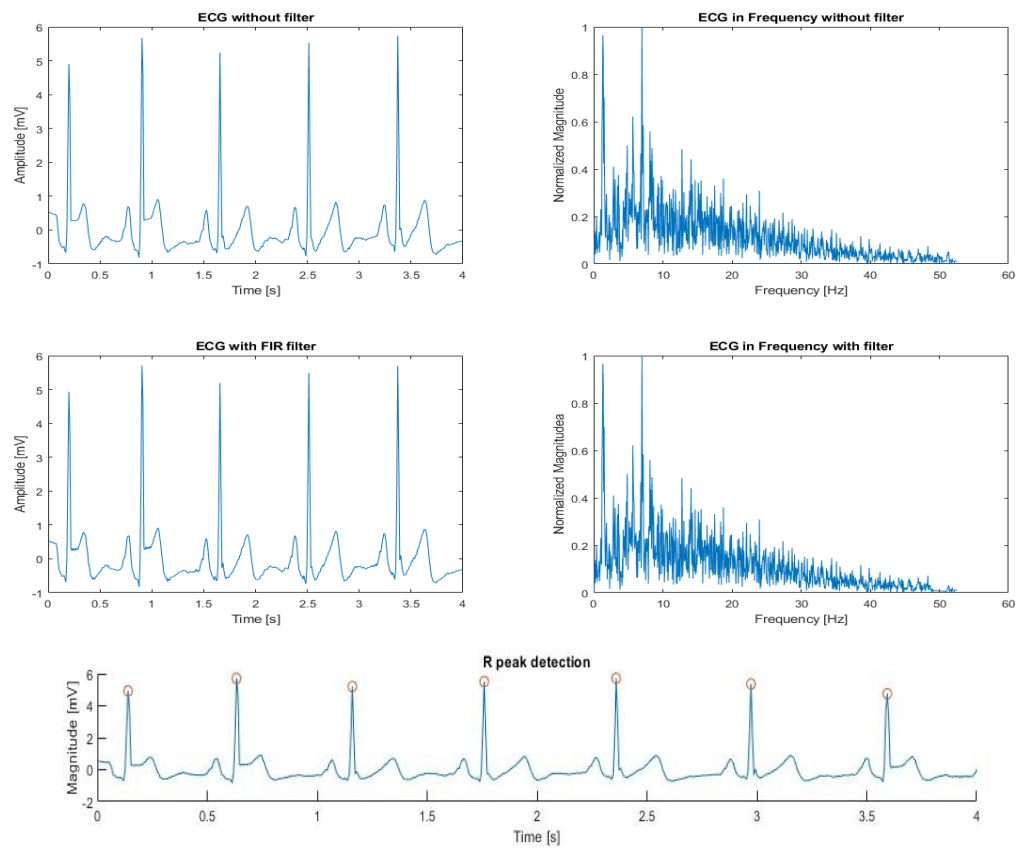


Figure C. 22: ECG and R peak analysis for subject 22.



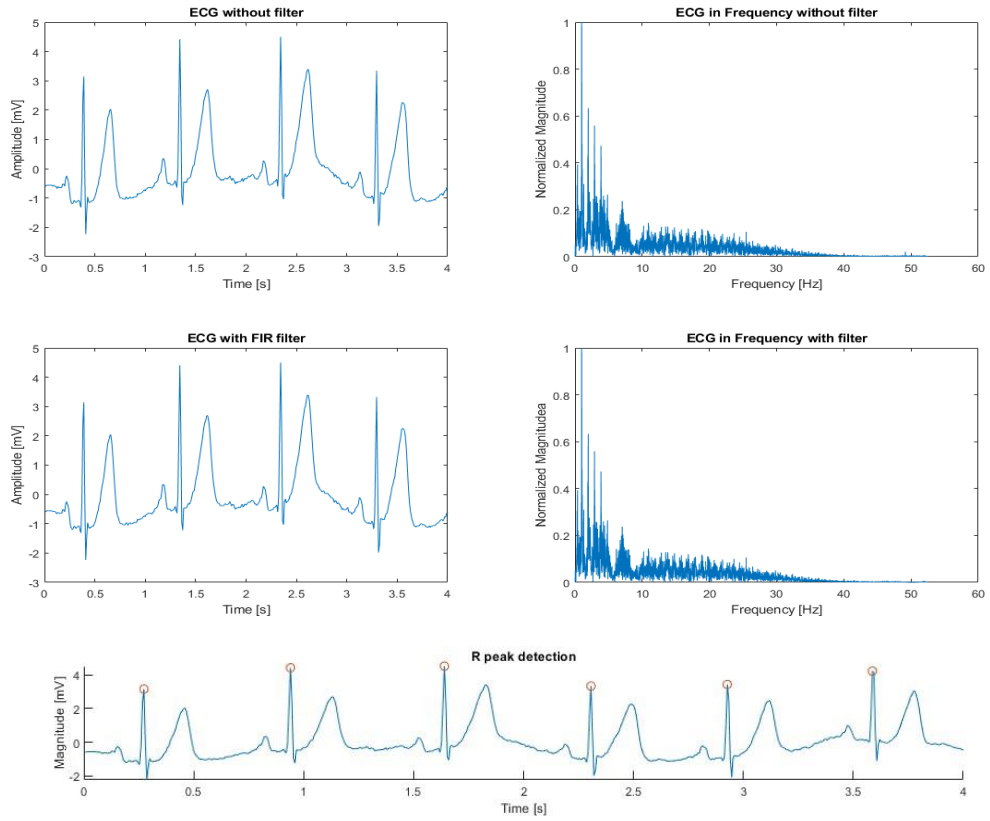


Figure C. 23: ECG and R peak analysis for subject 23.

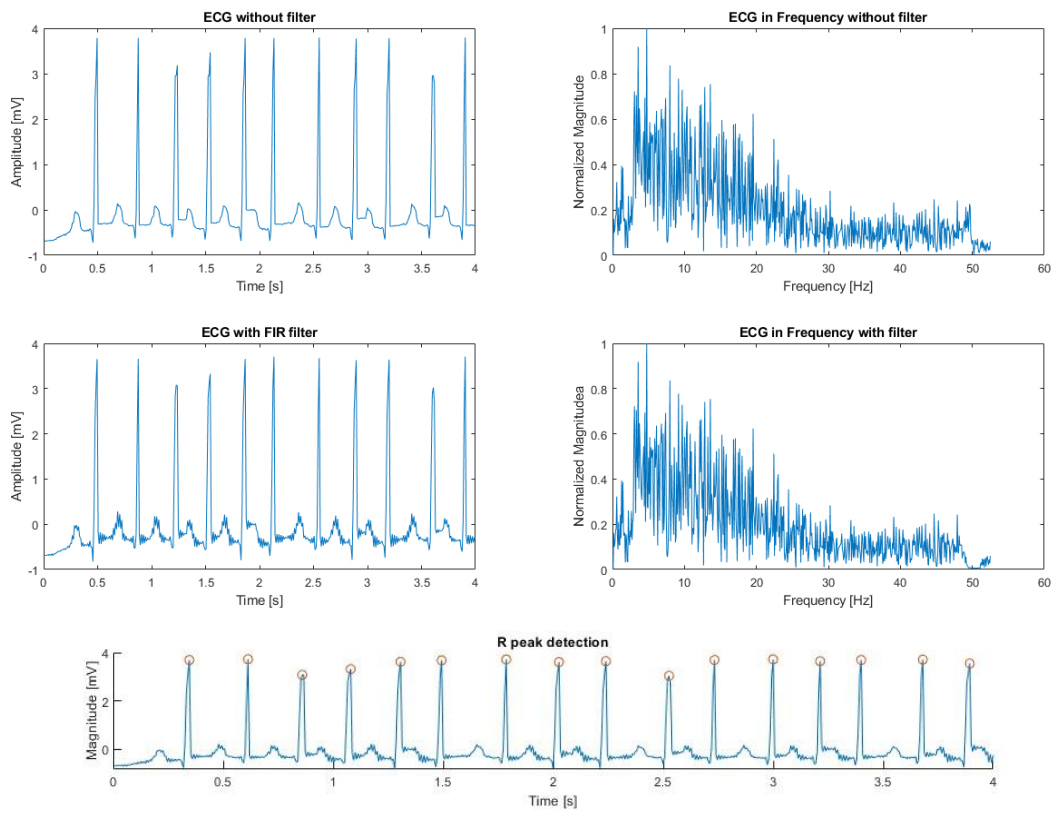


Figure C. 24: ECG and R peak analysis for subject 24.

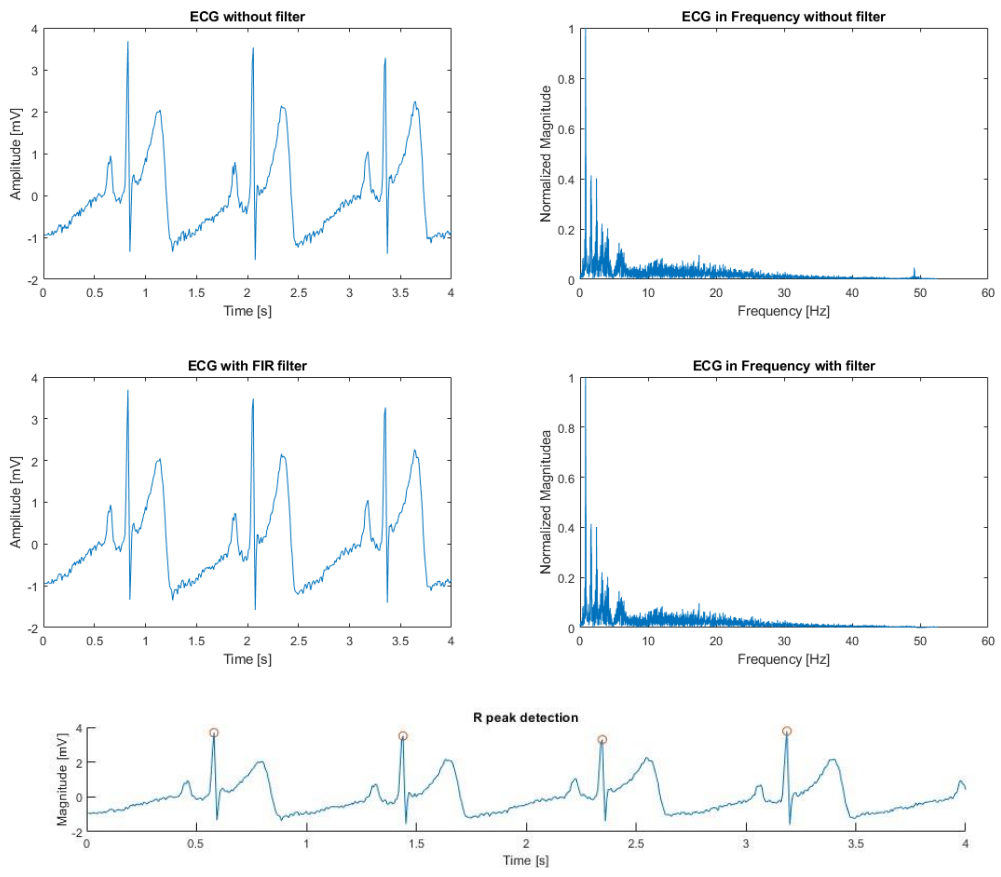
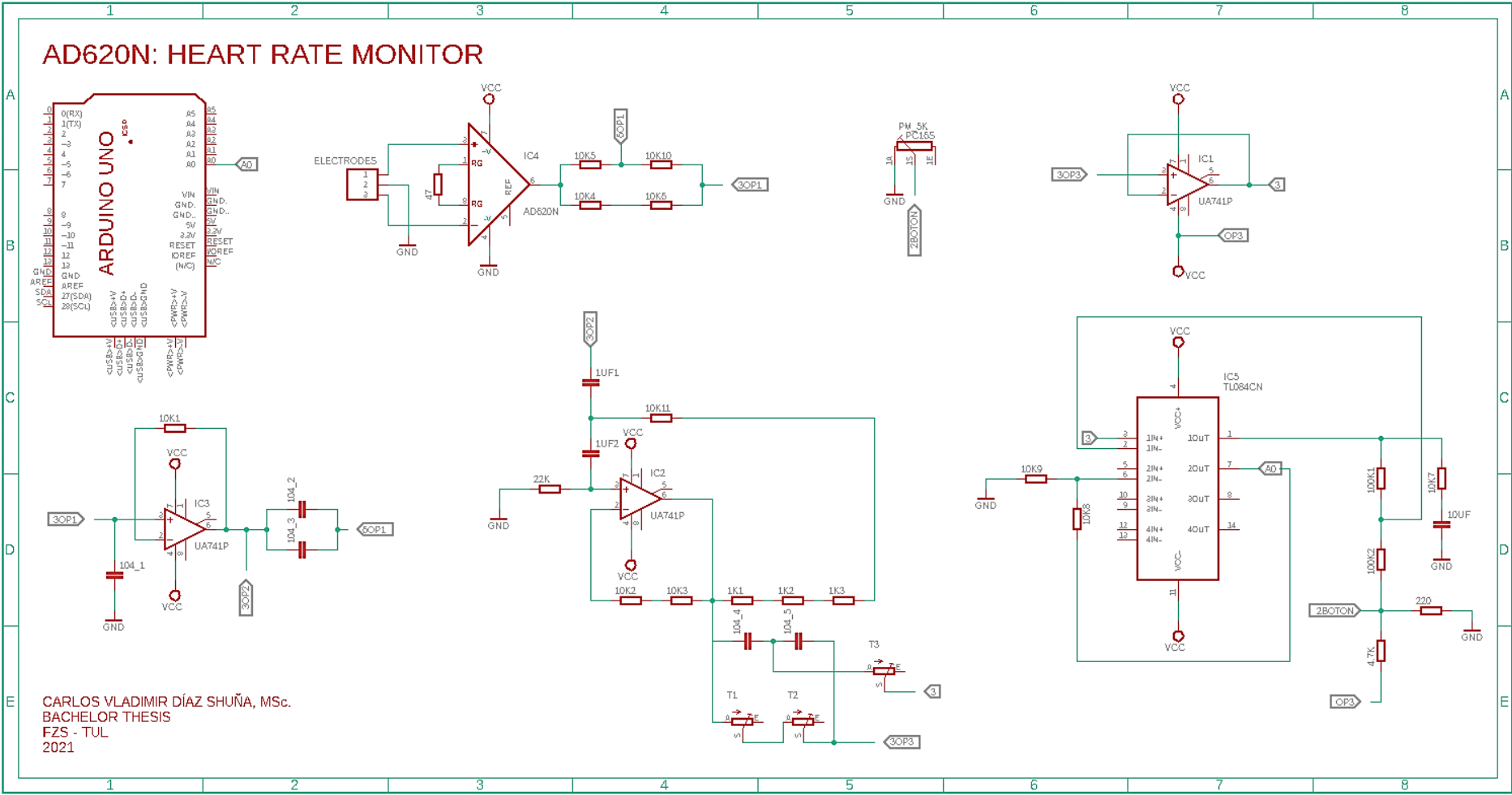
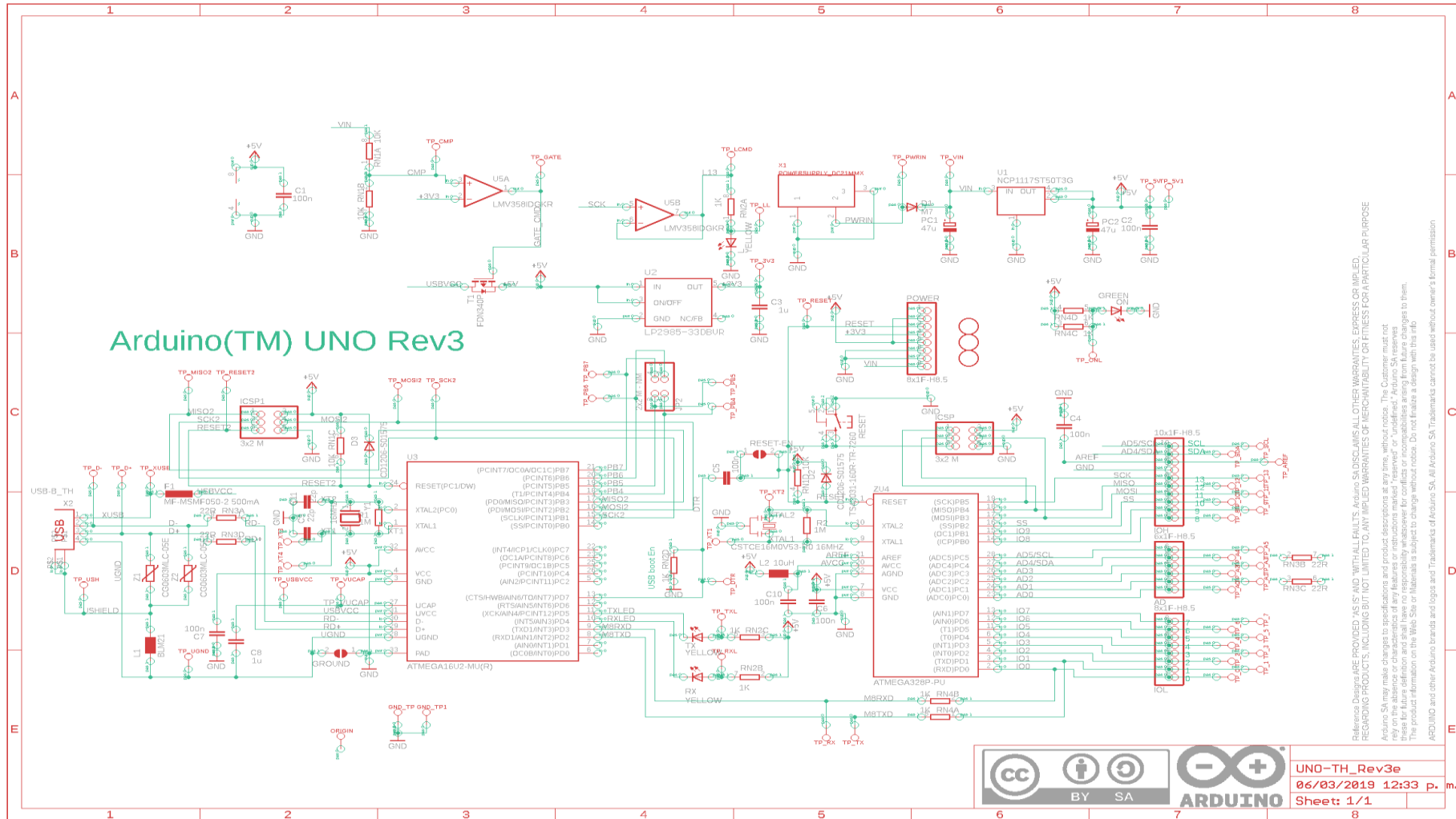


Figure C. 25: ECG and R peak analysis for subject 25.

# Appendix D: ECG's electronic diagram



# Appendix E: Arduino UNO board



## Appendix F: Content of attached CD.

### F.1 Bachelor thesis

- Thesis\_Diaz\_Shuna\_2021.pdf

### F.2 Complete source code

- ECG\_Diaz.ino
- HC05\_Diaz.ino
- ECG\_Diaz.m

### F.3 Circuit Diagram

- Proyecto.sch

### F.4 Source code for App